ABSTRACT

STORM, TYLER KEITH. Predicting Prestress Losses, Camber, and Deflection in Prestressed Concrete Members. (Under the direction of Dr. Sami Rizkalla.)

Accurate predictions of camber and prestress losses for prestressed concrete bridge girders are essential to minimizing the frequency and cost of construction problems. The time-dependent nature of prestress losses, variable concrete properties, and problems related to production variables make it difficult to predict camber accurately. The recent problems experienced by NCDOT during construction are mainly related to inaccurate predictions of camber. In this report, several factors related to girder production are shown to have a significant impact on the prediction of camber. These factors include differences between the specified and actual concrete strength, deformation of void forms in hollow girders, debonding and transfer length, thermal gradient effects and others. A detailed method and an approximate method for predicting camber that both utilize adjustments to account for the production factors are proposed. The detailed method uses time-dependent losses calculations and creep factors to predict camber, while the approximate method uses multipliers. The current NCDOT method and the proposed methods are analyzed and compared using an extensive database of field measurements. The proposed methods are shown to provide significant improvements to the camber predictions in comparison to the current NCDOT method. Recommendations for design and production practices are provided.

Predicting Prestress Losses, Camber, and Deflection in Prestressed Concrete Members

by
Tyler Keith Storm

A thesis submitted to the Graduate Faculty of
North Carolina State University
in partial fulfillment of the
requirements for the Degree of
Master of Science

Civil Engineering

Raleigh, North Carolina

2011

APPROVED BY:

_____	_____
Dr. Paul Zia	Dr. James Nau

_____
Dr. Sami Rizkalla
Chair of Advisory Committee

DEDICATION

To my family, for their patience and love.

BIOGRAPHY

Tyler Keith Storm was born December 4, 1986 in Kinston, North Carolina. He attended high school in Duplin County in North Carolina before pursuing undergraduate and then graduate studies in Civil Engineering at North Carolina State University. His interests are science, philosophy, and art. He also enjoys travel and sports.

ACKNOWLEDGEMENTS

I would like to first thank the members of my advisory committee, Dr. Sami Rizkalla, Dr. Paul Zia, and Dr. James Nau, for their guidance and direction during my studies. It has certainly been an honor and a pleasure to study under all of them.

I would also like to thank all of the students and staff at the Constructed Facilities Laboratory for their help and encouragement throughout my studies and research.

Sincere thanks are owed to the NCDOT steering committee who oversaw this project for their input and critical review. The steering committee includes the following members:

Brian Hanks, P.E. (Chair)
Kevin Bowen, P.E.
Victor Chao, P.E.
Aaron Earwood, P.E.
David Greene, P.E.
Gichuru Muchane, P.E.
Trudy Mullins
Rick Nelson, P.E.
Greg Perfetti, P.E.
Michael Robinson, P.E.
Moy Biswas, Ph.D., P.E.
Tom Drda, P.E.
Chris Peoples, P.E.
Neal Galehouse, P.E.
Dan Holderman, P.E.

A special thanks is owed to Trudy Mullins of the NCDOT Materials and Tests Unit for her assistance in collecting design and field data. She also acted as the primary liaison between the research team and the NCDOT inspectors and Resident Engineers.

The inspectors and Resident Engineers themselves were also invaluable to this project, as they performed the vast majority of the camber measurements.

A special thanks is also owed to Victor Chao and Gichuru Muchane of the NCDOT Structure Design Unit for their collaboration during the course of this research.

Thanks are owed to the management and staff of the following precast producers for accommodating the needs of this research:

Atlantic Wood Metrocast - Portsmouth, VA
Eastern Vault Company - Princeton, WV
Florence Concrete Producers - Sumter, SC
Prestress of the Carolinas - Charlotte, NC
Ross Prestress Concrete - Bristol, TN
S&G Prestress Concrete - Wilmington, NC
Standard Concrete Products - Atlanta, GA
Standard Concrete Products - Savannah, GA
Utility Precast - Concord, NC

TABLE OF CONTENTS

LIST OF TABLES

LIST OF FIGURES

LIST OF SYMBOLS

$95\%\ upper$ upper bound of the range that contains 95% of the data based on normal distribution

$95\%\ lower$ lower bound of the range that contains 95% of the data based on normal distribution

a factor to account for curing method and cement type

A_c area of section calculated using the gross composite concrete section properties of the girder and the deck and the deck-to-girder modular ratio

A_d area of composite deck concrete

A_g area of the gross section

A_{ps} total cross-sectional area of steel of all prestressing strands

$A_{ps,str}$ cross-sectional area of steel of a single prestressing strand

b factor to account for curing method and cement type

d depth of section

D_{ps} nominal diameter of prestressing strand

e eccentricity of prestressing force with respect to centroid of gross section, calculated at midspan (same as e_m)

e_d eccentricity of deck with respect to gross composite section

e_e eccentricity of prestressing force with respect to centroid of gross section, calculated at end of member

e_m eccentricity of prestressing force with respect to centroid of gross section, calculated at midspan (same as e)

e_{pc} eccentricity of prestressing force with respect to centroid of the composite section

E_c elastic modulus of concrete at 28 days

E_{cd} elastic modulus of deck concrete

E_{ci} elastic modulus of concrete at prestress transfer

E_p elastic modulus of prestressing strands

f_{cds} stress in concrete at level of strands due to superimposed dead loads applied after transfer; same as Δf_{cdp}

f_{cgp} stress in concrete at the level of the centroid of the prestressing steel due to self-weight and the prestressing force immediately after transfer

f'_c specified strength of concrete at 28 days

f'_{ci} specified strength of concrete at prestress transfer

f'_{c1} specified strength of concrete at time t_1

f^*_c estimated concrete strength at 28 days

f^*_{ci} estimated concrete strength at prestress transfer

f_{pi} stress in prestressing strands immediately after prestress transfer

f_{pj} jacking stress of prestressing strands; stress in strands before prestress transfer

f_{pu} ultimate stress of prestressing strands

f_{py} yield stress of prestressing strands

H average annual relative humidity (%)

I_c moment of inertia of section calculated using the gross composite concrete section properties of the girder and the deck and the deck-to-girder modular ratio

I_g moment of inertia of gross section

k_f factor for the effect of concrete strength

k_{hc} humidity factor for creep

k_{hs} humidity factor for shrinkage

k_s factor for the effect of the volume-to-surface area ratio of the member

k_{td} time-development factor

K_1 local aggregate adjustment factor for elastic modulus of concrete

K_{df} time-development factor for the time period between deck placement and final time

K_{id} transformed section coefficient that accounts for time-dependent interaction between concrete and bonded steel in the section being considered for the time period between transfer and deck placement

K_L factor for the type of prestressing steel used; to be taken as 30 for low-relaxation strands and 7 for other prestressing steel

L length of member

L_{db} average length of debonding at each end of the girder for debonded strands

L_m length of member

L_s length of span, from center to center of supports

L_t transfer length of prestressing strands

$M_{diaphragm}$ moment at midspan due to internal diaphragms of hollow girders

M_g moment at midspan due to girder self-weight

M_{sd} moment due to superimposed permanent loads

n_{str} number of prestressing strands in the girder

P total prestressing force

P_{28} total prestressing force at 28 days

P_{365} total prestressing force at 365 days

P_i total prestressing force immediately after transfer. (In the PCI Design Handbook: the initial prestressing force before transfer, after anchorage seating loss.)

P_j jacking force of the prestressing strands; prestress force prior to transfer

$P_{j,str}$ prestress force in a single strand prior to transfer

$(Pe)_{max}$ maximum girder moment due to prestressing only

t time

t_d time of deck placement, or time of girder erection for members without composite decks

t_f final time, typically taken as five years or 1825 days

t_i initial time (age of concrete at transfer)

V/S volume-to-surface area ratio of gross section; for members with poorly ventilated internal voids (such as box beams and cored slabs), only half the internal surface area should be included

w_c unit weight of concrete, by volume

w_g distributed load due to girder self-weight

w_{sd} distributed load due to superimposed dead loads

x_h distance from midspan to hold-down points of harped strands

y_c distance from the centroid of the gross section to the extreme bottom fibers of the section

y_{pse} distance from centroid of prestressing steel to extreme bottom fibers of the section, calculated at the end of the member

y_{psm} distance from centroid of prestressing steel to extreme bottom fibers of the section calculated at midspan

Δ net camber (positive upward)

$\Delta_{diaphragm}$ deflection due to internal diaphragms in hollow girders (positive downward)

Δ_{28} net camber at 28 days (positive upward)

Δ_{365} net camber at one year (365 days) (positive upward)

Δ_{ps} camber due to prestressing only (positive upward)

Δ_{sw} deflection due to girder self-weight (positive downward)

Δ_{cr} camber due to creep (positive upward)

Δ_{net} net camber (positive upward)

Δ_{sd} deflection due to superimposed dead load (positive downward)

Δ_T deflection due to thermal effects

Δf_{cd} change in concrete stress at the centroid of the strands due to long term losses between transfer and deck placement, combined with deck weight and superimposed loads

Δf_{cdf} change in concrete stress at the centroid of prestressing strands due to shrinkage of deck concrete

Δf_{cdp} change in concrete stress at center of gravity of prestressing steel due to permanent loads, with the exception of the load acting at the time the prestressing force is applied. Should be calculated at the same section or sections for which f_{cgp} is calculated.

Δf_p change in prestress

Δf_{pCR} loss of prestress due to creep

Δf_{pES}	loss of prestress due to elastic shortening
Δf_{pRE}	loss of prestress due to relaxation of prestressing steel
Δf_{pR1}	loss of prestress due to relaxation of prestressing steel before transfer
Δf_{pR2}	loss of prestress due to relaxation of prestressing steel after transfer
Δf_{pSD}	loss of prestress due to concrete shrinkage occurring after deck placement
Δf_{pSR}	loss of prestress due to concrete shrinkage
Δf_{pSS}	gain of prestress due to shrinkage of deck concrete
Δf_{pTL}	total prestress losses
ΔT	change in temperature
ε_{bdf}	shrinkage strain of the girder between deck placement and the final time
ε_{bid}	shrinkage strain of the girder between transfer and deck placement
ε_{ddf}	shrinkage strain of the deck concrete between deck placement and the final time
$\Psi(t_2, t_1)$	creep coefficient for the period between time t_1 and t_2
σ	standard deviation
μ	statistical mean
μ_c	coefficient of thermal expansion for concrete
μ_p	coefficient of thermal expansion for prestressing strands

LIST OF ABBREVIATIONS

AASHTO	American Association of State Highway and Transportation Officials
AASHTO 2004	AASHTO LRFD Bridge Design Specifications, 3rd Edition (2004)
AASHTO 2010	AASHTO LRFD Bridge Design Specifications, 5th Edition (2010)
ACI	American Concrete Institute
BB	box beam bridge girder
CS	cored slab bridge girder
EPS	expanded polystyrene, a foam material used to form the voids in box beams
LRFD	load and resistance factor design
MBT	modified bulb-tee bridge girder
NCDOT	North Carolina Department of Transportation
PCI	Precast/Prestressed Concrete Institute
Type III	AASHTO Type III bridge girder
Type IV	AASHTO Type IV bridge girder

1 INTRODUCTION

1.1 Background

Loss of prestress is a basic time-dependent characteristic of prestressed concrete. For pretensioned concrete, the magnitude of the prestress loss depends on the elastic and time-dependent properties of concrete, including elastic modulus, creep and shrinkage, as well as the relaxation characteristics of the prestressing steel. The prestress loss and creep in turn affect the camber of prestressed girders. The prediction of prestress losses and camber has been a subject of study by many investigators for nearly half a century since they directly affect the structural response and performance of prestressed concrete girders.

In recent years, NCDOT has experienced an increasing occurrence of problems resulting from discrepancies between predicted camber and actual camber of girders in the field. The most significant issues are overestimation of camber for box beams and cored slabs and differential camber among adjacent girders. Similar problems have also been experienced by other state transportation agencies as Chapter 2 discusses.

Problems caused by inaccurate camber predictions can be significant. For example, overestimation of camber can result in the need for additional deck concrete or asphalt in order to achieve the desired grade. This raises construction costs and increases the dead load acting on the bridge. In addition, differential camber between adjacent girders can cause construction problems in the field that can be difficult or impossible to overcome.

Currently, the camber predictions used by NCDOT engineers use a simplified multiplier method based on a paper by Leslie Martin published over 30 years ago (Martin, 1977). With the increasing use of newer types of prestressed concrete bridge girders, such as modified bulb-tees, box beams and cored slabs, this method seems to be inadequate. In addition, this method does not utilize detailed prestress loss predictions, instead relying on simplifying assumptions regarding the magnitude of prestress losses.

NCDOT engineers currently use the “refined” method specified in the *2004 AASHTO LRFD Bridge Design Specifications* for prediction of prestress losses. However, these specifications are now superseded the *2005-2006 Interim Revisions*, in which the loss predictions have become significantly more detailed. While earlier versions of the

specifications only provided estimates of the total losses, recent versions provide time-dependent estimates of the long-term losses. Since time-dependent estimates could provide improved camber predictions, this research focuses on evaluating the effectiveness of the current simplified prediction method, introducing possible modifications to improve the predictions, and recommending alternative prediction methods that utilize the time-dependent losses.

1.2 Research Objective and Scope

The objective of this research is to evaluate and improve the current NCDOT method for predicting camber and prestress losses for pretensioned prestressed concrete bridge girders with particular emphasis on the camber at the time of prestress transfer and at the time of girder erection. To accomplish this objective, the following tasks were pursued:

1) Review the method currently used by NCDOT to predict prestress losses and camber.
2) Review other methods for predicting prestress losses and camber.
3) Develop a camber prediction method that will utilize detailed prestress loss predictions.
4) Develop an extensive database of field measurements that includes camber data for various girder types and sizes.
5) Conduct site visits to prestressing plants to identify factors relating to production that could potentially impact prestress losses and camber.
6) Evaluate the effects of the production factors, and include adjustments for these factors in the prediction models for prestress losses and camber.
7) Evaluate and compare the prediction methods by utilizing the field measurements.
8) Propose a “refined” camber prediction method that utilizes detailed prestress losses predictions, as well as an “approximate” method that is suitable for simple hand calculations.

2 REVIEW OF LITERATURE

2.1 Introduction

Typically, the effect of the prestressing force, combined with the girder self-weight, causes a net upward deflection at the midspan of a precast prestressed girder before superimposed dead and live loads are applied. This upward deflection, or camber, helps to reduce the final downward deflection of the girder when the full service loads are in place. Prediction of camber and deflection is therefore an important design issue

The ability to predict camber accurately is critical for the design and construction of bridges. However, this is a complex task, since the camber is dependent on many variables, some of which are interdependent and change over time. Four of the most significant variables are the properties of the concrete, the creep of the concrete, concrete temperature, and the magnitude and location of the prestressing force. This chapter presents a brief review of research in the literature related to these factors and to the prediction of camber in general. It also provides a summary of the responses to a questionnaire that was sent by the research team to other state departments of transportation to learn about their experiences with camber prediction.

2.2 Concrete Properties

Since prestressed concrete bridge girders are usually designed in a manner that eliminates flexural cracking under service loads, elastic theory is typically used to predict camber and deflection. A key component of the various elastic deflection formulas is the elastic modulus of the concrete. One of the most prevalent models for predicting elastic modulus has been the following equation specified by the 2004 edition of the AASHTO LRFD Bridge Design Specifications (AASHTO, 2004):

$$E_c = 33000 w_c^{1.5} \sqrt{f_c'} \qquad 2\text{-}1$$

where:

$E_c =$ elastic modulus of concrete (ksi)

$w_c =$ unit weight of concrete (kcf)

$f_c' =$ specified concrete compressive strength (ksi)

However, several studies have revealed potential sources of error with this approach. Kelly et al. (1987) noted that the actual concrete compressive strength is often much higher than the specified strength. Based on a study of eight prestressed concrete girders with specified 28-day strengths of 6500 psi, they found that the average measured 28-day strength was approximately 9300 psi, which is more than 40% higher than the specified strength. This discrepancy results in a higher elastic modulus than predicted using the specified strength, consequently reducing the measured camber compared to the predicted value. Tadros et al. (2003) showed that the stiffness of the coarse aggregate used in the concrete, which typically varies with the aggregate source, can introduce significant errors when estimating elastic modulus. They recommended using introducing an aggregate adjustment factor, K_1, to account for the aggregate stiffness. This recommendation was subsequently adopted in the AASHTO specifications, beginning with the 2005-2006 Interim Revisions (AASHTO, 2006). Tadros et al. also observed that the elastic modulus measurements exhibited significant scatter even though the mix proportions were tightly controlled, suggesting that the elastic modulus and camber of prestressed girders will always have some inherent variability. They also noted that although it is typically assumed by the designer that the prestressing will be applied to the girders one day after casting, it is common in practice to allow girders to cure over the weekend, applying the prestressing after three days. This is sufficient time for the elastic modulus of the concrete at an early age to develop to a higher value than the value predicted for the time of prestress transfer, resulting in poor estimation of camber at this stage.

The compressive strength of the concrete, in addition to impacting the elastic modulus of the concrete, is also related to other factors affecting camber, such as creep and prestress losses. Bruce et al. (2001) showed that a potential source of error when predicting these factors is caused by a measured difference between the compressive strength of the concrete cylinders cured with the member and the strength of the concrete within the girder itself due to the higher curing temperatures within the more massive girder. By keeping the temperature of several cylinders the same as the temperature of the girder concrete using an

embedded thermocouple, they showed that the strength of the temperature-controlled cylinders was as much as 10% greater than the cylinders that were cured with the girder but without the thermocouple. This could lead to a greater than expected discrepancy between the specified and actual concrete strength at prestress transfer, resulting in poor predictions of elastic modulus and camber.

2.3 Creep of Concrete

Creep is a time-dependent deformation of concrete under sustained loading. The rate of creep controls the time-dependent growth of camber in bridge girders. Although creep of normal strength concrete has been extensively studied by many researchers over the years, the increasing popularity of high-strength concrete for prestressed girders in recent years has prompted new studies to analyze the creep effect for high-strength concrete.

The creep coefficient is defined as the percent increase in the initial strain over a given time due to sustained loading. Since the calculation for the creep coefficient specified by the AASHTO LRFD Bridge Design Specifications prior to 2005 was developed for girders with concrete strengths in the range of 4 to 5 ksi, Tadros et al. (2003) proposed adjusting the calculation to account for concrete strengths up to 15 ksi. Based on dozens of high-strength concrete cylinder tests, it was shown that the new creep predictions provided results that averaged 98% of the measured values, while the pre-2005 AASHTO method produced results that averaged 174% of the measured values. AASHTO implemented the recommended equation beginning with the 2005-2006 Interim Revisions to the specifications (AASHTO, 2006).

In addition to being related to the concrete strength, the creep is also a function of the volume-to-surface ratio of the girder, the ambient humidity, and the age of the concrete at which loading is applied.

2.4 Prestressing Force

The prestressing force is of critical importance when predicting camber. Due to various factors, the prestressing force tends to decrease after initial stressing. These prestress losses consist of instantaneous and time-dependent losses. The instantaneous loss of prestress is due

to elastic shortening of the girder at the level of the prestressing strands upon initial application of the prestressing. Time-dependent losses are due to creep, concrete shrinkage caused by drying, and relaxation of the prestressing strands. Based on the work of Zia et al. (1979), the Precast/Prestressed Concrete Institute adopted a set of simple equations to predict the prestress losses due to each of these sources. This was an improvement over the prior predictions, which required either substantial analytical analysis or calculation of a somewhat inaccurate lump-sum value. They showed that the proposed equations, which are still specified by PCI today, produced results similar to those predicted by detailed analytical methods (PCI, 2004).

Prior to 2005, the AASHTO LRFD Bridge Design Specifications also recommended simple equations for prestress losses. However, Tadros et al. (2003) showed that these calculations are not well-suited for high-strength concrete girders. Based on detailed measurements of seven bridge girders of various designs, it was shown that the pre-2005 AASHTO equations overestimated prestress losses by an average of 60%. One of the primary shortcomings of the AASHTO equations was that only the ultimate losses were calculated, rather than the time-dependent losses at various time intervals. Tadros et al. proposed equations to calculate the losses with respect to time and included adjustments to account for high-strength concrete. It was shown that these predictions as well as the PCI predictions were significantly more accurate for predicting prestress losses for high-strength girders than the pre-2005 AASHTO methods. The recommended equations were subsequently adopted by the AASHTO specifications beginning with the 2005-2006 Interim Revisions (AASHTO, 2006). A study by Byle et al. (1997) also showed that the pre-2005 AASHTO method overestimated losses for twelve girders constructed with high-strength concrete, although the margin was only 8%. They recommended an alternate set of time-dependent equations for prestress losses.

Another factor that can affect the prestressing force is thermal expansion of the prestressing strands caused by differential temperatures prior to prestress transfer. Bruce et al. (2001) showed that hydration-induced temperature increases in the concrete during curing can raise the temperature of the strands, resulting in a reduction of the prestress force by as much as 11% due to thermal expansion. However, since the concrete likely bonded with the

steel within six to eight hours after casting, a portion of the force would be regained upon cooling, and the final loss of prestress due to this effect was estimated to be approximately 6%.

2.5 Thermal Gradient Effect

As noted by Tadros et al. (2011), thermal gradients can develop through the depth of the girder due to differential cooling after curing or due to solar effects. This gradient can temporarily induce additional camber or deflection of the girder, thereby introducing scatter into the camber measurements. Byle et al. (1997) estimated that thermal gradient effects could produce deflections of approximately 1/2" for the U-girders that they studied, which were in the range of 115 to 145 feet in length.

2.6 Prediction of Camber

Prediction of camber is inherently imprecise due to variability of the concrete properties, differential shrinkage in composite sections, variation of when prestress transfer occurs, and many other factors (Martin, 1977). Because of the uncertainty in camber prediction, Martin developed a simple method to predict camber based on multiplying the predicted elastic camber and deflection at prestress transfer by standard factors to estimate the camber at later stages due to creep. This method is still being used by the PCI Design Handbook, and is one of the most commonly used methods for predicting camber. Ahlborn et al. (1995) tested two full-size composite I-girders constructed with high-strength concrete and measured the camber at various ages. The PCI method predicted camber reasonably well for one of the girders, which contained a limestone coarse aggregate, but overestimated camber by 40% for the other girder, which contained a glacial gravel.

Other methods for predicting camber include the incremental time-steps method and the approximate time-steps method (ACI Committee 435, 1995). The incremental time-steps method requires calculation of creep strains, shrinkage strains, and prestressing forces at numerous intervals, and is therefore typically only justified for very long spans or segmental bridge structures. Stallings et al. (2001) tested five AASHTO BT54 bulb-tee girders constructed with high-strength concrete with an average 28-day strength of 10 ksi. Based on

the camber measurements, the PCI multiplier method significantly overestimated the camber at the time of girder erection. The approximate time-steps method and the incremental time-steps method predicted camber reasonably well.

Although several methods for predicting camber exist, most studies show significant scatter in the camber measurements. Kelly et al. (1987) noted that the camber for eight identical AASHTO Type IV girders that were 127 feet in length varied from 2 to 6 inches at the time of prestress transfer.

A detailed summary of the existing methods for predicting prestress losses and camber that are considered in this report is provided in Chapter 3.

2.7 Camber Experiences of Other States

A brief questionnaire was sent to bridge design engineers at the Nebraska Division of Roads (NDOR), the Texas Department of Transportation (TXDOT), and the Florida Department of Transportation (FDOT). These questionnaires were designed to explore the methods used by these states to predict prestress losses and camber. They also requested information about any problems experienced with the prediction of camber. This section provides a summary of the responses. The full text of the responses are provided in Appendix C.

2.7.1 Nebraska Division of Roads (NDOR)

NDOR uses both the "approximate method" and the "refined method" of the *2004 AASHTO LRFD Bridge Design Specifications* to estimate prestress losses. In their experience, both give approximately the same prediction of camber at the time of the erection of the bridge, which is assumed to be 30 days after casting.

NDOR has observed that the camber predictions are often higher than the measured values, particularly for very long spans (over 150 feet) when the specified concrete strength exceeds 10 ksi.

2.7.2 Texas Department of Transportation (TXDOT)

TXDOT typically uses the "refined method" of the *2004 AASHTO LRFD Bridge Design Specifications* to estimate prestress losses. To predict camber, they use a single set of assumed creep values for all girders.

In contrast with NDOR, TXDOT has observed that their camber predictions are often significantly lower than the measured values for long span girders. In rare cases, the girders had to be re-cast. In addition, TXDOT has observed that girders cast at the same time will often have different cambers on the bridge if the project phasing requires that some girders remain in storage in the casting yard longer than others. They observed that these differential camber problems are most problematic with box beam girders since these are placed immediately adjacent to each other on the bridge.

2.7.3 Florida Department of Transportation (FDOT)

FDOT uses the AASHTO equation (Equation 2-1) to calculate the elastic modulus of concrete. They use the specified concrete strength and a concrete unit weight of 145 pcf. For concrete made with coarse aggregate native to Florida, which is typically limestone, the elastic modulus is factored by 0.9.

FDOT estimates prestress losses using the refined calculations specified by the 2004 AASHTO LRFD Bridge Design Specifications. Camber is calculated using either the PCI multiplier method or the approximate time-step method. FDOT engineers have not experienced persistent problems with camber prediction using either method, although construction difficulties related to camber occasionally occur.

Problems related to camber prediction are prevented to some extent by FDOT's practice of requiring that the contractor measure the camber of the girders before setting the seat elevations on the bridge bents.[1]

[1] The fact of this practice was related to the researchers in a private communication.

3 EXISTING PREDICTION METHODS

3.1 Introduction

There are several methods in the literature and in various codes normally used to predict prestress losses and camber for prestressed concrete girders. The current NCDOT method, the PCI method, and the AASHTO 2010 method are presented in this chapter, although it should be noted that the AASHTO 2010 method predicts only prestress losses.

Throughout this report, some of the symbols have been altered from those of the source materials for the purposes of uniformity and comparison. The symbols used here are consistent with the definitions in the "List of Symbols" provided in this report.

In addition, the equations presented here pertain only to pretensioned girders using normal-weight concrete and low-relaxation strands with a nominal strength of 270 ksi. The calculations and assumptions may differ for other applications.

3.2 Prestress Losses

The three existing methods for predicting prestress losses considered in this study are the current NCDOT method, the method specified by the Precast and Prestressed Concrete Institute (the PCI method), and the "refined" method specified in the *2010 AASHTO LRFD Bridge Design Specifications* (the AASHTO 2010 method).

All of the prediction methods provide estimates of the instantaneous loss that occurs at transfer of prestressing due to elastic shortening, as well as estimates of the time-dependent losses including concrete shrinkage, creep, and strand relaxation. However, a fundamental difference between the three methods is that the AASHTO 2010 method provides estimates of the time-dependent losses as functions of time, while the NCDOT method and the PCI method provide estimates of only the ultimate time-dependent losses.

3.2.1 Current NCDOT Method

The current NCDOT method for predicting prestress losses is based on the "refined" method specified in the *2004 AASHTO LRFD Bridge Design Specifications*. In this method,

the predictions of the time-dependent losses are not expressed as functions of time. Rather, they are estimates of the ultimate time-dependent losses only.

3.2.1.1 Total Prestress Loss

The total prestress loss is determined by combining the effects of elastic shortening, concrete shrinkage, creep, and strand relaxation, as follows:

$$\Delta f_{pTL} = \Delta f_{pES} + \Delta f_{pSR} + \Delta f_{pCR} + \Delta f_{R2} \quad \text{3-1}$$

where:

$\Delta f_{pES} =$ elastic shortening loss

$\Delta f_{pSR} =$ total shrinkage loss

$\Delta f_{pCR} =$ total creep loss

$\Delta f_{R2} =$ total relaxation loss after prestress transfer

Although some strand relaxation occurs prior to transfer of the prestressing force, it is commonly accepted that the producer will compensate for this loss by overstressing the strands. Therefore, only the relaxation loss that occurs after transfer is included in the total losses.

3.2.1.2 Elastic Shortening Loss

Elastic shortening loss occurs instantaneously at the time of prestress transfer as a result of the shortening of the girder caused by the application of the prestressing force. This prestress loss is estimated as the product of the stress applied to the concrete at the level of the centroid of the strands and the modular ratio, as follows:

$$\Delta f_{pES} = \frac{E_p}{E_{ci}} f_{cgp} \quad \text{3-2}$$

where:

$E_p =$ elastic modulus of the prestressing strands

$E_{ci} =$ elastic modulus of the girder concrete at transfer

$f_{cgp} =$ stress in the concrete at the level of the centroid of the prestressing strands immediately after transfer due to prestressing and girder self-weight

$$= \left(\frac{P_i}{A_g} + \frac{P_i e^2}{I_g}\right) - \frac{M_g e}{I_g}$$

$P_i =$ total prestressing force immediately after transfer

$e =$ eccentricity of the centroid of the prestressing strands at midspan with respect to the centroid of the girder

$A_g =$ area of the gross cross-section of the girder

$I_g =$ moment of inertia of the gross cross-section of the girder

$M_g =$ moment at midspan due to girder self-weight, assuming simply supported conditions

$$= \frac{w_g L^2}{8}$$

$w_g =$ uniformly distributed load due to girder self-weight

$L =$ girder length

Since the initial prestressing force after transfer, P_i, depends on the elastic shortening loss, this calculation is iterative. On the first iteration, the initial prestressing force after transfer is assumed to be 90% of the specified jacking force. After computing the elastic shortening loss, the prestressing force after transfer is determined for the second iteration by reducing the specified jacking stress by the calculated loss. This process is then repeated until convergence occurs.

3.2.1.3 Shrinkage Loss

Shrinkage loss occurs gradually as a result of the shortening of the girder caused by the drying shrinkage of the concrete. It is determined as follows:

$$\Delta f_{pSR} = 17.0 - 0.150H \ \ (ksi) \qquad 3\text{-}3$$

where:

$H =$ average annual ambient relative humidity (%). Typically taken as 70 for North Carolina per Figure 5.4.2.3.3-1 of AASHTO 2004.

3.2.1.4 Creep Loss

Creep is the time-dependent deformation of the girder concrete caused by sustained stresses due to prestressing, self-weight, and superimposed dead loads. Prestress loss occurs due to the shortening of the girder at the level of the centroid of the strands. In this method, the creep loss is considered to be proportional to the applied stresses. Since the superimposed dead loads are typically applied at a later time than are the prestressing force and self-weight, the stress due to the superimposed dead loads is considered to impact creep less significantly than the other loads. This fact is accounted for in the following equation by the two different coefficients of 12.0 and 7.0:

$$\Delta f_{pCR} = 12.0 f_{cgp} - 7.0 f_{cds} \geq 0 \qquad 3\text{-}4$$

where:

$f_{cds} =$ concrete stress at the level of the centroid of the strands due to superimposed dead loads applied after transfer.

$$= \frac{M_{sd} e}{I_g} \qquad 3\text{-}5$$

$M_{sd} =$ midspan moment due to superimposed dead loads.

3.2.1.5 Relaxation Loss

Under the sustained loading of the prestressing force, the strand steel gradually relaxes. The resulting reduction in prestress is the relaxation loss. This method divides the relaxation loss calculations into two parts, including the loss before transfer and the loss after transfer.

Before Transfer

The relaxation loss that occurs between initial stressing and prestress transfer is estimated as follows:

$$\Delta f_{pR1} = \frac{\log(24.0t)}{40.0}\left[\frac{f_{pj}}{f_{py}} - 0.55\right] f_{pj} \qquad 3\text{-}6$$

where:

$t =$ time (days) between stressing and transfer. Typically assumed to be 2 days.

$f_{py} =$ specified yield strength of the prestressing strands. Taken as 90% of the nominal strength for low relaxation strands.

$f_{pj} =$ stress in the strand after jacking. Taken as 75% of the nominal strength.

After Transfer

The relaxation loss that occurs after transfer accounts for the interaction with the other components of losses, and is estimated for low relaxation strands as follows:

$$\Delta f_{pR2} = 0.30\left[20.0 - 0.4\Delta f_{pES} - 0.2\left(\Delta f_{pSR} + \Delta f_{pCR}\right)\right] \ (ksi) \qquad 3\text{-}7$$

3.2.2 PCI Method

The method recommended by the Precast and Prestressed Concrete Institute for estimating prestress losses is similar to the current NCDOT method in that it only estimates the ultimate time-dependent losses rather than time-specific values. However, the prediction equations themselves are different.

3.2.2.1 Total Losses

The total prestress loss is the summation of the losses due to elastic shortening, shrinkage, creep, and relaxation, as follows:

$$\Delta f_{pTL} = \Delta f_{pES} + \Delta f_{pSR} + \Delta f_{pCR} + \Delta f_{RE} \qquad 3\text{-}8$$

3.2.2.2 Elastic Shortening

The elastic shortening loss is determined using the same equation used in the NCDOT method, as follows:

$$\Delta f_{pES} = \frac{E_p}{E_{ci}} f_{cgp} \quad \text{3-9}$$

Unlike the NCDOT method, however, this method does not compute the loss iteratively. It is instead determined by applying a reduction factor of 0.9 to the specified jacking force as follows:

$$f_{cgp} = \left[\frac{0.9P_j}{A_g} + \frac{0.9P_j e^2}{I_g}\right] - \frac{M_g e}{I_g} \quad \text{3-10}$$

where:

$P_j =$ specified jacking force; taken as 75% of the nominal strength multiplied by the total strand area for 270 ksi low-relaxation strands

The factor of 0.9 is used to approximate the prestressing force after elastic shortening by assuming that the elastic shortening is ten percent of the jacking force. This is similar to the first iteration of the NCDOT prediction. However, the calculation is not iterative for this method as it is for the NCDOT method.

3.2.2.3 Shrinkage Loss

This method accounts for the average annual ambient humidity and the volume-to-surface area ratio of the girder. Girders with high volume-to-surface area ratios experience less shrinkage, and vice versa. The shrinkage loss is estimated as follows:

$$\Delta f_{pSR} = (8.2x10^{-6}) E_p \left(1 - 0.06\frac{V}{S}\right)(100 - H) \quad \text{3-11}$$

where:

$\frac{V}{S} =$ volume-to-surface area ratio of the girder.

3.2.2.4 Creep Loss

In the following equation, creep loss is proportional to the applied stresses. However, unlike the NCDOT method, this method proportions the stresses due to prestressing and the stresses due to superimposed dead loads equally using the same creep factor of 2.0 for both, as follows:

$$\Delta f_{pCR} = 2.0 \frac{E_p}{E_c}\left(f_{cgp} - f_{cds}\right) \quad \text{3-12}$$

3.2.2.5 Relaxation Loss

In the following equation for relaxation loss, each loss is treated equally, regardless of when it occurs. This differs from the NCDOT method, in which the elastic shortening loss is given greater influence due to its instant application at transfer.

$$\Delta f_{pRE} = \left(5000 - 0.040\left(\Delta f_{pSR} + \Delta f_{pCR} + \Delta f_{pES}\right)\right) \quad \text{3-13}$$

3.2.3 AASHTO 2010 Method

Unlike the previous two methods, the method specified in the *2010 AASHTO LRFD Bridge Design Specifications* can be used to estimate prestress losses at any time. In addition, the predictions of the time-dependent losses are calculated in two parts—the losses occurring before deck placement and those occurring after deck placement.

The calculations for this method are more detailed than are those for the NCDOT and PCI methods. One major reason is that the creep loss and shrinkage loss calculations also require the calculation of creep coefficients and shrinkage strains. This method also includes provisions to account for the effects of composite deck systems.

Since the creep coefficients and shrinkage strains are used in multiple equations in the losses calculations, they are presented first, followed by the predictions of the losses.

3.2.3.1 Creep Coefficient

The general form of the equation for the creep coefficient at a time t_2 is as follows:

$$\Psi(t_2, t_1) = 1.9 k_s k_{hc} k_f k_{td} t_1^{-0.118} \quad \text{3-14}$$

where:

$k_s =$ factor to account for the effect of the volume-to-surface area ratio

$$= 1.45 - 0.13\frac{V}{S} \geq 0 \quad \text{3-15}$$

$k_{hc} =$ humidity factor for creep

$$= 1.56 - 0.008H \quad \text{3-16}$$

$k_f =$ factor for the effect of concrete strength

$$= \frac{5}{1 + f'_{ci}} \quad \text{3-17}$$

$k_{td} =$ time development factor

$$= \frac{t_2 - t_1}{61 - 4f'_{ci} + (t_2 - t_1)} \quad \text{3-18}$$

$t_1 =$ age of concrete at time of loading for creep calculations or at time of prestress transfer for shrinkage calculations (days)

$t_2 =$ age of concrete at time of consideration of creep or shrinkage effects (days)

$f'_{ci} =$ specified compressive strength of concrete at time of prestressing (ksi)

The creep coefficient for the period between times t_2 and t_3 due to loading applied at time t_1 is determined as follows:

$$\Psi(t_3, t_2) = \Psi(t_3, t_1) - \Psi(t_2, t_1) \quad \text{3-19}$$

where:

$\Psi(t_3, t_1) =$ creep coefficient at time t_3 due to loading applied at time t_1 per equation 3-14

$\Psi(t_2, t_1) =$ creep coefficient at time t_2 due to loading applied at time t_1 per equation 3-14

3.2.3.2 Shrinkage Strain

The concrete shrinkage strain is determined by applying various factors to a base shrinkage strain of 0.48×10^{-3}. The factors account for the effects of concrete strength, ambient humidity, volume-to-surface area ratio, and time. The general form of the equation for shrinkage strain ε_{sh} is as follows:

$$\varepsilon_{sh} = k_s k_{hs} k_f k_{td} 0.48x10^{-3} \quad 3\text{-}20$$

where:

$k_{hs} =$ humidity factor for shrinkage

$$= 2.00 - 0.014H \quad 3\text{-}21$$

$k_{td} =$ time development factor

$$= \frac{t}{61 - 4f'_{ci} + t} \quad 3\text{-}22$$

$t =$ time between prestress transfer and time under consideration for shrinkage effects (days)

3.2.3.3 Total Prestress Loss

The total prestress loss is the summation of all of the losses:

$$\Delta f_{pTL} = \Delta f_{pES} + \left(\Delta f_{pSR} + \Delta f_{pCR} + \Delta f_{R1}\right)_{id} + \quad 3\text{-}23$$

$$\left(\Delta f_{pSD} + \Delta f_{pCD} + \Delta f_{pR2} - \Delta f_{pSS}\right)_{df}$$

where:

$(\Delta f_{pSR} + \Delta f_{pCR} + \Delta f_{R1})_{id} =$ summation of the time-dependent losses between the time of prestress transfer and the time of deck placement

$(\Delta f_{pSD} + \Delta f_{pCD} + \Delta f_{pR2} - \Delta f_{pSS})_{df} =$ summation of the time-dependent losses occurring after deck placement

3.2.3.4 Elastic Shortening

The elastic shortening loss is determined using the same procedure as described by the NCDOT method (equation 3-2).

3.2.3.5 Shrinkage Loss

The time-dependent shrinkage loss is calculated in two steps, including the loss occurring prior to deck placement and the loss occurring after deck placement. The times can be adjusted to predict the loss at any time.

Prior to Deck Placement

The shrinkage loss that occurs prior to deck placement is determined by first calculating the concrete shrinkage strain at the time of deck placement. This strain is then converted into prestress loss using the elastic modulus of the strands. Finally, a time-development factor is used to account for the time-dependent interaction between the concrete and the bonded steel. The shrinkage loss is determined as follows:

$$\Delta f_{pSR} = \varepsilon_{bid} E_p K_{id} \qquad 3\text{-}24$$

where:

$\varepsilon_{bid} =$ concrete shrinkage strain at time of deck placement per equation 3-20.

$K_{id} =$ transformed section coefficient that accounts for time-dependent interaction between concrete and bonded steel in the section being considered for the time period between transfer and deck placement

$$= \frac{1}{1 + \frac{E_p A_{ps}}{E_{ci} A_g}\left(1 + \frac{A_g e^2}{I_g}\right)\left(1 + 0.7\Psi\left(t_f, t_i\right)\right)} \quad \text{3-25}$$

$A_{ps} =$ total area of the prestressing strands

$\Psi\left(t_f, t_i\right) =$ ultimate creep coefficient due to loading applied at transfer per equation 3-14

After Deck Placement

The shrinkage loss after deck placement is determined in a manner similar to the shrinkage loss before deck placement, as follows:

$$\Delta f_{pSD} = \varepsilon_{bdf} E_p K_{df} \quad \text{3-26}$$

where:

$\varepsilon_{bdf} =$ shrinkage strain for the period between deck placement and the final time per equation 3-20.

$K_{df} =$ time development factor for the period between deck placement and the final time.

$$= \frac{1}{1 + \frac{E_p A_{ps}}{E_{ci} A_c}\left(1 + \frac{A_c e_{pc}^2}{I_c}\right)\left(1 + 0.7\Psi\left(t_f, t_i\right)\right)} \quad \text{3-27}$$

$A_c =$ area of section calculated using the gross composite concrete section properties of the girder and the deck and the deck to girder modular ratio

$I_c =$ moment of inertia of the section calculated using the gross composite concrete section properties of the girder and the deck and the deck-to-girder modular ratio at service

$e_{pc} =$ eccentricity of the prestressing force with respect to the centroid of the composite section.

3.2.3.6 Creep Loss

The time-dependent creep loss prediction is also separated into two parts, including the loss occurring prior to deck placement and the loss occurring after deck placement.

Prior to Deck Placement

The creep loss that occurs prior to deck placement is determined as follows:

$$\Delta f_{pCR} = \frac{E_p}{E_{ci}} f_{cgp} \Psi(t_d, t_i) K_{id} \qquad 3\text{-}28$$

where:

$\Psi(t_d, t_i) =$ creep coefficient at time of deck placement due to loading applied at transfer per equation 3-14

$t_d =$ age of concrete at time of deck placement (days)

After Deck Placement

The prestress loss (if positive) or gain (if negative) due to creep that occurs after deck placement is determined as follows:

$$\Delta f_{pCD} = \frac{E_p}{E_{ci}} f_{cgp} \left(\Psi(t_f, t_i) - \Psi(t_d, t_i) \right) K_{df} + \frac{E_p}{E_c} \Delta f_{cd} \Psi(t_f, t_d) K_{df} \qquad 3\text{-}29$$

where:

$\Delta f_{cd} =$ change in concrete stress at the centroid of the strands due to time-dependent losses between transfer and deck placement, combined with deck weight and superimposed loads. Negative if compressive concrete stress is reduced.

3.2.3.7 Relaxation Loss

Similar to the other time-dependent losses, the relaxation loss calculation is separated into two parts, including the loss occurring prior to deck placement and the loss occurring after deck placement.

Prior to Deck Placement

The relaxation loss that occurs prior to deck placement is estimated as follows:

$$\Delta f_{pR1} = \frac{f_{pi}}{30}\left(\frac{f_{pi}}{f_{py}} - 0.55\right) \quad 3\text{-}30$$

where:

$f_{pi} =$ stress in prestressing strands immediately after transfer

$$= f_{pj} - \Delta f_{pES} \quad 3\text{-}31$$

After Deck Placement

The relaxation loss occurring after deck placement is considered to be equal to the relaxation loss before deck placement:

$$\Delta f_{pR2} = \Delta f_{pR1} \quad 3\text{-}32$$

3.2.3.8 Prestress Gain due to Deck Shrinkage

As the composite deck concrete shrinks, the girder is deflected downward, resulting in an increase in the strand force. This prestress gain is determined as follows:

$$\Delta f_{pSS} = \frac{E_p}{E_c}\Delta f_{cdf} K_{df}\left(1 + 0.7\Psi\left(t_f, t_i\right)\right) \quad 3\text{-}33$$

where:

$\Delta f_{cdf} =$ change in concrete stress at the centroid of prestressing strands due to shrinkage of deck concrete.

$$= \frac{\varepsilon_{ddf} A_d E_{cd}}{1 + 0.7\Psi\left(t_f, t_d\right)}\left(\frac{1}{A_c} - \frac{e_{pc} e_d}{I_c}\right) \quad 3\text{-}34$$

$\varepsilon_{ddf} =$ ultimate shrinkage strain of deck concrete per equation 3-20.

$A_d =$ area of deck concrete.

$E_{cd} =$ modulus of elasticity of the deck concrete.

$e_d =$ eccentricity of the deck with respect to the gross composite section.

$\Psi(t_f, t_d) =$ ultimate creep coefficient of the deck concrete due to loading applied immediately after deck placement per equation 3-14.

3.3 Camber

All camber prediction methods estimate the camber at the time of prestress transfer by using elastic beam theory to determine the deflections due to the prestressing force and the self-weight. Prediction methods differ in the calculation of the camber at later ages. Common methods for predicting camber typically utilize "multipliers" applied to the initial deflections to estimate the camber at the time of bridge erection. The multipliers approximate the effect of creep, which increases the deflections over time. Multiplier methods do not utilize detailed prestress losses predictions and are simple enough for hand calculations.

The current NCDOT method and the PCI method both utilize multipliers to predict long-term camber. The PCI multipliers were developed by Leslie Martin (Martin, 1977). The NCDOT multipliers were derived in a similar manner, but are larger than those recommended by Martin.

The AASHTO 2010 specifications do not provide a method to predict camber.

3.3.1 Current NCDOT Method

The NCDOT method is a multiplier method that predicts camber at the time of prestress transfer and at the time of bridge erection.

3.3.1.1 Camber at Transfer

The two components of net camber at the time of transfer are the upward deflection due to prestressing and the downward deflection due to self-weight. The net camber is determined as follows:

$$\Delta_i = \Delta_{ps,i} - \Delta_{sw,i} \qquad 3\text{-}35$$

where:

$\Delta_i =$ net camber at transfer

$\Delta_{ps,i} =$ upward deflection due to prestressing

$$= \frac{P_i}{E_{ci} I_g} \left(\frac{e_m L^2}{8} - (e_m - e_e) \frac{(L/2 - x_h)^2}{6} \right) \quad \text{3-36}$$

$\Delta_{sw,i} =$ downward deflection due to girder self-weight

$$= \frac{5 w_g L^4}{384 E_{ci} I_g} + \Delta_{diaphragm} \quad \text{3-37}$$

$P_i =$ prestressing force immediately after transfer

$e_m =$ eccentricity of the centroid of the strands at midspan with respect to the centroid of the gross section

$e_e =$ eccentricity of the centroid of the strands at the end of the girder with respect to the centroid of the gross section. Debonding is neglected.

$L =$ girder length

$E_{ci} =$ elastic modulus of the concrete at transfer

$I_g =$ moment of inertia of the gross section

$w_g =$ linearly distributed self-weight load

$x_h =$ distance from harp point to center of span

$\Delta_{diaphragm} =$ deflection due to internal diaphragms in hollow girders; diaphragms are treated as point loads; deflection depends on number and location; zero for solid girders.

3.3.1.2 Camber at Time of Bridge Erection

To estimate the net camber at the time of bridge erection, the components of initial deflection at transfer are adjusted by multipliers. The downward deflection due to superimposed loads applied at bridge erection is also included if superimposed loads are present:

$$\Delta = 2.26\,\Delta_{ps,i} - 2.31\,\Delta_{sw,i} - \Delta_{sd} \quad \text{3-38}$$

where:

$\Delta =$ net camber

$\Delta_{sd} =$ deflection due to superimposed dead loads applied at bridge erection

$$= \frac{5 w_{sd} L^4}{384 E_c I_g} \quad \text{3-39}$$

$w_{sd} =$ weight of superimposed loads applied at bridge erection

$E_c =$ elastic modulus of the concrete at bridge erection

3.3.2 PCI Method

The PCI method also uses multipliers to predict camber at prestress transfer, at bridge erection, and at an arbitrary "final" time in the distant future, which represents the ultimate deflection.

3.3.2.1 Camber at Transfer

The calculation of the camber at prestress transfer is identical to the NCDOT method (Equation 3-35).

3.3.2.2 Camber at Time of Bridge Erection

In estimating the camber at the time of bridge erection, the PCI method is similar to the NCDOT method except that the multipliers are reduced:

$$\Delta = 1.80\,\Delta_{ps,i} - 1.85\,\Delta_{sw,i} - \Delta_{sd} \quad \text{3-40}$$

where $\Delta_{ps,i}$, $\Delta_{sw,i}$, and Δ_{sd} are calculated according to Equations 3-36 through 3-39.

3.3.2.3 Camber at Final Time

The net camber at an arbitrary "final" time in the distant future is estimated using additional multipliers for the initial deflections. The deflection due to superimposed loads applied at bridge erection, if such loads are present, is also adjusted by a multiplier.

$$\Delta = 2.45\ \Delta_{ps,i} - 2.70\ \Delta_{sw,i} - 3.00\ \Delta_{sd} \qquad 3\text{-}41$$

If the superimposed load applied at bridge erection is a composite topping, then its contribution to deflection is multiplied by 2.30 instead of 3.00 in the above equation.

4 FIELD MEASUREMENTS AND SITE VISITS

4.1 Introduction

A significant part of the effort of this study was the development of an extensive database of field measurements that could be used to evaluate the various prediction models. The field data included camber, concrete properties, and production details. The development of the database is discussed in Section 4.2.

In addition to collecting camber data, the research team conducted site visits to several producers to observe the production process to identify factors that may have an effect on the prediction of camber. During the visits, measurements of the strand tension were also taken during casting using load cells. The camber of the girders was also measured by the research team at various stages of production. The site visits are discussed in Section 4.3

4.2 Field Measurements

To develop the extensive database of field measurements, it was necessary to enlist the help of NCDOT inspectors and Resident Engineers. For quality assurance purposes, the inspectors are required to be present during the casting of every prestressed bridge girder produced for NCDOT. Since there is an NCDOT inspector stationed at each precasting yard, they were well-positioned to take camber measurements before the girders were shipped. The resident engineers, on the other hand, are present at the erection of the bridge and were thus able to take camber measurements once the girders were in place.

4.2.1 Camber Data Sheets

In order to collect the camber measurements and the related girder data, a data sheet was developed on which the inspectors would record the measurements and data at the precasting yards. Once the girders were sent to the construction site, the data sheets were sent by the inspectors to the resident engineers so that the camber measurement of the in-place girder could also be recorded.

The measurements and data included on the data sheets consisted of the following items:

- position of each girder along the casting bed
- curing method used
- ultimate compressive strength of the concrete at transfer
- ultimate compressive strength of the concrete at a later age
- locations of the supports in storage
- exposure conditions and geologic orientation during storage
- measurements of the camber at transfer, at the beginning of storage, at the end of storage, and in place on the bridge
- weather and temperature at the time of each camber measurement

An example of the data sheet is given in Appendix D.

4.2.2 Method of Camber Measurement

In the past, researchers have used a variety of techniques to measure the camber of prestressed girders. Often, the research is focused on a very limited number of girders, usually for a single bridge project. In these cases, highly accurate and sophisticated measuring techniques are warranted. For this study, however, the goal was to develop an extensive database containing measurements for a large number of girders. It was critical that the method of measurement be simple, since a number of different people would perform the measurements. It was also necessary for the method to be a relatively fast process to avoid delays to the production schedule, since camber measurements needed to be taken just after transfer but before the girders were removed from the bed. Therefore, an effective method of measurement was developed that balanced the need for simplicity and accuracy. The procedure was as follows:

1) Two pieces of steel reinforcing bar (rebar) are notched near their ends.
2) One rebar is embedded in each end of the girder during casting, with the notched end protruding several inches from the top surface of the concrete.

3) A string is pulled tautly from one rebar to the other, spanning the length of the girder, and fastened at the level of the notch.

4) Using paint or by indenting the wet concrete, a mark is made at midspan on the surface of the girder directly under the string where measurements will be taken. The setup of the girder and string is shown in Figure 4-1.

5) Before prestress transfer, the vertical distance at midspan from the string to the mark on the girder is measured. This is considered to be the datum measurement.

6) When prestress transfer is complete but before removing the girder from the casting bed, the distance from the string to the girder is measured again. The difference between this value and the datum measurement from step 5 is the measured net camber due to prestressing and self-weight.

7) Additional measurements are made at the beginning of storage, prior to shipment, and when the girder is in place on the bridge, for a total of four camber measurements for each girder.

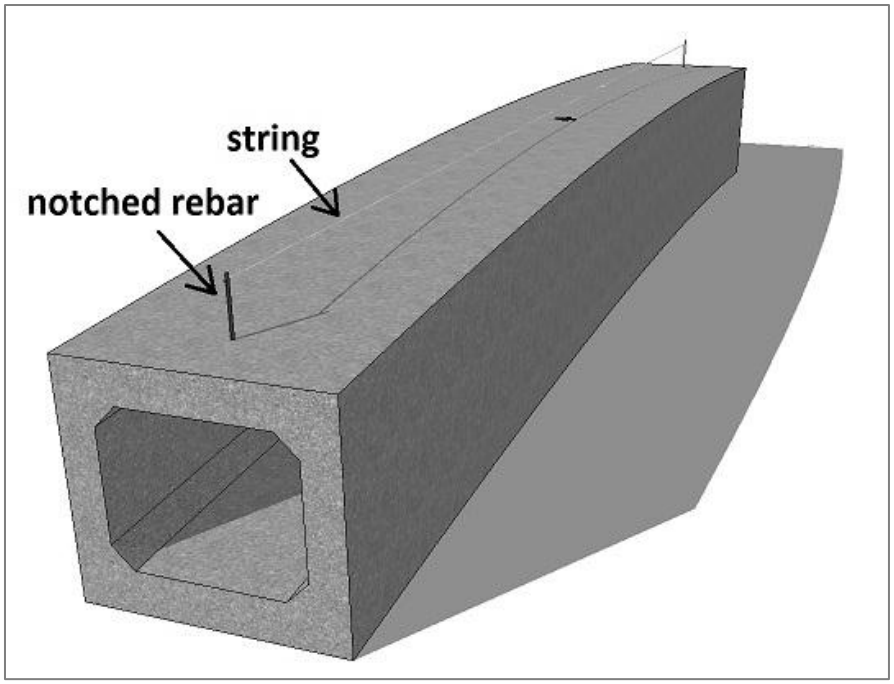

Figure 4-1 Girder with rebar and string in place for camber measurements.

4.2.3 Extent of Collected Data

As girders were produced at various precast plants during the data collection phase, the NCDOT inspectors were asked to select one to two girders from each casting to record the camber. For this reason, the number and types of girders for which data were collected depended on the production schedules at the plants.

Camber data were collected via the data sheets over a period of about one year. This amount of time was necessary in order to obtain a sufficient amount of data on each girder type to be studied, since some types were produced less often than others were. The following sections describe the types of girders studied and the typical prestressing strands used.

4.2.3.1 Girder Types

This study focused only on precast, pretensioned girders. The types and sizes of the girders that were considered in this study are given in Table 4-1. The shapes of the sections are shown in Figure 4-2.

Table 4-1 Types and typical sizes of girders considered in this study.

Girder Type	Depth	Length
AASHTO Type III	36”	57’
AASHTO Type IV	45”	43’ to 104’
Box Beam	27”, 33”, 39”	44’ to 100’
Cored Slab	18”, 21”, 24”	24’ to 68’
Modified Bulb-Tee	63”, 72”	73’ to 142’

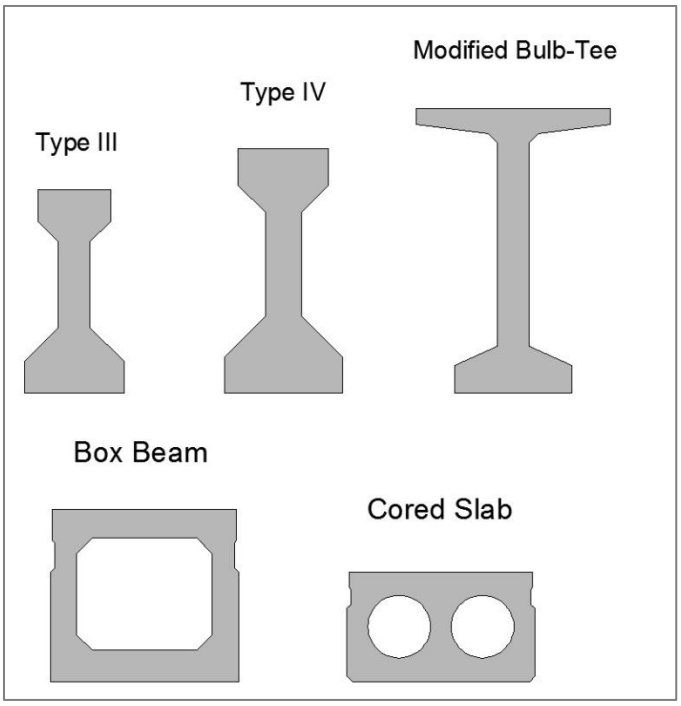

Figure 4-2 Typical sections of the girder types considered in this study.

The number of each type of girder considered in this study is given in Table 4-2. Again, these numbers are in proportion to the rate at which each girder type was produced for NCDOT bridges over the period when data was collected.

Table 4-2 Number of girders of each type considered in this study.

Member Type	No. of Girders
Type III	4
Type IV	21
Box Beam	114
Cored Slab	194
Bulb-Tee	49

It should be noted that while all of the girders represented in the database were measured for camber after prestress transfer, some measurements of camber at later stages were not completed due to scheduling or other circumstances.

4.2.3.2 Prestressing Strands

NCDOT uses low-relaxation seven-wire strand with 270 ksi nominal strength. During this study, some girders contained 0.5-inch diameter strand and some contained 0.6-inch strand. The specified initial tensioning stress for low-relaxation strands is 75 percent of the nominal strength, or 202.5 ksi for 270 ksi strand.

4.3 Site Visits

The research team conducted a series of site visits to precast producers and bridge construction sites in order to identify possible factors during production that could affect the prediction of camber. During the visits, the research team observed casting of girders for four bridge projects selected by NCDOT. One casting was observed for each project. Two of the projects involved casting of cored slabs, while the other two involved box beams. Strand tension measurements were taken during casting using load cells placed on selected strands. Camber measurements of the selected girders were also taken, following the measurement

procedure described in Section 4.2.2. When the girders were shipped, follow-up site visits were conducted to observe the transport of the girders from the producer to the bridge construction site and to measure the camber once the girder was in place on the bridge.

4.3.1 Observations

The following notable observations were made during the site visits:

1) The casting of multiple girders along the same casting bed requires multiple batches of concrete. Because batches of concrete are prone to variability, this could result in girders cast in the same bed having different concrete properties, including strength, unit weight, and elastic modulus. There are also occasional delays in the batching process, which could result in girders having different strengths at the time of prestress transfer since some would experience longer curing times than others would. Any of these factors could cause camber variations among girders cast in the same bed. The effect of concrete properties on camber is discussed in detail in Section 5.4.
2) For cored slabs, it was observed that there is a local deformation of the void tubes at the hold-down points during casting in the range of 3/8” to 5/8”. There was also additional flexural deflection between hold-downs in the range of 1/8” to 3/8”. For box beams, it was observed that local deformation of the expanded polystyrene (EPS) internal voids during casting was about 1/8” to 3/8”. The flexural deflection of the box beam voids was approximately 1/8”. The effects of void deformation on camber are discussed in detail in Section 5.5.
3) Curing times and methods vary from casting to casting, even for girders intended to be placed adjacent to each other on a span. Girders are typically cured with either heat or water and are released the day after casting. However, if the girders are cast on Friday, the producer will often wait until the following Monday to release the girders. In these cases, heat curing is often not used since the girders have enough time to reach the specified concrete strength for

prestress transfer without heat curing. Because of this difference in curing, girders that are intended to be placed adjacent to each other in a span may have different cambers.

4) Girders were typically supported near their design bearing locations close to the ends of the girder while in storage. Therefore, the effect of storage support locations is not considered a significant source of error in the camber predictions.

4.3.2 Strand Tension Measurements

During the site visits, the research team instrumented several strands with load cells to measure the prestressing forces during tensioning and casting, as shown in Figure 4-3. Measurements were taken at the following stages:

1) After tensioning
2) Prior to casting the concrete
3) After casting the concrete
4) Prior to prestress transfer

At each stage, the ambient temperature was also recorded. During the site visit to Eastern Vault in Princeton, West Virginia, the approximate temperature of the strands was recorded at each stage by noting the air temperature before casting and the concrete temperature after casting.

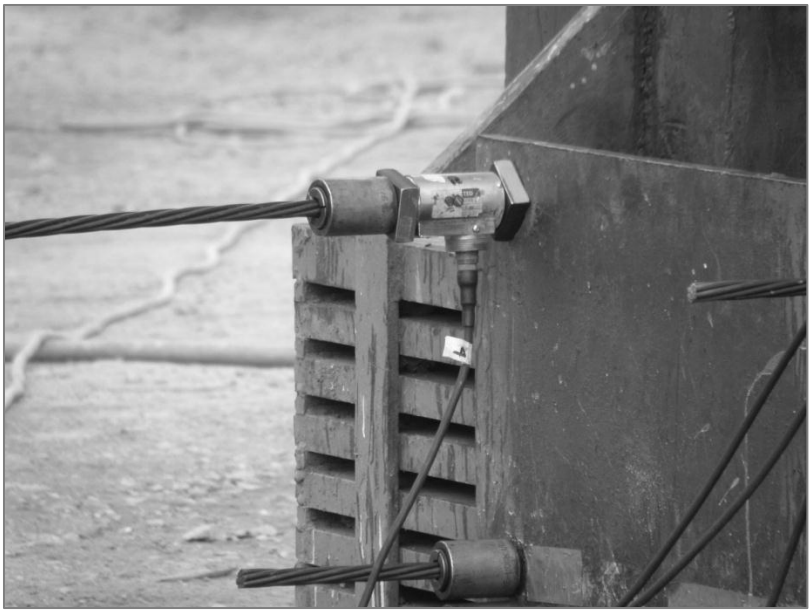

Figure 4-3 Load cells placed on selected strands to measure the prestressing force.

Based on the tension measurements, it was observed that the prestressing force in the strands varied significantly between tensioning and prestress transfer. In addition, by comparing the prestressing force and strand temperature measurements taken during the site visit to Eastern Vault, shown in Figure 4-5 and Figure 4-4, respectively, it can be seen that the prestressing force is reduced as strand temperature increases, and vice versa. This is due to thermal expansion of the strands. The effect of strand temperature on the prestressing force and camber is discussed in detail in Section 5.3.

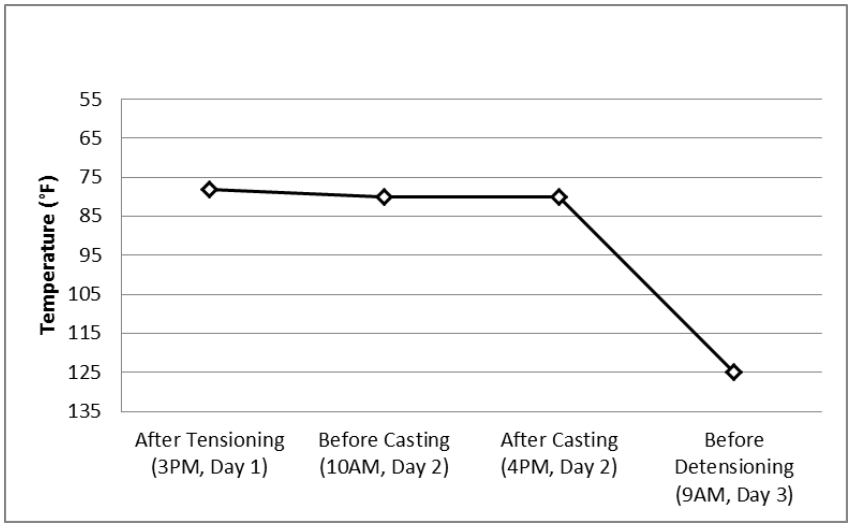

Figure 4-4 Approximate temperature of the strands at various stages of production for box beams cast during the site visit to Eastern Vault in Princeton, WV. The vertical axis is inverted.

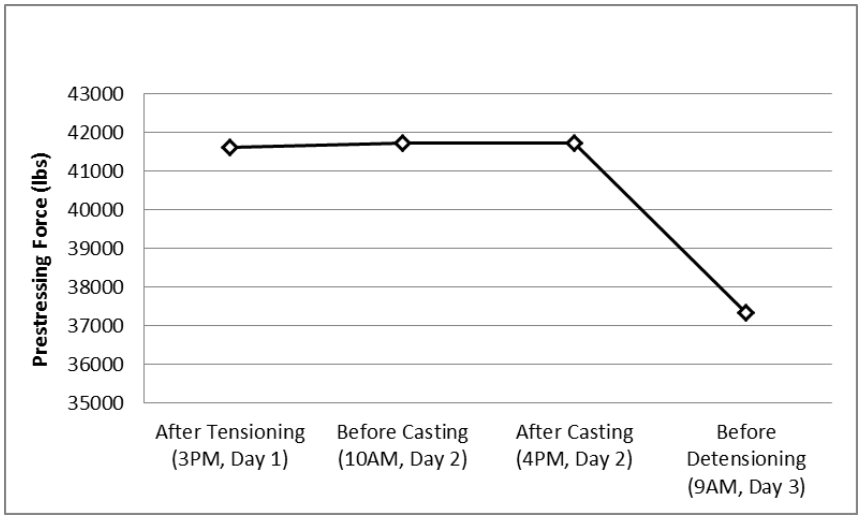

Figure 4-5 Average prestressing force at various stages for box beams cast during the site visit to Eastern Vault in Princeton, WV.

4.3.3 Camber Measurements

During the site visits, the research team measured the camber of the girders at the following four stages using the method described in Section 4.2.2:

1) In the casting bed after detensioning
2) At the beginning of storage
3) Prior to shipment
4) In place on the bridge

The camber measurements are discussed and compared with the predicted values in Section 7.3.4.

5 EVALUATION OF PRODUCTION FACTORS

5.1 Introduction

Throughout this research, several production variables were identified as factors that could affect the prediction of camber. In this chapter, these production factors are evaluated to consider their effects. Recommendations to account for these factors to improve the predictions are provided.

5.2 Debonding and Transfer Length

One factor that can have an impact on the prediction of camber is debonding of the strands at the end of the girder. Debonding is typically achieved by covering a portion of the strand with a sheath. It is often specified for prestressed girders to reduce the stresses caused by a large eccentricity of the strands at the end region. Debonding reduces the curvature of the girder in the end regions and therefore reduces the camber. Current NCDOT practice is to neglect the effect of debonding in the camber predictions.

Another factor that affects the camber predictions is the prestress transfer length. In pretensioned girders, the full prestressing force is only developed in the strands after a distance from the end of the girder known as the transfer length, which is the length of embedment required for a strand to develop the full prestressing force. Currently, NCDOT estimates camber based on the assumption that the full prestressing force is developed at the very ends of the girder, which ignores the effect of the transfer length.

To evaluate the effect of debonding and transfer length on the prediction of camber, the net camber was determined twice for each girder considered in the database—once by neglecting the effects of debonding and transfer length, and again by including their effects. The two predictions were then compared.

The camber due to prestressing only was determined by analyzing the moment profile due to prestressing. Since the shape of the actual bending moment pattern in the girder is complex when multiple debonded lengths are specified, a linear approximation was used to represent the moment profile. This approximation is illustrated in Figure 5-1 for a typical girder with two debonded lengths. In the figure, L_t is the transfer length, L_{d1} and L_{d2} are the

two debonded lengths, and $(Pe)_{max}$ is the moment due to the fully developed prestressing force. The camber due to prestressing was then calculated based on the approximate moment profile. The net camber was determined by combining the camber due to prestressing and the deflection due to self-weight.

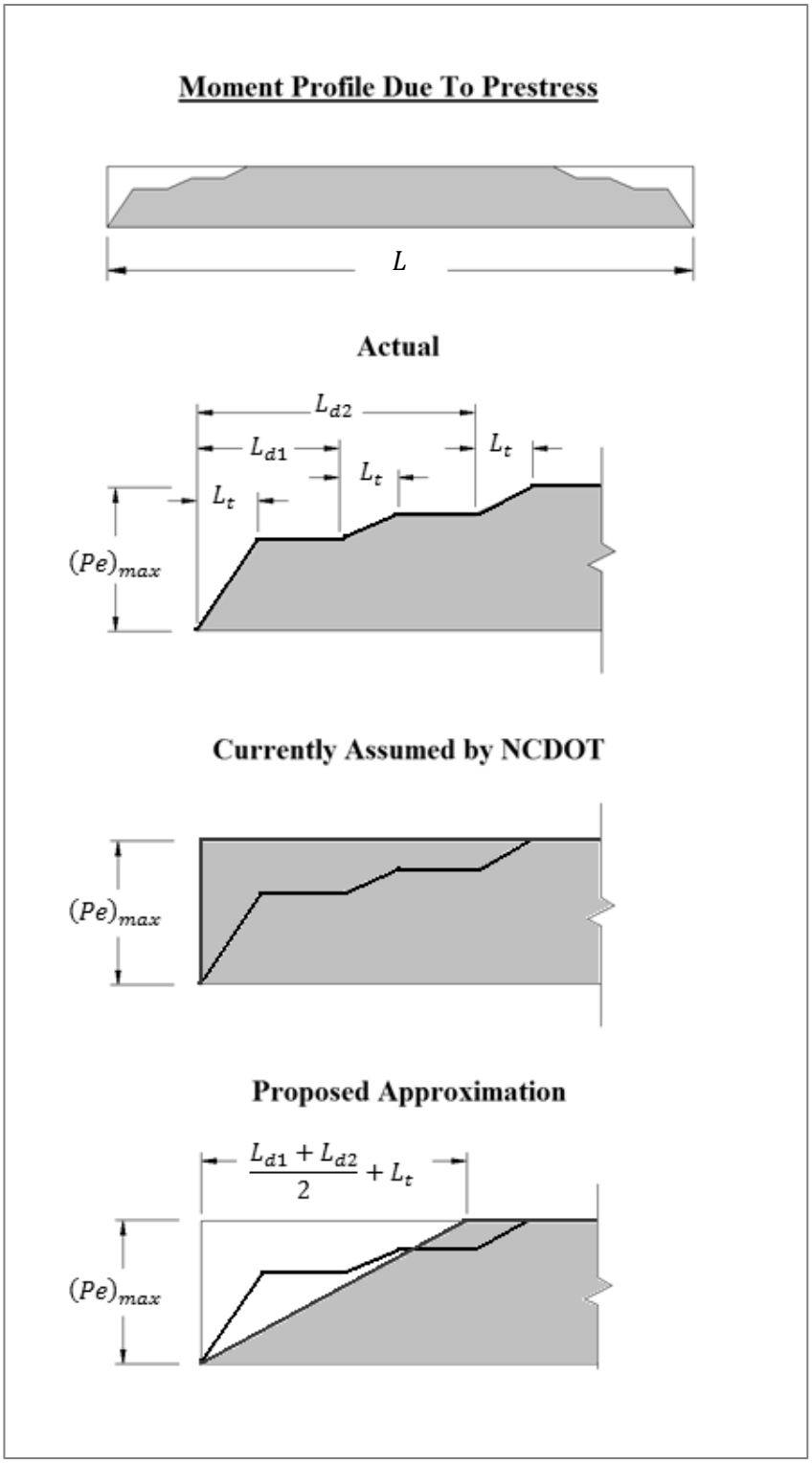

Figure 5-1 Approximation of the moment profile due to prestressing as affected by debonding and transfer length.

Using this linear approximation, the net camber for girders with only straight strands is determined as follows:

$$\Delta = \frac{Pe}{E_c I_g}\left(\frac{L^2}{8} - \frac{(L_{db} + L_t)^2}{6}\right) - \frac{5 w_g L^4}{384 E_c I_g} \qquad 5\text{-}1$$

where:

$L_{db} =$ average debonded length of the debonded strands

$L_t =$ transfer length of the prestressing strands; assumed to be 36 inches for 0.6" strands

The analysis revealed that debonding and transfer length typically reduces the camber predictions by 0.5% to 3%, although the effect is greater than this for very short girders and for those with long debonded lengths. The maximum calculated error was about 13%, which occurred for girders with specified debonded lengths of 10 feet or greater.

Based on this analysis, it is recommended that the effects of debonding and transfer length be considered for the prediction of camber. This is especially important for very short girders and for those with long debonded lengths. Section 5.10 contains the general recommended adjustment equation, which can be used for girders with or without harped strands.

5.3 Temperature of the Strands

Variations in the temperature of the strands between the time of initial stressing and the time of prestress transfer can cause changes in the prestressing force. As the temperature increases, thermal expansion causes the strands to relax, consequently reducing the prestressing force, which can affect the camber.

Before casting of the concrete, the temperature of the strands fluctuates due to both the ambient air temperature and solar effects. Soon after the concrete is cast, the strands are subject to significant heat caused by the cement hydration process. If heat curing is used, this also contributes significantly to the high temperature of the strands. Research by Roller and

Russell (Roller & Russell, 2003) has confirmed that the prestressing force can be reduced, at least temporarily, by these factors.

The impact of thermal effects can be estimated based on the thermal expansion coefficient of steel cable, μ_p, and the estimated change in temperature, ΔT. The change in the stress in the strand can be determined as follows:

$$\Delta f_p = E_p \, \mu_p \, \Delta T \qquad 5\text{-}2$$

Research has shown that the coefficient of thermal expansion for prestressing strands is approximately $8x10^{-6}$ strain per degree Fahrenheit (Chen, Liu, & Sun, 2011). In addition, it is reasonable to assume that the temperature increase is about 60°F. This temperature fluctuation is typical of the case where heat curing is used, causing the temperature of the strands to rise from the ambient temperature to approximately 140°F shortly after casting. The resulting reduction in the stress in the strands is then as follows:

$$\Delta f_p = (28.5x10^6 \, psi)\left(8x10^{-6}\frac{in}{in}/°F\right)(60°F)$$

$$\Delta f_p \approx 13.7 \, ksi$$

The resulting stress reduction of 13.7 ksi is equivalent to a 7% reduction of the typical initial prestress of 202.5 ksi for strands with 270 ksi nominal strength. This error is outside the typical industry tolerance of 5%, illustrating the fact that strand temperature fluctuations can have a potentially significant effect on the prestressing force and, consequently, on the camber. As noted by Roller and Russell, however, it is difficult to determine how much of the prestressing is permanently lost and how much will be regained after the girder cools down, since this will depend on when the concrete fully bonds to the strands.

Since the strand temperature history is unknown at the time of design, no specific recommendation can be made to adjust the prediction of camber due to this factor.

5.4 Concrete Properties

Predictions of prestress losses and camber are highly dependent on the properties of the concrete used for the girder. The elastic modulus of the concrete is used for predicting

deflections and prestress loss due to elastic shortening. The compressive strength of the concrete is used to predict losses and elastic modulus. The unit weight of concrete is also needed to determine the self-weight load, and it influences the elastic modulus equations provided by AASHTO, PCI, and ACI.

Due to the importance of the concrete properties in the predictions, the research team used physical tests and collected data to evaluate these properties. The following sections describe the tests, the collected data, and the analyses of these properties.

5.4.1 Testing and Collected Data

A large number of concrete cylinders were collected from the producers and tested. The cylinders represented a variety of typical mix designs used for NCDOT bridge girders. They were tested for compressive strength, elastic modulus, and unit weight. A total of 88 cylinders were tested for unit weight, 153 were tested for elastic modulus, and 218 were tested for strength. Many of the cylinders were tested for more than one property. Appendix E contains detailed information about the testing program.

In addition to the cylinder testing, an extensive amount of concrete strength data was collected from the producers. For each girder included in the database, the concrete strength at transfer and at a later date was recorded on the camber data sheets by the NCDOT inspectors. This data was then used to analyze the relationship between the specified and actual concrete strength.

5.4.2 Unit Weight of Concrete

The 88 cylinders that were tested for unit weight were tested in 29 sets of three or four cylinders. As shown in Figure 5-2, the average unit weight of the cylinder sets was 148 lbs/ft^3. The data ranged from approximately 140 to 154 lbs/ft^3.

Currently, NCDOT engineers assume a unit weight of 150 lbs/ft^3 for the elastic modulus and deflection predictions. Due to the weight of the reinforcing steel in the girder, it is reasonable to assume that the actual unit weight of the section will be slightly higher than the measured value of 148 lbs/ft^3. Therefore, the value of 150 lbs/ft^3 currently used by NCDOT engineers for design is considered appropriate.

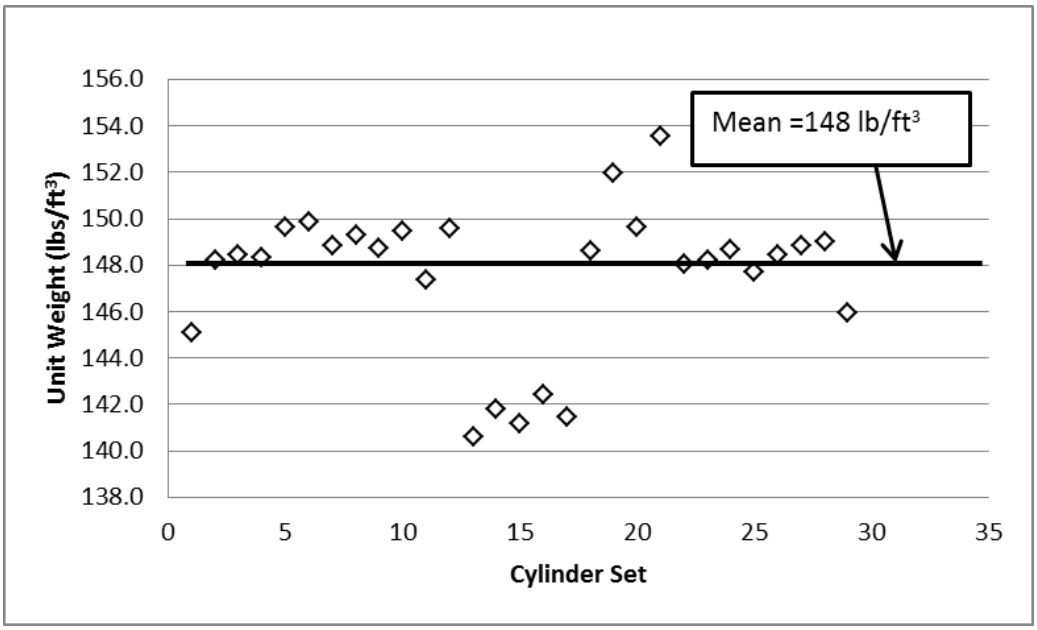

Figure 5-2 Measured unit weight of concrete cylinders.

5.4.3 Compressive Strength

NCDOT engineers currently use the specified concrete compressive strength to estimate the elastic modulus of the concrete. Since the specified strength is always lower than the actual strength, the elastic modulus is likely to be underestimated when the specified strength is used. The prestress losses, which also depend on the concrete strength, are likely to be overestimated. To improve the predictions of the camber and prestress losses, it is critical to use an estimated actual concrete strength for the elastic modulus and losses calculations.

To estimate the actual concrete strength, it is necessary to determine the typical relationship between the specified strength and the observed strength for typical bridge girders. In addition, since there are two specified strength values for pretensioned girders—one at the time of prestress transfer and one at 28 days—and since both of these values are used for the losses and camber calculations, it is necessary to determine realistic ratios for both of these stages.

Recommended Strength At Transfer

Before the prestressing force is transferred to the girder, the producer must test concrete cylinders from the cast to ensure that the concrete has reached the specified transfer strength. Cylinders are made from batches of concrete at each end of the casting bed, and the average strength of these two batches is considered to be the strength of all of the girders in the same casting bed.

The concrete strength at transfer for each girder was reported on the camber data sheets by the NCDOT inspectors. Data was collected for 381 girders. As shown in Figure 5-3, the average ratio of measured strength to specified strength was 1.24 with a range of approximately 1.0 to 2.1.

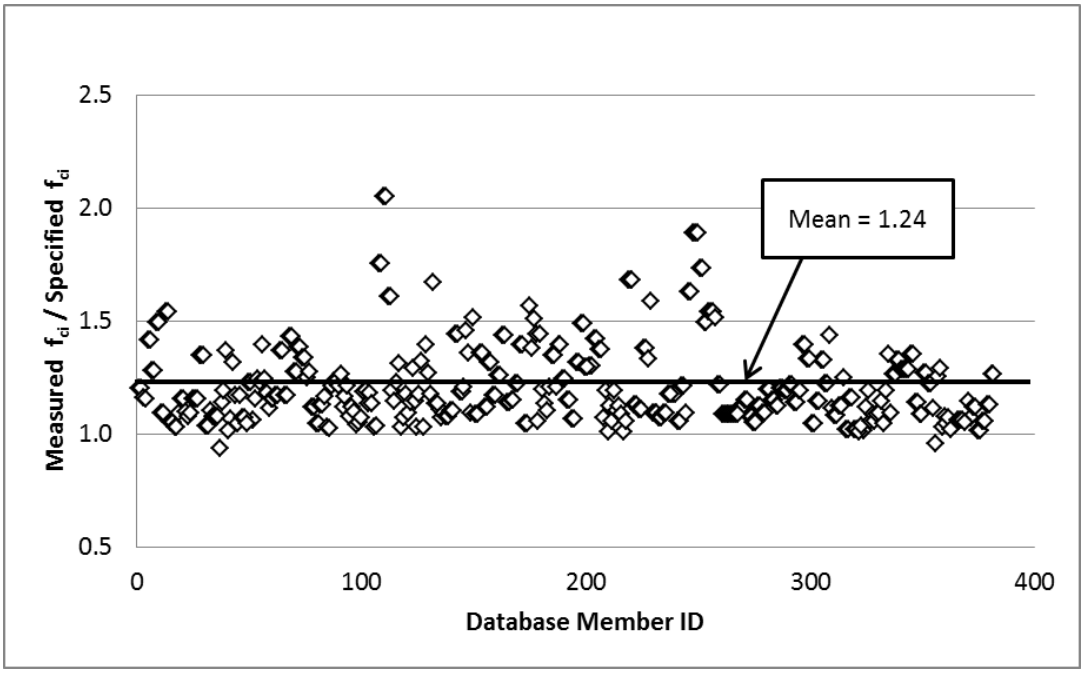

Figure 5-3 Ratio of measured concrete strength to specified strength at the time of prestress transfer.

Based on this analysis, the recommended concrete strength at transfer to be used for the prediction of prestress losses and elastic modulus for camber calculations is as follows:

$$f_{ci}^{*} = 1.25 f_{ci}' \quad \text{5-3}$$

where:

$f_{ci}' =$ the specified concrete strength at transfer

Recommended Strength at 28 Days

The concrete strength at 28 days was analyzed by computing the ratio of the measured strength to the specified 28-day strength for the cylinders that were collected from the producers and tested in the lab. However, since many of the cylinders were tested at ages other than 28 days, the measured strengths were adjusted to estimate the 28-day strengths. The ratio of the estimated 28-day strength to the specified strength was then calculated.

To estimate the 28-day strength based on the strength measured at different times, the measured strength was adjusted using the time function provided by the *ACI Committee Report 209R* as follows:

$$f_c' = f_c \frac{a + bt}{t} \quad \text{5-4}$$

where:

$f_c' =$ concrete strength at 28 days

$f_c =$ measured concrete strength at an age other than 28 days

$a =$ factor to account for curing method and cement type

$b =$ factor to account for curing method and cement type

$t =$ concrete age at time of strength measurement

It should be noted that the above equation is highly sensitive when the concrete strength is measured at very early ages. Therefore, this analysis only included cylinders that were measured for strength at ages greater than 5 days. In addition, strengths measured after 28 days were not adjusted.

The analysis included 70 sets of cylinders comprising 200 individual specimens. As shown in Figure 5-4, the average ratio of the estimated 28-day strength to the specified 28-day strength was 1.45 with a range of approximately 1.0 to 2.2.

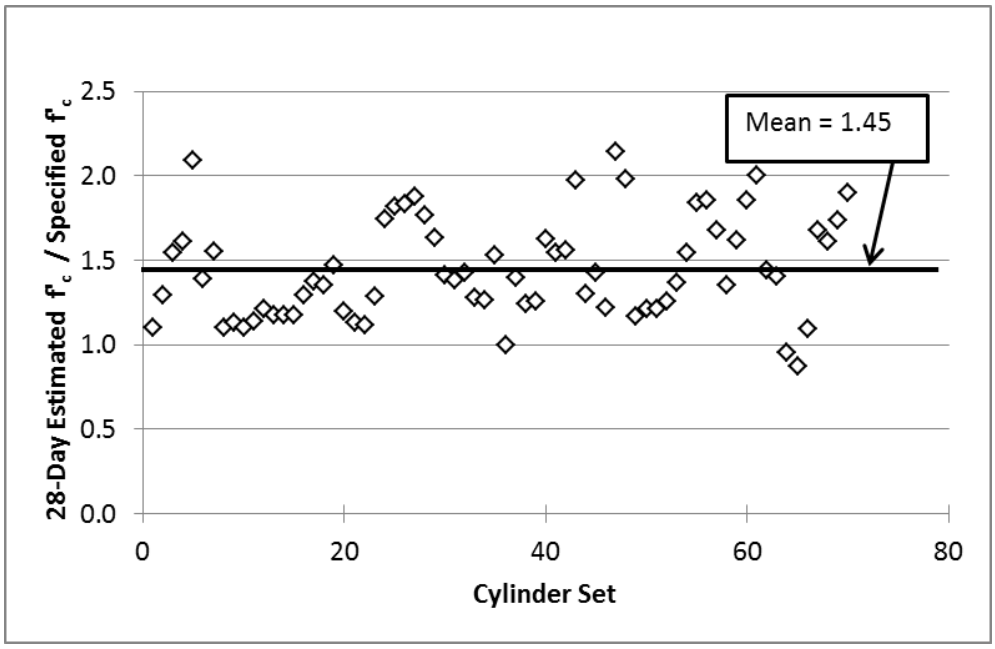

Figure 5-4 The ratio of the estimated actual 28-day strength to the specified 28-day strength for tested concrete cylinders.

Based on this analysis, the recommended 28-day concrete strength to be used for the prediction of prestress losses and elastic modulus for camber calculation is as follows:

$$f_c^* = 1.45 f_c' \qquad 5\text{-}5$$

where:

$f_c' =$ the specified 28-day concrete strength

5.4.4 Elastic Modulus

Currently, NCDOT engineers use the following formula to estimate the elastic modulus of concrete, which is based on the *2004 AASHTO LRFD Specifications*:

$$E_c = 33\, w_c^{1.5} \sqrt{f_c} \qquad 5\text{-}6$$

where:

$w_c =$ unit weight of concrete (lb/ft^3)

$f_c =$ concrete compressive strength

In 2007, the AASHTO specifications introduced into the equation a factor to account for the effects of aggregates on concrete stiffness, as follows:

$$E = 33\ K_1 w_c^{1.5} \sqrt{f_c} \qquad 5\text{-}7$$

In the above equation, K_1 is the aggregate adjustment factor, which is assumed to be 1.0 unless otherwise determined by physical tests.

To evaluate the accuracy of the AASHTO equation for estimating the elastic modulus of concrete for girders produced for NCDOT bridges, the ratio of the measured elastic modulus to the predicted elastic modulus was calculated for the cylinders tested in the lab. For the predictions, the unit weight was assumed to be 150 lbs/ft^3 as recommended in Section 5.4.2, and the measured concrete strength of each cylinder set was used.

This analysis included 70 sets of cylinders comprising 153 individual specimens. As shown in Figure 5-5, the average ratio of measured elastic modulus to predicted elastic modulus was 0.85. The ratio for individual sets of cylinders ranged from approximately 0.62 to 1.15.

Based on this analysis, it is recommended that the new AASHTO prediction (Equation 5-7) be used to predict elastic modulus for NCDOT bridge girders. In the equation, K_1 should be 0.85, the unit weight of concrete should be 150 lbs/ft^3, and the value of concrete strength should be based on Equation 5-3 or 5-5.

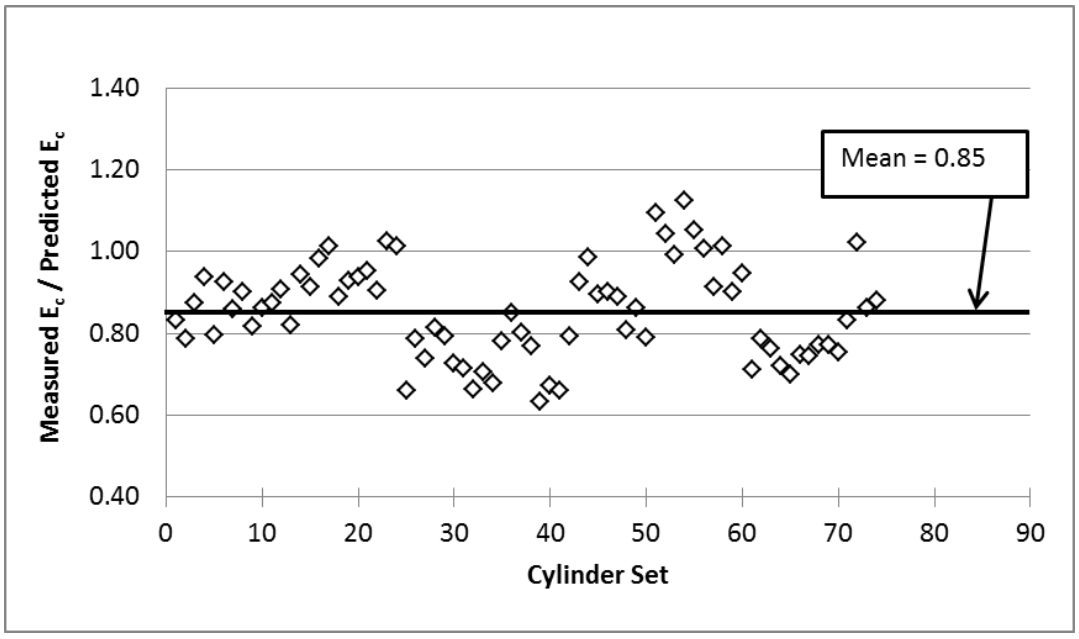

Figure 5-5 Ratio of measured elastic modulus to predicted elastic modulus for the tested cylinders.

5.5 Void Deformation

As mentioned in section 4.2.3, two of the most commonly used girder types for NCDOT bridges are box beams and cored slabs. Both of these girder types have hollow cross-sections and are constructed using permanent internal void forms. In the case of box beams, the void forms consist of blocks of expanded polystyrene (EPS) foam, as illustrated in Figure 5-6 and Figure 5-7.

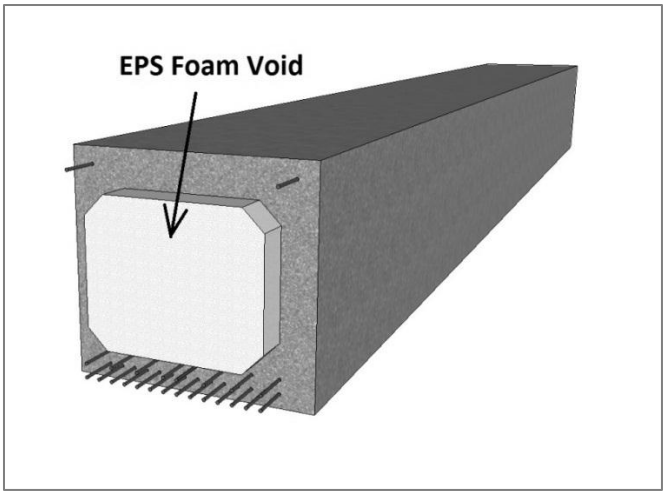

Figure 5-6 Expanded polystyrene blocks are used to form the internal voids in a box beam.

Figure 5-7 Expanded polystyrene void forms are placed in the casting bed during casting of box beams.

For cored slabs, the internal void forms consist of hollow paper tubes, as shown in Figure 5-8 and Figure 5-9.

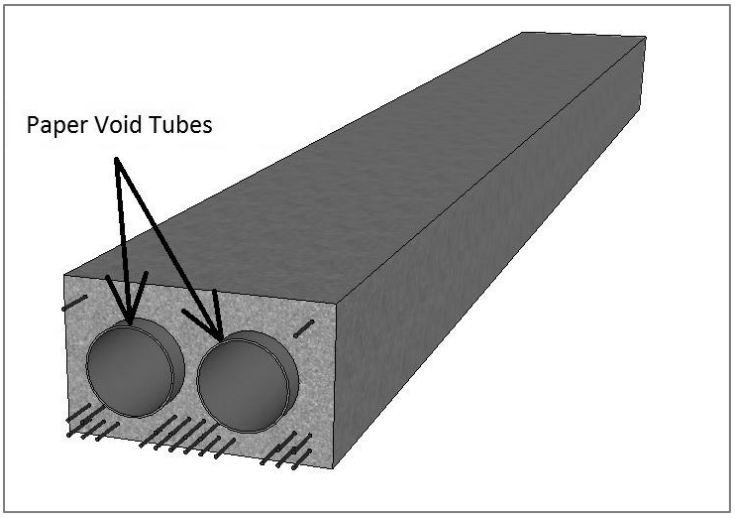

Figure 5-8 Paper tubes are used for the internal voids in cored slabs.

Figure 5-9 Paper tubes have been placed in the casting bed to form the internal voids of cored slabs. The tubes are held in place with an external hold-down system.

Due to the natural buoyancy of the void forms used for box beams and cored slabs, they tend to float up in the fresh concrete during casting. To prevent this from happening, a void hold-down system is typically used. However, due to the flexibility of the voids, there is a tendency for the voids to deflect upward in the span between the hold-down supports. In

addition, there is potential for local deformation at the location of the hold-down supports. In the case of box beams, there can also be significant compressive deformation of the EPS foam voids that occurs due to the hydrostatic pressure of the fresh concrete during casting.

Deformation of the void forms alters the section properties of hollow girders from the original design section properties. This could have a significant impact on the predictions of prestress losses and camber. Section 5.5.1 introduces two different hold-down systems, while Sections 5.5.2 and 5.5.3 discuss the effects of void deformation on the camber predictions for cored slabs and box beams.

5.5.1 Hold-down Systems

Two types of hold-down systems are typically used for box beams and cored slabs. External hold-down systems consist of rigid braces attached to the casting bed. These braces are external to the cross section. Typically, reinforcing bars are extended down from the braces and contact the void tubes, holding them in place. The braces are typically spaced three to four feet apart along the length of the casting bed. An example of an external hold-down system is shown in Figure 5-9.

Some producers use internal hold-down systems, in which the tensioned prestressing strands are used as braces. Steel straps are placed around the strands and the voids, and the strands prevent the voids from floating upward during concrete casting. The strap spacing of internal hold-down systems is typically similar to that of external systems.

During the site visits to the precasting plants, the research team observed that the two cored slab projects and one of the two box beam projects utilized external hold-down systems, while the other box beam project utilized an internal hold-down system.

For any hold-down system used, local deformation at the hold-down supports and flexural deformation between the supports should be minimized. If the internal system is used, then the producer should verify that the buoyancy force is not shifting the strands upward. This can be verified by measuring the distance from the strands to the bottom of the casting bed before and after casting at a location between two girders near the middle of the bed.

5.5.2 Cored Slabs

To analyze the impact of void deformation on the camber of cored slabs, the section properties were adjusted to account for flexural deflection and local deformation of the voids. The adjusted section properties were then used to predict the girder deflections, and these deflections were compared to those calculated based on the original design section properties.

The extent of local deformation that occurs in cored slab voids was determined by direct measurement during the site visits to the producers. However, the severity of local deformation was observed to depend on the specific design of the hold-down system used. During the two site visits in which cored slabs were cast, two different devices were used to contact the void tubes in the hold-down systems. At one producer, the contact devices consisted of a thin metal plate with dimensions of 3 inches by 5 inches, as shown in Figure 5-10. At another producer, the hold-down contact was a molded plastic device, as seen in Figure 5-11.

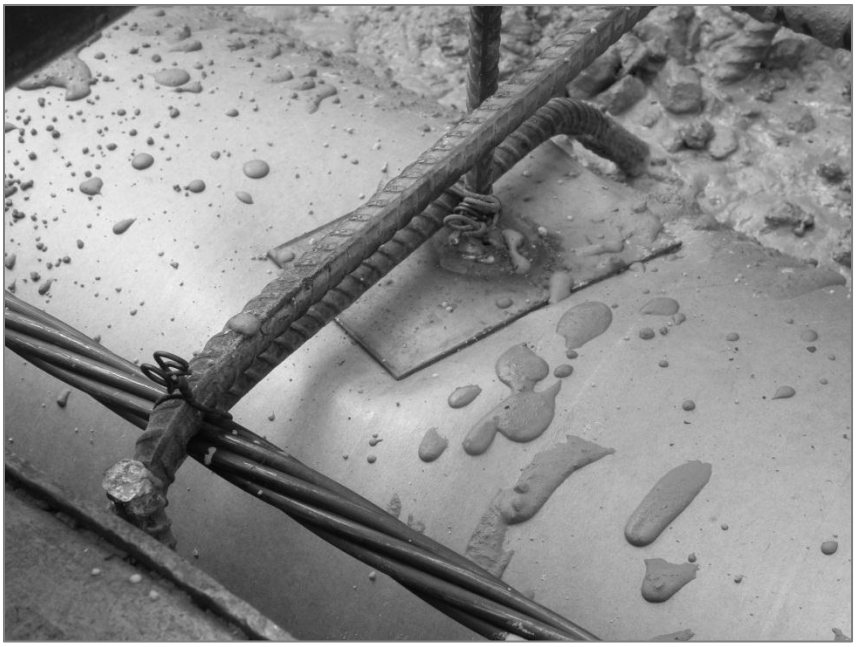

Figure 5-10 A thin metal plate is used to contact the void tube for the hold-down system, resulting in significant local deformation.

Figure 5-11 A molded plastic device is used to contact the void tube in the external hold-down system.

It was observed that when the flat metal plates were used, the void tube was locally deformed by approximately one-half to five-eighths of an inch at the hold-downs due to the buoyancy of the voids. When the molded plastic contact devices were used, the local deformation was less severe—typically one-quarter to three-eighths of an inch. This is because the molded plastic device contoured to the shape of the void tube and therefore provided some horizontal confinement while the metal plate did not. It was also observed that the local deformation is more severe for large diameter voids.

The measured flexural deflection of the voids between the hold-down points was approximately one-quarter of an inch.

To determine the adjusted section properties of the cored slabs after casting, the voids were assumed to shift upward by a certain amount. Based on the observed behavior, voids that were eight inches in diameter were assumed to shift by one-half inch; voids that were ten inches in diameter were assumed to shift by five-eighths of an inch, and those that were twelve inches in diameter were assumed to shift by three-fourths of an inch. The concrete

centroid and the moment of inertia of the section were then calculated and compared to the original design values.

Six cored slab sections with various depths and with voids of varying diameters were analyzed. The effects of void deformation on the section properties are summarized in Table 5-1, in which y_c is the location of the concrete centroid relative to the bottom of the girder, and I_g is the moment of inertia of the section. The percent change in the properties is calculated relative to the original sections.

Table 5-1 Percent change in section properties due to void deformation, relative to the original sections.

Cored Slab (Depth/Void ϕ)	y_c % Change	I_g % Change
18"/10"	-2.3%	-0.6%
21"/8"	-0.7%	-0.1%
21"/10"	-1.6%	-0.4%
21"/12"	-3.1%	-0.8%
24"/12"	-2.3%	-0.5%
26"/12"	-1.8%	0.5%

After adjusting the section properties, the effect of void deformation on the camber predictions was evaluated for several typical cored slab designs by predicting the deflections using both the original section properties and the modified section properties. The percent changes in the predicted deflections due to prestress, Δ_{ps}, deflection due to self-weight, Δ_{sw}, and the typical change in the net camber, Δ_{net}, are summarized in Table 5-2. It should be noted that the changes in the prestress deflection and self-weight deflection depend only on the section and not the girder length or prestressing, while the change in the net camber depends on all of these factors. Therefore, the typical range is given for the effect of void deformation on net camber.

Table 5-2 Percent change in deflections and net camber due to void deformation, relative to the original sections.

Cored Slab (Depth/Void ϕ)	Δ_{ps} % Change	Δ_{sw} % Change	Δ_{net} % Change
18"/10"	-3.4%	0.6%	5%-12% (typical)
21"/8"	-2.9%	0.1%	
21"/10"	-2.7%	0.4%	
21"/12"	-5.2%	0.9%	
24"/12"	-4.5%	0.5%	
26"/12"	-5.5%	-0.5%	

As shown in the table, the calculated net camber was reduced by approximately five to twelve percent when the void deformation was considered. It is important to note that the net camber is affected more significantly than either the camber due to prestress or the deflection due to self-weight. This result arises due to the fact the magnitude of the net camber is small in comparison to the magnitude of the prestress deflection alone. Therefore, small changes in the prestress deflection will have a significant impact on net camber. An example of this calculation is provided in Appendix A.

Based on this analysis, it is apparent that void deformation can have a significant effect on the camber predictions. To avoid this, the local deformation and flexural deflection of the voids should be minimized, either by reducing the spacing between hold-down supports, by using more effective contact devices, or by using stiffer void tubes. However, absent any changes to current production practices, the adjusted section properties tabulated in Appendix A should be used to improve the camber and prestress losses predictions.

5.5.3 Box Beams

The EPS foam voids used for box beams also deflect and deform during casting. In addition to undergoing flexural deflection and local deformation, the voids are compressed due to the hydrostatic pressure of the fresh concrete, as shown in Figure 5-12. This increases the amount of concrete required for the section, resulting in increased dead load. Since the compression is greater near the bottom of the void, this could also shift the centroid of the

section closer to the strands, consequently reducing the eccentricity of the prestressing force. The moment of inertia of the section is also changed when the void is deformed. Therefore, in the analysis of the box beam voids, all three effects—flexural deflection, local deformation at the hold-downs, and hydrostatic compression—were considered.

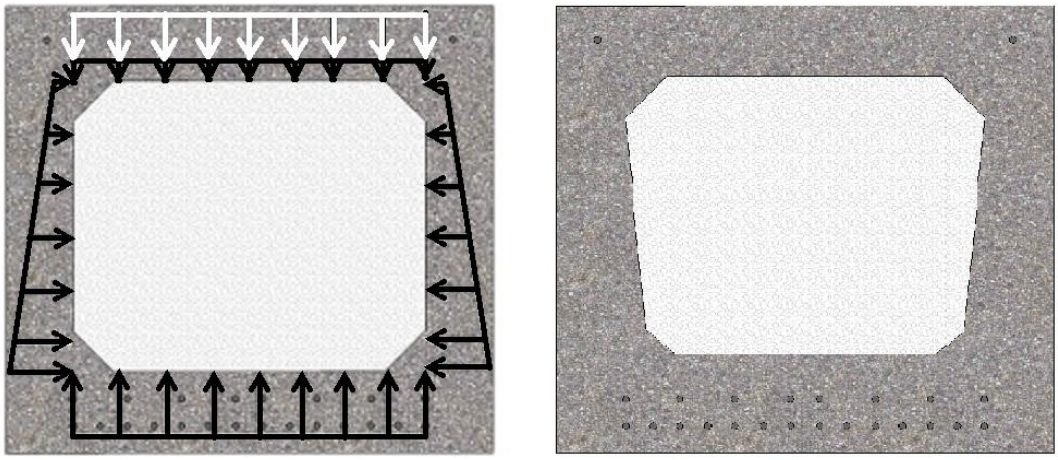

Figure 5-12 Distribution of the assumed pressures acting on the box beam EPS void form and the resulting deformed shape. The black arrows represent the hydrostatic pressure, while the white arrows represent the magnitude of the hold-down support reaction if it were evenly distributed along the entire top surface of the EPS form.

Similar to the analysis for cored slabs, the effect of void deformations was determined by calculating the adjusted section properties and the resulting camber. Based on measurements made during the site visits, the box beam void was assumed to shift upward by 1/4 of an inch due to local deformation at the hold-down supports. The flexural deflection of the void was calculated using elastic beam formulas by modeling the void as a continuous beam with a uniformly distributed load acting upward due to the buoyancy of the void. The extent of hydrostatic compression was determined by assuming that the EPS void material behaves linearly and has an elastic modulus of 170 psi. These values are representative of typical EPS voids used for NCDOT box beams, which have an average density of 1.0 lb/ft^3. Linearity of the EPS material under the calculated loads was confirmed by physical tests

conducted at the NCSU Constructed Facilities Laboratory. The details of the testing are reported in Appendix F.

Similar to the cored slab analysis, the effects of the void deformation depend on the section used. The calculated percent changes in the section properties of various box beam sizes are shown in Table 5-3, where A_g is the area of the section, y_c is the location of the centroid relative to the bottom of the section, I_g is the moment of inertia of the section, and w_g is the distributed self-weight load. The percent changes in the predicted deflection due to prestress, Δ_{ps}, deflection due to self-weight, Δ_{sw}, and the net camber, Δ_{net}, are summarized in Table 5-4.

Table 5-3 Percent changes in section properties due to void deformation in box beams.

Box Beam Depth	A_g % Change	y_c % Change	I_g % Change	w_g % Change
27"	1.2%	-2.5%	-0.2%	1.2%
33"	1.9%	-2.5%	0.5%	1.9%
39"	2.7%	-2.7%	1.3%	2.7%

Table 5-4 Percent changes in deflection and net camber predictions due to void deformation in box beams.

Box Beam Depth	Δ_{ps} % Change	Δ_{sw} % Change	Δ_{net} % Change (typical)
27”	-4.8%	1.4%	5%-10%
33”	-5.5%	1.4%	15%-25%
39”	-6.2%	1.4%	20%-25%

As shown in Table 5-4, the percent change in net camber is more significant than for either the camber due to prestress alone or the deflection due to self-weight. As discussed in Section 5.5.2, this is because the magnitude of the net camber is typically significantly less

than the magnitude of the deflection due to prestress only. Therefore, small changes to the prestress deflection will have a significant impact on the net camber prediction.

Based on the above analysis, it is recommended that void deflection and deformation be minimized by using a void material that is significantly stiffer than the typical EPS that is currently used, which has an elastic modulus of approximately 170 psi. However, to improve the camber predictions for current production materials, the camber predictions may be improved by the using the adjusted section properties, which are summarized in Appendix A.

5.6 Temperature of the Concrete

Since the top surface of a girder stored in the casting yard is usually exposed to the sun while the bottom surface is shaded, the girder is subject to temporary thermal gradients through the depth of the girder. Due to thermal expansion, this thermal gradient can cause temporary changes in camber throughout the day. In addition, the effect on the camber for box beams and cored slabs could be more severe than it is for other girder types since these are often stored immediately adjacent to one another in the yard, which keeps the bottom surfaces relatively cooler.

Since the effect of the thermal gradient causes scattering of the collected camber data, it is important to evaluate the impact that this effect can have on the camber measurements. For the case of a linear thermal gradient, the increase in camber due to thermal effects can be estimated using the following integral:

$$\Delta_T = \int_0^{\frac{L}{2}} \frac{\mu_c \Delta T}{d} x \qquad 5\text{-}8$$

where:

$\Delta_T =$ deflection due to thermal gradient effects

$L =$ girder length

$\mu_c =$ coefficient of thermal expansion for concrete; approximately $6\text{x}10^{-6}$ strain/°F

$\Delta T =$ total temperature difference in the girder

$d =$ depth of the girder

This equation can be simplified to the following form:

$$\Delta_T = \frac{\mu_c \Delta T L^2}{8d} \qquad 5\text{-}9$$

For the example case of a 33-inches deep, 75-feet long box beam with a 40-degrees temperature differential, the increase in camber is estimated as follows:

$$\Delta_T = \frac{(6x10^{-6})(40)(75x12)^2}{(8)(33)} = 0.74\ in$$

Box beams of this size typically have a camber of 1 to 2 inches, so the thermal gradient effect can temporarily increase the measured camber by 40 to 80 percent for this example. For the case of non-linear thermal gradients, which are more likely, the estimated impact of the thermal gradient could be even more significant.

Based on Equation 5-9, the effect of the thermal gradient on camber is more severe for long girders with shallow depths. Since girders are being designed increasingly longer by the use of greater amounts of prestressing, this could explain why camber variability seems to be more of a problem in recent years. In addition, newer girder types such as box beams and cored slabs are especially susceptible to thermal gradient effects due to their relatively low depth-to-width ratio and their high span-to-depth ratio.

Based on this analysis, it is recommended that future camber measurements be taken before dawn whenever practical to avoid the effect of the thermal gradient induced by the sun. No adjustment for this factor is recommended for the prediction of camber at the design stage since the effects are temporary.

5.7 Curing Method

The two primary curing methods used for precast, pretensioned girders are moist curing and heat (or steam) curing. Moist curing typically consists of using a hose to drip water on the top surface of the girder, while heat curing involves the use of steam lines to heat the girder, consequently accelerating the cement hydration process.

As discussed in Section 5.3, the temperature of the strands can affect the prestressing force through thermal expansion and relaxation of the strands. When heat curing is used, the temperature of the girders and strands rises very quickly after casting. Therefore, girders that

are heat cured could experience a greater reduction in the prestressing force than moist cured girders due to the effect of the strand temperature.

In addition to affecting the prestressing force, heat curing can also generate a thermal gradient within the girder since the girder is typically heated from below while the top of the girder is more exposed to cooling. This could reduce the camber of the girder at the time of prestress transfer due to differential thermal expansion, as discussed in Section 5.6.

The effect of the curing method on camber is evidenced by the analysis of the collected camber data, which is discussed in detail in Section 7.3. The data suggest that the camber at the time of prestress transfer is significantly reduced for heat cured members as compared to moist cured members. The data also suggest that the effect seems to depend on the girder type. For box beams, the camber at transfer for heat cured members is roughly 50% lower than for moist cured members; for cored slabs, the difference is approximately 75%; and for Type IV girders, the difference is approximately 20%. For modified bulb-tees, there is not a significant difference in the camber at transfer for heat cured versus moist cured girders.

Although the effect of curing method on the camber at the time of transfer is significant, analysis of the camber measurements at later ages suggests that the effect may be only temporary, since the difference between the camber measurements for heat cured and moist cured girders is significantly reduced at ages greater than 24 days.

Based on these observations, it is concluded that the effect of curing method on camber prediction accuracy can be significant at the time of transfer, although it varies for different girder types. In addition, the fact that the effect of the curing method is most significant for shallow girders such as cored slabs and box beams leads to the conclusion that thermal gradients present at the time of transfer may be a significant cause of camber discrepancy at this stage for heat cured members. This conclusion is drawn from the fact that thermal gradients with the same temperature differential tend to cause a greater deflection in shallow members than in deep members, as discussed in Section 5.6.

This analysis leads to the further conclusion that the measured camber at the time of transfer is not necessarily a reliable indicator of the eventual long-term camber since the camber at this early stage may be temporarily reduced due to effects related to the curing method.

Adjustments to the camber predictions due to this factor are not practical since the curing method is generally not known at the design stage. However, for camber analysis, girder data should be grouped according to the curing method used.

5.8 Transport and Handling

The effects of girder transport and handling on camber were evaluated by observing handling practices during the site visits and by measuring the camber at various stages.

During the site visits, camber was measured just before the girders were moved from the storage yard and again when they were in place on the bridge. In all cases except one, the camber did not change during shipping. In the case of one cored slab shipment, however, the camber of the cored slabs was observed to decrease by about 20%. It is possible that this change is the result of dissipation of the thermal gradient in the cored slabs during shipping. When the camber was measured before the girders were shipped, the slabs were exposed to the sun in the storage yard, and it is likely that a thermal gradient developed within the slabs at this time, producing additional camber. However, during shipment, the wind across the girder during travel likely dissipated the thermal gradient, reducing the camber. The impact of the thermal gradient effect is discussed in detail in Section 5.6.

Based on these observations, it is concluded that current transportation and handling practices are appropriate. However, if camber is to be measured before and after shipping for comparison purposes, the measurements should be taken just before dawn when the thermal gradient effect is minimal.

5.9 Project Scheduling

Factors related to project scheduling can also affect the camber predictions. For example, predictions of the camber at the time of prestress transfer as well as predictions of losses are based on the assumption that prestress transfer occurs one day after casting, which is typically the case. However, it is also common for girders cast on a Friday to have the prestressing transferred on the following Monday, three days after casting. During this extra time, the strength and elastic modulus of the concrete increases significantly. As a result, these properties can be significantly greater than the specified values used in the camber and

prestress loss predictions. In addition, the increased strength could result in significantly less creep than predicted. Therefore, two girders cast for the same bridge could have very different cambers if the prestressing force is transferred to the girders at different ages.

Another factor related to project scheduling that could affect the camber predictions is the amount of time between prestress transfer and erection of the bridge. There is often wide variation in this respect from project to project. For example, it is not uncommon for cored slabs to be erected within 15 days of casting, while other girder types may be in storage for six months or more before being erected. Due to the effects of creep on the measured camber, this could result in significant discrepancies between predicted and measured camber since the time of bridge erection is typically assumed to be 28 days in the predictions.

Due to the inherent scheduling uncertainties involved with bridge projects, adjustments to account for the project scheduling at the design stage are not practical. However, camber behavior will be more consistent among the girders in a particular bridge or span if they experience the same amounts of time between casting, prestress transfer, and bridge erection.

5.10 Summary of the Proposed Adjustments

Many of the factors discussed in this chapter introduce errors in the camber predictions that are additive. Specifically, the effects of neglecting debonding, transfer length, concrete over-strength, and void deformation in the camber predictions all tend to overestimate the actual camber. When considered together, the impact of these effects can be significant. Therefore, it is recommended that the adjustments for all four of these factors be included in the predictions.

The following recommended adjustments should be used when predicting camber and when predicting prestress losses for the camber calculations. The adjustments are summarized as follows:

Concrete Strength

The specified concrete strength at transfer, f'_{ci}, should be adjusted to determine the best estimate of the actual concrete strength at transfer, f^*_{ci}, as follows:

$$f_{ci}^{*} = 1.25\, f_{ci}' \quad \text{5-10}$$

The specified 28-day concrete strength, f_c', should be adjusted to determine the best estimate of the actual 28-day strength, f_c^*, as follows:

$$f_c^{*} = 1.45\, f_c' \quad \text{5-11}$$

These adjusted strengths should replace the specified strengths in all of the calculations, including concrete elastic modulus, creep coefficients, shrinkage strains, losses, and deflections.

Concrete Elastic Modulus

The AASHTO equation to estimate the elastic modulus of concrete at transfer should be adjusted by a factor of 0.85 to account for local production factors, as follows:

$$E_{ci} = (0.85)33 w_c^{1.5} \sqrt{f_{ci}^{*}} \quad \text{5-12}$$

The 28-day elastic modulus equation should be similarly adjusted:

$$E_c = (0.85)33 w_c^{1.5} \sqrt{f_c^{*}} \quad \text{5-13}$$

Void Deformation

To account for the effect of void deformation as discussed in section 5.5, the section properties of cored slabs and box beams should be modified from their original design values. For cored slabs, the modified properties include the section centroid and the moment of inertia. For box beams, the modified properties include the section centroid, the moment of inertia, and the area of the section. See the appendices for details regarding calculation of the modified section properties as well as a summary of all section properties used in this study.

Debonding and Transfer Length

The reduction in camber due to debonding and transfer length, discussed in section 5.2, is currently neglected by NCDOT engineers. To account for this effect, the elastic deflection due to prestressing only should have the following general form:

$$\Delta_{P,elastic} = \frac{P}{E_c I_g}\left(\frac{e_m L^2}{8} - (e_m - e_e)\frac{(L/2 - x_h)^2}{6} - \frac{e_m(L_{db} + L_t)^2}{6}\right) \qquad 5\text{-}14$$

where:

$P =$ prestressing force

$e_m =$ eccentricity of the centroid of the strands at midspan with respect to the centroid of the gross section

$e_e =$ eccentricity of the centroid of the strands at the girder end with respect to the centroid of the gross section

$E_c =$ elastic modulus of concrete

$I_g =$ moment of inertia of the gross section

$L =$ girder length

$L_{db} =$ average debonded length of the debonded strands

$L_t =$ transfer length; assumed to be 36 inches

$x_h =$ distance from the harp point to the center of the span

In Equation 5-14, the third term in the parenthesis represents the adjustment for debonding and transfer length based on the linear approximation of the prestress moment profile as discussed in Section 5.2.

6 PROPOSED CAMBER PREDICTION METHODS

6.1 Introduction

As stated in Chapter 1, one of the main tasks of this research is to develop and recommend two methods that will provide improved predictions of the camber of prestressed concrete bridge girders. One is an "approximate" method intended for hand calculations and does not require detailed prestress loss estimates. The other is a "refined" method that makes use of the detailed, time-specific prestress loss calculations.

In addition to these two proposed methods, a modified version of the current NCDOT method is also presented. All three methods utilize the recommended adjustments for the production factors discussed in Chapter 5.

Since the primary focus of this research is to predict the camber at prestress transfer and immediately prior to the placement of the deck, the procedures outlined below do not include the effects of superimposed dead loads applied after erection of the girder. In the following discussion, camber is predicted at the time of transfer (assumed to be one day), at 28 days, and at one year assuming that the superimposed dead loads have not been placed. This provides a one-year predicted time-history of camber prior to deck placement. Based on these three camber predictions, the predicted camber at other times can be interpolated.

6.2 Adjustment of the Section and Material Properties

For the two proposed methods and the modified NCDOT method, the section and material properties are adjusted to account for the effects of the production factors summarized in Chapter 5 as follows:

1) If the girder is a box beam or cored slab, the section properties should be modified to include the effects of internal void deformation. The proposed modified properties for girders produced with the void materials that were typical at the time of this research are summarized in Appendix A.

2) Estimate concrete strength at transfer and at 28 days by adjusting the specified values according to Equations 5-10 and 5-11, respectively.

3) Estimate concrete elastic modulus at transfer and at 28 days according to Equations 5-12 and 5-13 using the concrete strength estimated in step 2.

Use the adjusted properties from steps 1 through 3 for all subsequent calculations.

6.3 Modified NCDOT Method

The modified NCDOT method is based on the current NCDOT method discussed in Chapter 3. It uses the same losses predictions and the same camber multipliers. However, this method includes the adjustments for the production factors as recommended in Section 6.2.

The proposed prediction procedure for the modified NCDOT method is as follows:

1) Estimate the elastic shortening loss according to the current NCDOT procedure provided in Section 3.2.1 using the properties determined in Section 6.2.
2) Determine the initial prestressing force after transfer as follows:

$$P_i = A_{ps}\left(f_{pj} - \Delta f_{pES}\right) \quad \text{6-1}$$

where:

$P_i =$ initial prestressing force after transfer, where transfer is assumed to occur one day after casting.

$f_{pj} =$ stress in the strand after jacking. Taken as 75% of the nominal strength.

$\Delta f_{pES} =$ elastic shortening loss

$A_{ps} =$ total area of the prestressing strands

3) Predict the net camber at transfer as follows:

$$\Delta_i = \Delta_{ps,i} - \Delta_{sw,i} \quad \text{6-2}$$

where:

$\Delta_i =$ net camber at transfer

$\Delta_{ps,i} =$ upward deflection due to prestressing

$$= \frac{P_i}{E_{ci} I_g} \left(\frac{e_m L^2}{8} - (e_m - e_e) \frac{(L/2 - x_h)^2}{6} - \frac{e_m (L_{db} + L_t)^2}{6} \right) \quad \text{6-3}$$

$\Delta_{sw,i}=$ downward deflection due to girder self-weight

$$= \frac{5 w_g L^4}{384 E_{ci} I_g} + \Delta_{diaphragm} \quad \text{6-4}$$

$e_m =$ eccentricity of the centroid of the strands at midspan with respect to the centroid of the gross section

$e_e =$ eccentricity of the centroid of the strands at the end of the girder with respect to the centroid of the gross section. Debonding is neglected.

$L =$ girder length

$E_{ci} =$ elastic modulus of the concrete at transfer

$I_g =$ moment of inertia of the girder cross section

$w_g =$ uniformly distributed girder self-weight

$x_h =$ distance from harp point to center of span

$L_{db} =$ average debonded length of the debonded strands

$L_t =$ transfer length; assumed to be 36 inches

$\Delta_{diaphragm}=$ deflection due to internal diaphragms cast in hollow girders; diaphragms are treated as point loads; deflection depends on number and location; zero for solid girders.

4) Predict the net camber at 28 days using the current NCDOT multipliers for the time of bridge erection, as follows:

$$\Delta_{28} = 2.26\, \Delta_{ps,i} - 2.31\, \Delta_{sw,i} \quad \text{6-5}$$

5) Since the current NCDOT method does not provide multipliers to calculate the camber beyond the time of bridge erection, the net camber at one year, Δ_{365}, is assumed to be equal to the camber at 28 days.

$$\Delta_{365} = \Delta_{28} \quad \text{6-6}$$

6.4 Proposed Approximate Method

The proposed approximate method is based on the PCI method for predicting prestress losses and camber outlined in Chapter 3. Since the camber is predicted using multipliers, this method does not require calculation of the time-dependent losses to predict camber. Instead, the deflections at transfer due to prestressing and self-weight are adjusted by multipliers to estimate camber at later stages.

The prediction procedure for the proposed approximate method is as follows:

1) Estimate the elastic shortening loss according to the PCI procedure provided in Section 3.2.2 using the properties determined in Section 6.2.
2) Determine the initial prestressing force after transfer as follows:

$$P_i = A_{ps}\left(f_{pj} - \Delta f_{pES}\right) \quad \text{6-7}$$

where:

$P_i =$ initial prestressing force after transfer
$f_{pj} =$ stress in the strand after jacking, taken as 75% of the nominal strength
$\Delta f_{pES} =$ elastic shortening loss
$A_{ps} =$ total area of the prestressing strands

3) Predict the camber at transfer in the same manner as step 3 of the modified NCDOT method.
4) Predict the camber at 28 days by using the PCI multipliers for the time of girder erection as follows:

$$\Delta_{28} = 1.80\ \Delta_{ps,i} - 1.85\ \Delta_{sw,i} \quad \text{6-8}$$

5) Predict the camber at one year by using the PCI multipliers for final long-term camber, as follows:

$$\Delta_{365} = 2.45\ \Delta_{ps,i} - 2.70\ \Delta_{sw,i} \quad \text{6-9}$$

6.5 Proposed Refined Method

As stated in Chapter 3, the 2010 *AASHTO LRFD Bridge Design Specifications* provide estimates of prestress losses at specific times. However, they do not specify a procedure to predict camber. Therefore, it was necessary to develop a method to predict camber utilizing the time-specific losses calculations as discussed in Section 3.2.3.

The 2010 AASHTO specifications contain provisions for calculating the creep coefficient for any period of time, as outlined in section 3.2.3. Since the instantaneous deflection at transfer due to prestressing and self-weight is proportional to the internal stresses induced in the girder, the creep coefficients, which are used to estimate the effect of creep on strains, can also be used to estimate the additional deflections due to creep. Therefore, the components of the initial deflection can be multiplied by the creep coefficients to estimate the deflections at specified times.

The proposed refined method outlined below is a time-step method that uses two time-steps. It is similar to the approximate time-steps method described by the ACI Committee 435 (ACI Committee 435, 1995), although the formulation is somewhat different. It can be used to predict camber at any time before or immediately after placement of the deck or superimposed dead loads. However, since the time of girder erection is not known during the design stage, it is recommended that losses and camber be estimated at transfer, at 28 days, and at one year assuming that the deck has not been placed. The deflection at other specific times can be estimated by interpolating between these values.

The prediction procedure for the proposed approximate method is as follows:

1) Estimate the elastic shortening loss according to the AASHTO 2010 procedure provided in Section 3.2.3.4 using the properties determined in Section 6.2.
2) Estimate the time-dependent losses including shrinkage, creep, and strand relaxation at 28 days according to the AASHTO 2010 procedure provided in Section 3.2.3 using only the calculations that apply to the losses prior to deck placement. Assume that t_i equals 1 day, t_d equals 28 days, and t_f equals 1825 days (five years).
3) Estimate the time-dependent losses including shrinkage, creep, and strand relaxation at one year (365 days) according to the AASHTO 2010 procedure provided in Section 3.2.3 using only the calculations that apply to the losses prior to deck placement. Assume that t_i equals 1 day, t_d equals 365 days, and t_f equals 1825 days (five years).
4) Determine the initial prestressing force after transfer, at 28 days, and at one year as follows:

$$P_i = A_{ps}\left(f_{pj} - \Delta f_{pES}\right) \quad \text{6-10}$$

$$P_{28} = A_{ps}\left(f_{pj} - \left[\Delta f_{pES} + \Delta f_{pSR,28} + \Delta f_{pCR,28} + \Delta f_{pRE,28}\right]\right) \quad \text{6-11}$$

$$P_{365} = A_{ps}\left(f_{pj} - \left[\Delta f_{pES} + \Delta f_{pSR,365} + \Delta f_{pCR,365} + \Delta f_{pRE,365}\right]\right) \quad \text{6-12}$$

where:

$P_i =$ initial prestressing force after transfer

$P_{28} =$ prestressing force at 28 days

$P_{365} =$ prestressing force at 365 days

$f_{pj} =$ stress in the strand after jacking, taken as 75% of the nominal strength.

$A_{ps} =$ total area of the prestressing strands

$\Delta f_{pES} =$ elastic shortening loss

$\Delta f_{pSR,28} =$ shrinkage loss between transfer and 28 days

$\Delta f_{pSR,365} =$ shrinkage loss between transfer and 365 days

$\Delta f_{pCR,28} =$ creep loss between transfer and 28 days

$\Delta f_{pCR,365} =$ creep loss between transfer and 365 days

$\Delta f_{pRE,28} =$ relaxation loss between transfer and 28 days

$\Delta f_{pRE,365} =$ relaxation loss between transfer and 365 days

5) Predict the net camber at transfer by following the procedure defined for the Modified NCDOT method in Section 6.3.

6) Predict the net camber at 28 days, Δ_{28}, as follows:

$$\Delta_{28} = \Delta_{ps,28} - \Delta_{sw,28} + \Delta_{cr,28} \quad \text{6-13}$$

where:

$\Delta_{ps,28} =$ deflection at 28 days due to prestressing only

$$= \Delta_{ps,i} - \frac{P_i - P_{28}}{\left(\frac{E_{ci} + E_c}{2}\right) I_g}\left(\frac{e_m L^2}{8} - \frac{(e_m - e_e)\left(\frac{L}{2} - x_h\right)^2}{6} - \frac{e_m (L_{db} + L_t)^2}{6}\right) \quad \text{6-14}$$

$\Delta_{sw,28} =$ deflection at 28 days due to self-weight only; equivalent to self-weight deflection at transfer

$= \Delta_{sw,\mathrm{i}}$

$\Delta_{cr,28} =$ deflection at 28 days due to creep

$$= \Psi(28, t_i)\left(\frac{\left(\frac{P_i + P_{28}}{2}\right)}{E_{ci} I_g}\left(\frac{e_m L^2}{8} - \frac{(e_m - e_e)\left(\frac{L}{2} - x_h\right)^2}{6} - \frac{e_m (L_{db} + L_t)^2}{6}\right) - \Delta_{sw,\mathrm{i}}\right) \quad \text{6-15}$$

$\Psi(28, t_i) =$ creep coefficient at 28 days due to loading applied at transfer per equation 3-14

7) Predict the net camber at one year, Δ_{365}, as follows:

$$\Delta_{365} = \Delta_{ps,365} - \Delta_{sw,365} + \Delta_{cr,365} \quad \text{6-16}$$

where:

$\Delta_{ps,365} =$ deflection at 365 days due to prestressing only

$$= \Delta_{ps,28} - \frac{P_{28} - P_{365}}{E_c I_g}\left(\frac{e_m L^2}{8} - \frac{(e_m - e_e)\left(\frac{L}{2} - x_h\right)^2}{6} - \frac{e_m (L_{db} + L_t)^2}{6}\right) \quad \text{6-17}$$

$\Delta_{sw,365} =$ deflection at 365 days due to self-weight only; equivalent to self-weight deflection at transfer

$= \Delta_{sw,\mathrm{i}}$

$\Delta_{cr,365} =$ deflection at 365 days due to creep

$$= \Delta_{cr,28} + \Psi(365,28)\left(\frac{\left(\frac{P_{28} + P_{365}}{2}\right)}{E_{ci} I_g}\left(\frac{e_m L^2}{8} - \frac{(e_m - e_e)\left(\frac{L}{2} - x_h\right)^2}{6} - \frac{e_m (L_{db} + L_t)^2}{6}\right) - \Delta_{sw,\mathrm{i}}\right) \quad \text{6-18}$$

$\Psi(365,28) =$ creep coefficient for the period between 28 days and 365 days due to loading applied at transfer per Equation 3-19

7 EVALUATION OF PREDICTION METHODS

7.1 Introduction

To evaluate the accuracy of the methods for predicting camber, the predicted values from each method were compared to the field measurements. The following four prediction methods were compared:

1) *current NCDOT method*
2) *modified NCDOT method*
3) *proposed approximate method*
4) *proposed refined method*

The detailed calculations for these methods are given in Chapters 3 and 6. All of the methods except the current NCDOT method include adjustments to account for the effects of the production factors and material properties as discussed in Chapter 5.

7.2 Method of Comparison

A series of spreadsheets was developed to predict the camber of each girder in the database using each prediction method. Since no camber measurements were taken after placement of superimposed dead loads, the predictions were limited to consider only the camber up to the time of girder erection.

For each method, camber was predicted at three specific times—at transfer, at 28 days after casting, and at one year after casting. For the current NCDOT method, the camber was predicted according to the procedure outlined in Section 3.3.1, where the multipliers for the camber at bridge erection were used to determine the camber at 28 days, and the camber at one year was assumed to be equal to the camber at 28 days. For the other methods, the camber was predicted following the procedures discussed in Chapter 6.

Linear interpolation between the predicted cambers for each method was performed to determine the predicted camber at the time of measurement. For example, if camber was measured at 60 days, then linear interpolation was performed using the 28-day and one year predictions from a given method to determine the prediction at 60 days. This interpolated

value was then compared to the measured camber. An example of the resulting bilinear prediction curves is shown in Figure 7-1.

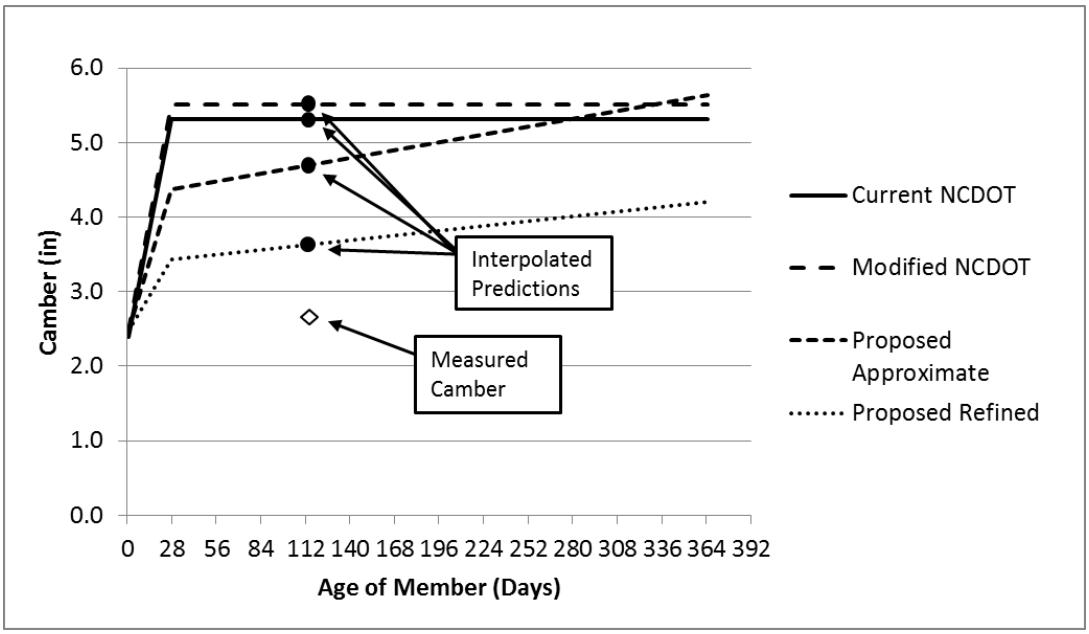

Figure 7-1 Camber is predicted at transfer, at 28 days, and at one year for each prediction method to obtain a bilinear prediction curve. Linear interpolation between these points is performed to determine the predicted value at the time that camber is actually measured.

Since the camber significantly increases in the early days after transfer and the rate of increase reduces over time, the linear interpolation is expected to significantly underestimate the camber between roughly 3 days and 24 days for any given method, even if the method itself is accurate. Therefore, only measurements taken either at the time of transfer or at ages beyond 24 days were used to evaluate the prediction models.

The camber data were grouped by girder type, curing method, and the time at which camber was measured (e.g. at transfer or at ages greater than 24 days).

To compare the predicted camber to the measured camber, the difference between the predicted and measured camber was determined as follows:

$$difference = \Delta_{predicted} - \Delta_{measured} \qquad 7\text{-}1$$

For each group of camber data, the mean and the standard deviation of the normally-distributed difference data was determined. The upper and lower bounds of the 95% range of the data were determined using the standard deviation and the mean, as follows:

$$(95\%\ upper)_{diff} = \mu_{diff} + 2\sigma_{diff} \quad 7\text{-}2$$

$$(95\%\ lower)_{diff} = \mu_{diff} - 2\sigma_{diff} \quad 7\text{-}3$$

where:

$(95\%\ upper)_{diff}$ = upper bound of the range that contains 95% of the "difference" values for a given group of data based on normal distribution

$(95\%\ lower)_{diff}$ = lower bound of the range that contains 95% of the "difference" values for a given group of data based on normal distribution

μ_{diff} = mean of the "difference" values for a given group of data

σ_{diff} = standard deviation of the "difference" values for a given group of data

The mean and the upper and lower bounds of the 95% range of the difference data were determined relative to the average measured camber for each group of data, as follows:

$$\mu_{\%\ error} = \frac{\mu_{diff}}{\mu_{measured}} \quad 7\text{-}4$$

$$(95\%\ upper)_{\%\ error} = \frac{(95\%\ upper)_{diff}}{\mu_{measured}} \quad 7\text{-}5$$

$$(95\%\ lower)_{\%\ error} = \frac{(95\%\ lower)_{diff}}{\mu_{measured}} \quad 7\text{-}6$$

where:

$\mu_{\%\ error}$ = mean relative percent error

$\mu_{measured}$ = average measured camber of the group of data

$(95\%\ upper)_{\%\ error}$ = upper bound of the range that contains 95% of the "difference" values for a given group of data, converted to "relative percent error"

$(95\%\ lower)_{\%\ error}$ = lower bound of the range that contains 95% of the "difference" values for a given group of data, converted to "relative percent error"

Using this approach, the mean difference and the mean relative percent error for a group of data for any given prediction method will be close to zero if the prediction method is accurate. By analyzing all of the data for each group of girders and curing methods, the overall best prediction method can be selected.

7.3 Results and Analysis

The analysis of the camber data collected in the database for 382 girders revealed significant scatter in the camber measurements as well as significant differences in typical camber behavior between the different girder types and curing methods, as discussed in the following sections.

7.3.1 Scatter of Data

Since the data comparing predicted to measured camber is normally distributed, the degree of scatter was evaluated by comparing the upper and lower bounds of the range containing 95% of the data as determined by Equations 7-1 to 7-6. The prediction method that has the narrowest 95% range for a given group of data has the least scatter of data.

The results of this analysis indicate that the scatter of the relative percent error of the camber predictions was similar for each prediction method considered in nearly every group of data. In a few cases, the scatter was slightly narrower for the proposed approximate method and the proposed refined method than it was for the two NCDOT methods, as illustrated in Figure 7-2 for the case of moist cured cored slabs measured at ages greater than 24 days. In general, however, the relative percent error had a wide scatter for all prediction

methods due to the various factors discussed in Chapter 5 related to concrete properties, temporary temperature effects, and other variables.

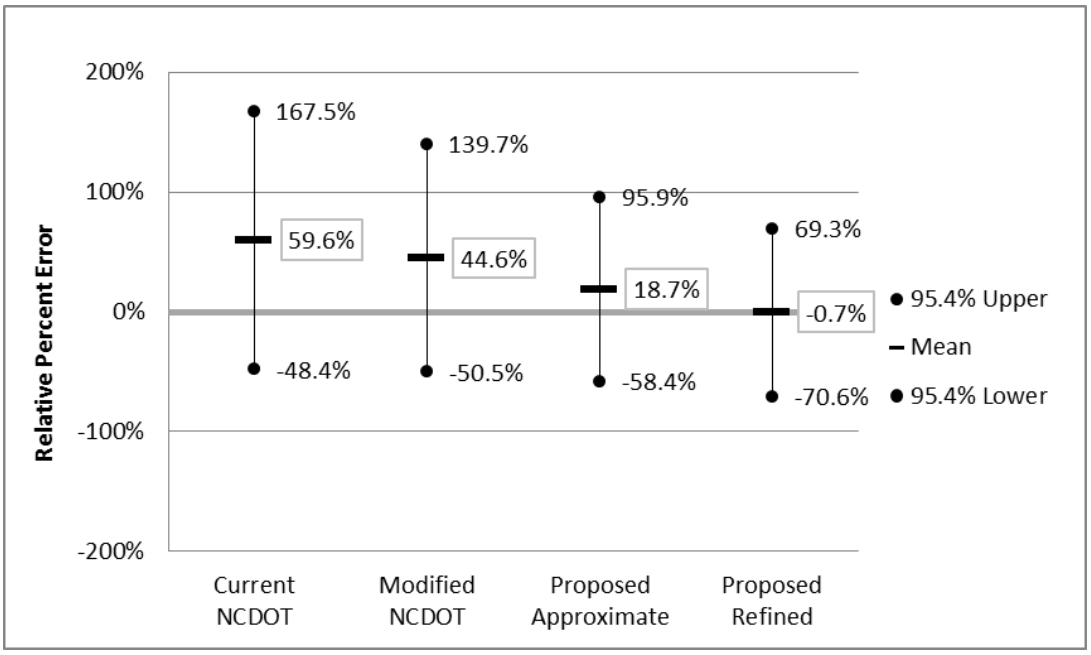

Figure 7-2 Distribution of relative percent error for moist cured cored slabs; includes camber measurements taken at 24 days or greater.

It is concluded that there is not a significant difference in the scatter of the data between prediction methods due to uncontrollable variables. For this reason, the remainder of the data analysis compares the prediction methods using only the mean of the data for each prediction method.

7.3.2 Camber at Transfer

The calculation of the camber at prestress transfer is nearly identical for all methods. The primary difference is that the recommended adjustments to account for the effects of the production factors described in Chapter 5 are included for the modified NCDOT method, the proposed approximate method, and the proposed refined method, while they are not included for the current NCDOT method. The results shown in Figure 7-3 indicate that the adjustments significantly improve the prediction of camber for box beams and cored slabs,

while the predictions for the other girder types are not significantly affected. This suggests that the majority of the improvement is due to the adjustments for the void deformation in hollow sections. The adjustments improved the predictions of camber at transfer for box beams and cored slabs by approximately ten to twenty percent.

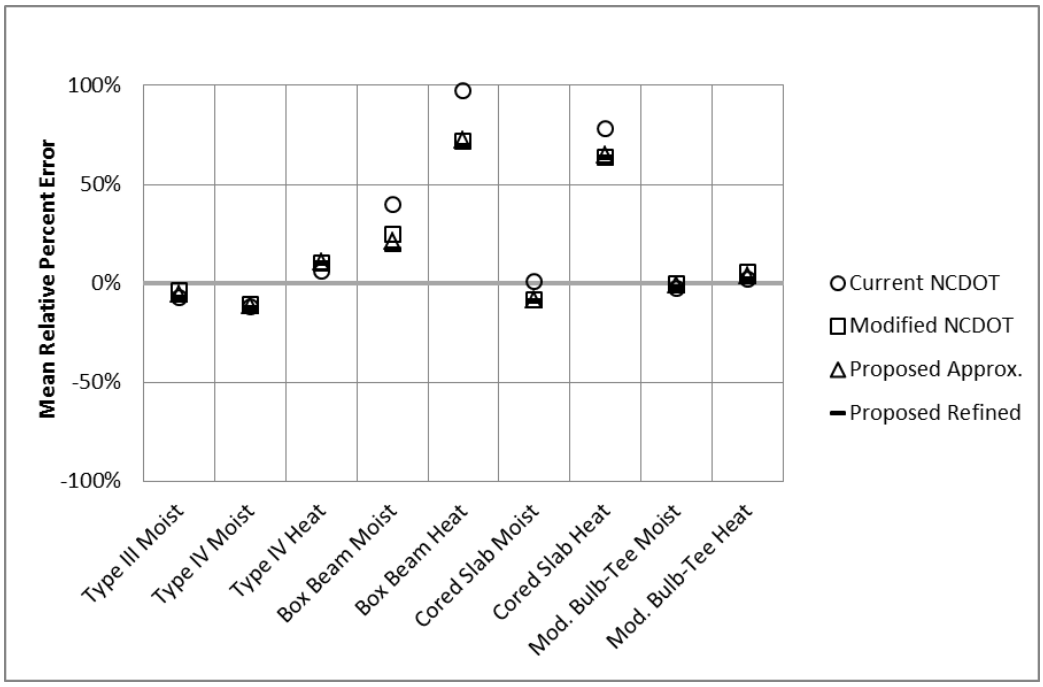

Figure 7-3 Mean relative percent error of the camber predictions for measurements taken at prestress transfer.

It can also be observed from Figure 7-3 that the effect of the curing method on the camber at transfer is significant. For cored slabs and box beams, the mean relative percent error of the camber predictions is approximately 50% to 70% less for moist cured girders than for heat cured girders. For Type IV girders, the difference in the percent error between moist cured and heat cured girders is approximately 20%. For modified bulb-tees, there is not a significant difference in the prediction error between curing methods. Since the predicted camber is the same for moist cured and heat cured girders, it is concluded that the measured camber at transfer is significantly less for heat cured girders than for moist cured girders. This discrepancy may be caused by the presence of a thermal gradient within the concrete at

transfer due to the heat curing or by the reduction in the prestressing force discussed in Chapter 5. It may also be due to other unknown factors.

To illustrate the performance of the camber predictions in absolute terms, Figure 7-4 shows the average difference between the predicted and measured camber at transfer for each group of data. From the analysis results shown in the figure, it is clear that the average camber for heat cured box beams and cored slabs is approximately 1/4" to 1/2" less than predicted. The predictions for the rest of the girder types and for moist cured girders are relatively accurate.

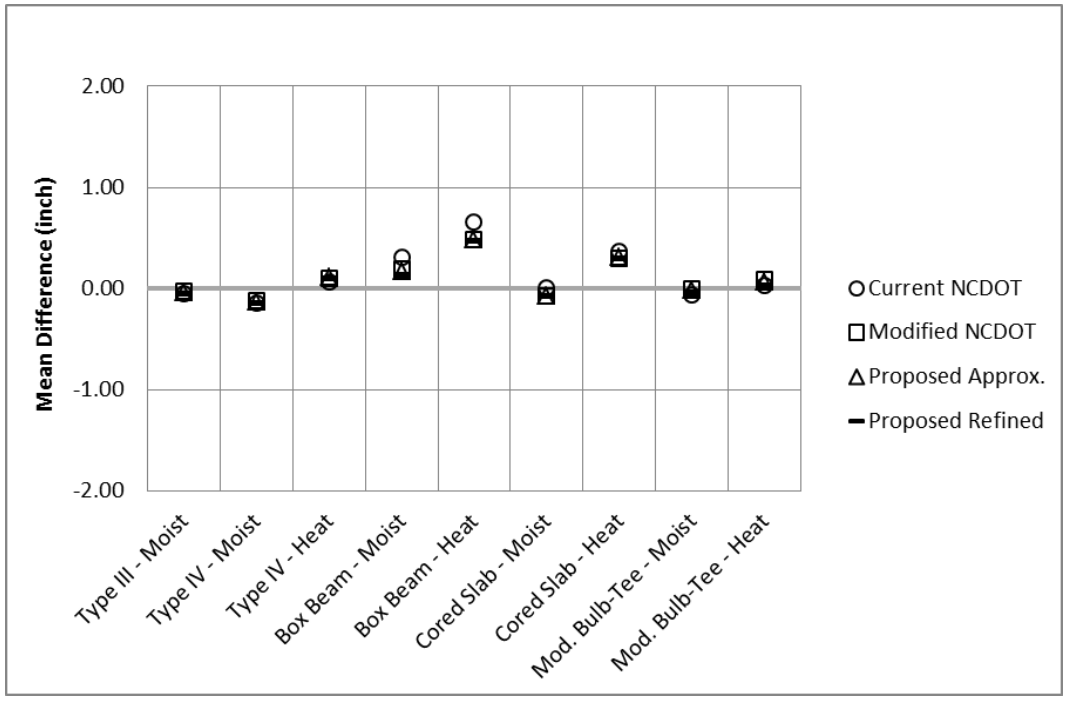

Figure 7-4 Mean difference (predicted camber - measured camber) at prestress transfer.

7.3.3 Camber at 24 Days and Later

The data for camber measurements taken at 24 days or more after casting provide a more reliable comparison for the performance of the prediction methods since the bilinear approximations of the prediction curves more closely represent the realistic camber growth

during this time. This analysis is of primary importance since the focus for this research is to improve the prediction of the camber at the time of girder erection, which typically occurs several weeks after casting.

The analysis indicates that both the proposed approximate method and the proposed refined method provide significant improvement to the camber predictions compared to the current NCDOT method and the modified NCDOT method, as shown by the data in Table 7-1 and Figure 7-5. The most significant improvement to the predictions was seen for the box beams and cored slabs. When the proposed refined method is used, the average error for these girder types is reduced to nearly 0%, compared to an error of between 50% and 90% for the current NCDOT method. When the proposed approximate method is used, the average error is between 13% and 30% for these girder types.

Table 7-1 Average relative percent error for camber measurements taken at 24 days or later.

		No. of Data Points	Current NCDOT	Modified NCDOT	Proposed Approx.	Proposed Refined
Type III	Type III Moist	8	21%	26%	10%	-8%
	Type III Heat	0				
Type IV	Type IV Moist	16	16%	18%	-4%	-23%
	Type IV Heat	8	30%	35%	15%	-4%
Box Beam	Box Beam Moist	11	57%	40%	14%	-7%
	Box Beam Heat	142	90%	59%	30%	4%
Cored Slab	Cored Slab Moist	74	60%	45%	19%	-1%
	Cored Slab Heat	114	49%	35%	13%	-6%
Modified Bulb-Tee	Mod. Bulb-Tee Moist	26	38%	43%	18%	-8%
	Mod. Bulb-Tee Heat	27	5%	8%	-5%	-26%
All Girder Types	All Moist	135	43%	39%	14%	-8%
	All Heat	291	57%	40%	17%	-6%
	All	**426**	**52%**	**39%**	**16%**	**-6%**

It is apparent from Figure 7-5 that the proposed approximate method and the proposed refined method both provide significantly improved predictions of camber compared to the current NCDOT method.

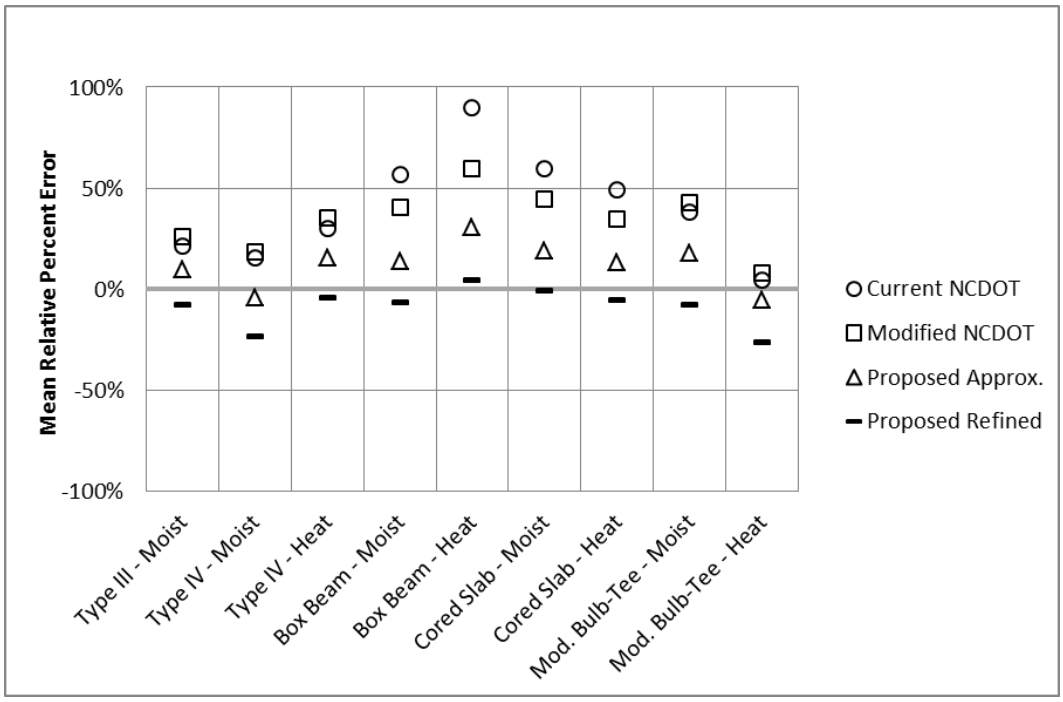

Figure 7-5 Mean relative percent error of the camber predictions for measurements taken at 24 days or later.

The averages of the difference between the predicted and measured camber for measurements taken at 24 days or later are shown in Figure 7-6. The analysis indicates that the proposed refined method provides the best overall prediction of camber with the exceptions of moist cured Type IV girders and heat cured modified bulb-tees, for which it underestimates the camber by an average of 1/2" and 1", respectively. The proposed approximate method overestimates camber by 1/4" to 1/2" for most girder types. The current NCDOT method and the modified NCDOT method overestimate the camber by 1/4" to 1 1/2" depending on the girder type.

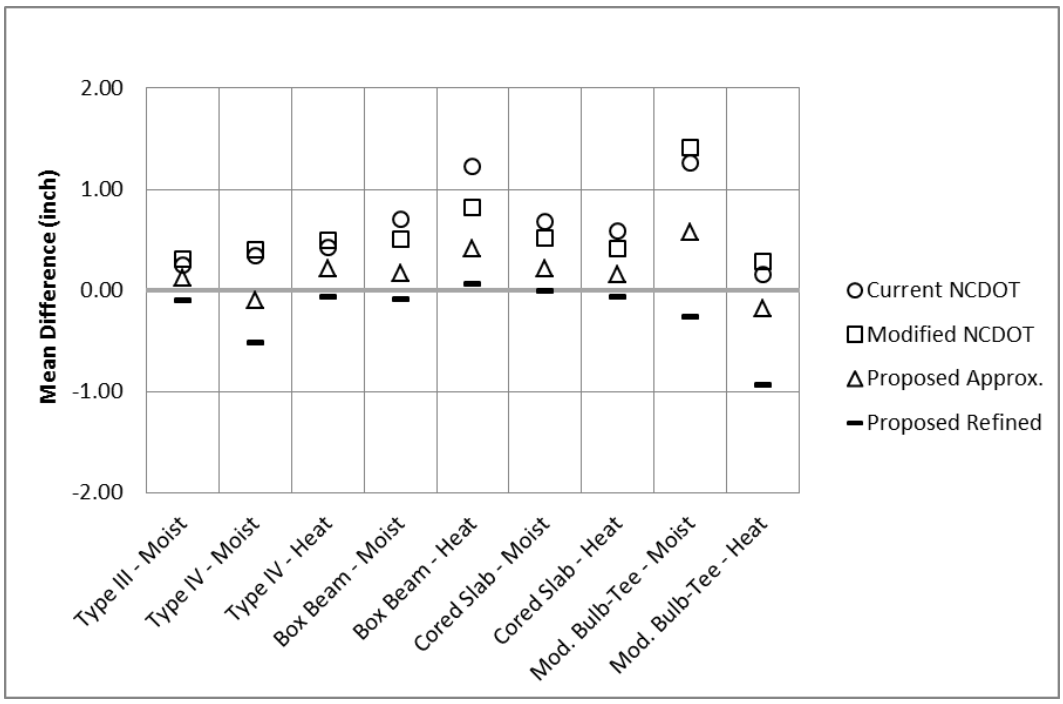

Figure 7-6 Mean difference (predicted camber - measured camber) at 24 days or later.

Based on this analysis, the proposed refine method is recommended as the most accurate camber prediction method. The proposed approximate method is recommended when simpler calculations are desired, since it does not require calculation of time-dependent losses.

7.3.4 Evaluation of Camber Data from Site Visits

The camber measurements made by the research team during the site visits support the conclusions reached in the previous sections. The measurements for the observed cored slabs show that camber varies significantly, especially at early ages, even for identical girders cast in the same casting bed, as shown in Figure 7-7 and Figure 7-8.

In addition, the comparison of the measured to predicted camber for the observed box beams shows that the current NCDOT method tends to overestimate camber, while the proposed approximate method and the proposed refined method provide improved predictions, as shown in Figure 7-9 and Figure 7-10.

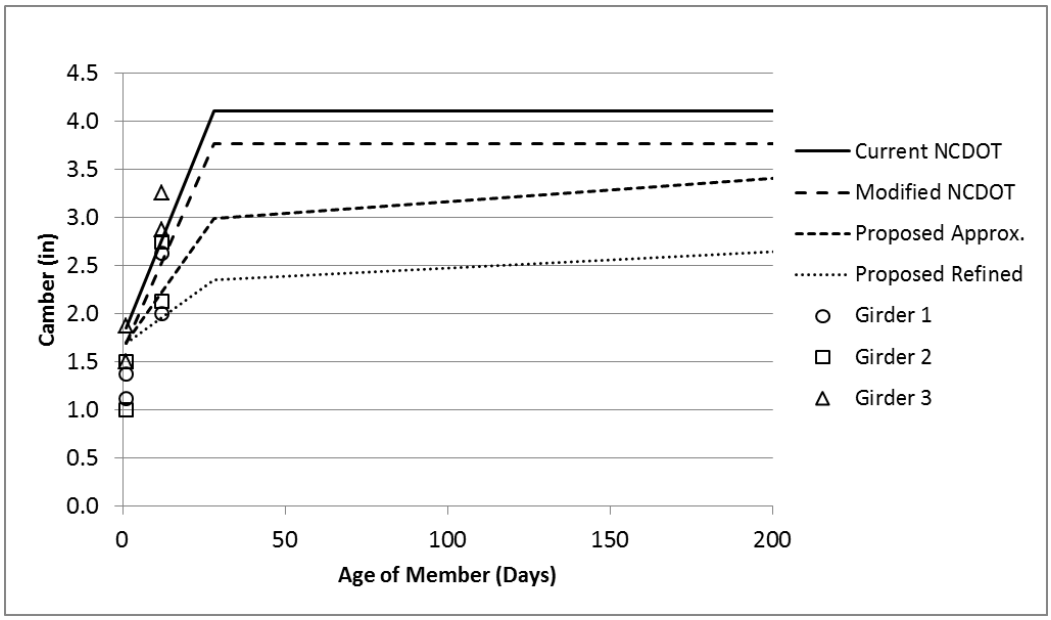

Figure 7-7 Predicted and measured cambers for three identical cored slabs observed during site visits to Utility Precast in Concord, NC. The camber varies widely at early ages.

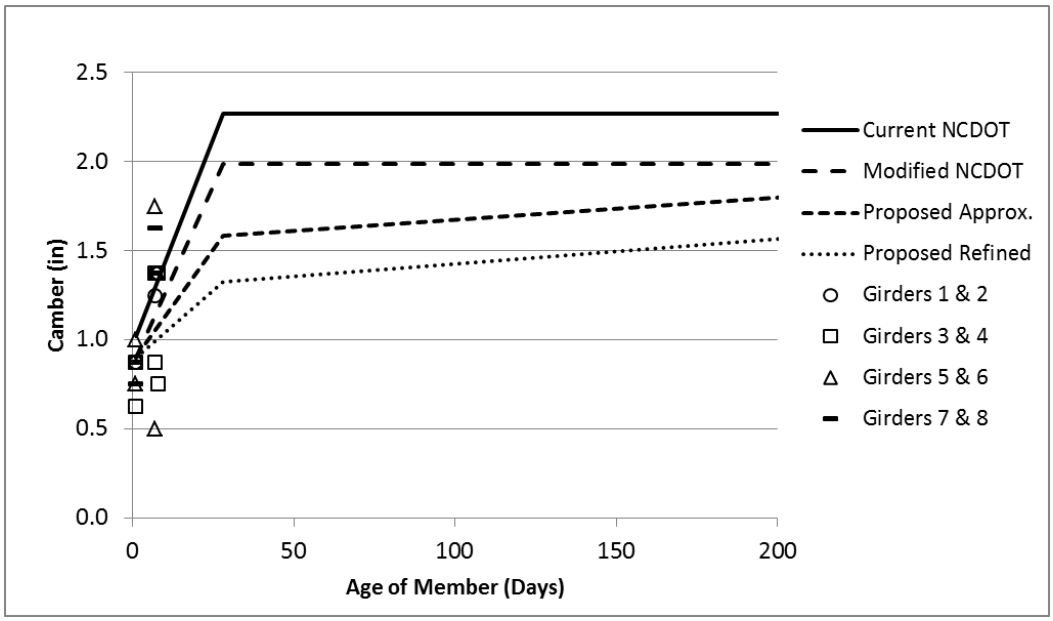

Figure 7-8 Predicted and measured cambers for eight identical cored slabs observed during site visits to S&G Prestress in Wilmington, NC. The camber varies widely at early ages.

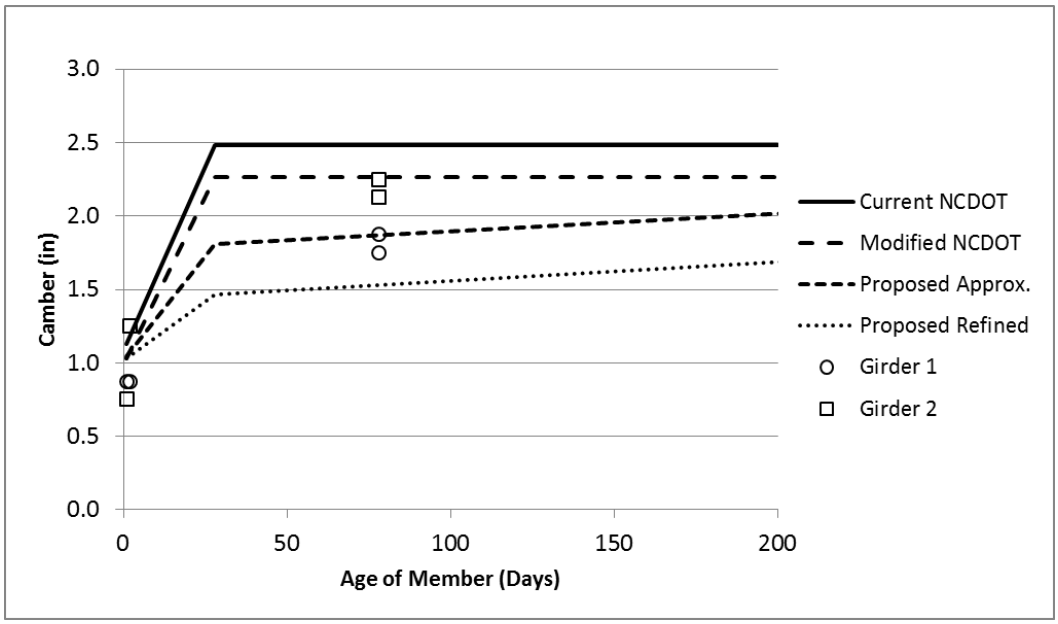

Figure 7-9 Predicted and measured cambers for two identical box beams observed during site visits to Ross Prestress in Bristol, TN. The proposed methods provide improved predictions of camber compared to the current NCDOT method.

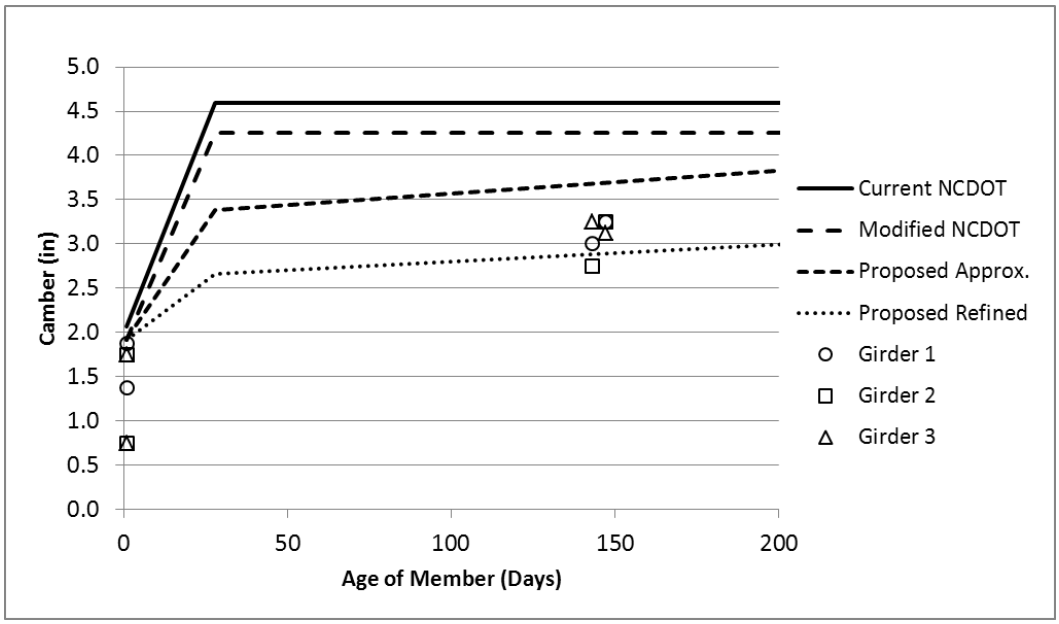

Figure 7-10 Predicted and measured cambers for three identical box beams observed during site visits to Eastern Vault in Princeton, WV. The proposed methods provide improved predictions of camber compared to the current NCDOT method.

8 CONCLUSIONS AND RECOMMENDATIONS

8.1 Conclusions

Based on the field measurements collected by NCDOT personnel, site visits by the research team, consultation with transportation authorities in other states, material tests conducted at NCSU, and the comprehensive analysis of various prediction methods provided in the literature, the major findings and conclusions of this research are summarized as follows:

1) Many factors related to the design of girders as well as the production process can have significant impacts on the prediction of camber and prestress losses. These factors include the following:

    a) *Debonding and transfer length.* Neglecting the reduced curvature at the ends of the girder due to debonding and transfer length can result in overestimation of camber. For most girders, the effect on camber is less than 3%. However, for girders with especially long debonded lengths (10 feet or greater), the camber may be overestimated by as much as 13% if this effect is not considered.

    b) *Temperature of the strands.* The prestressing force can undergo significant fluctuations between the time of tensioning and the time of prestress transfer due to temperature changes in the strands caused by the ambient temperature, solar effects, and concrete curing temperatures. This can affect the camber of the girder.

    c) *Concrete properties.* The accurate estimation of the concrete properties is essential to obtaining reliable predictions of camber and prestress losses. NCDOT currently uses the specified concrete strength in the predictions, which is often significantly different from the actual concrete strength of the girder. A survey of cylinder test data as well as tests conducted by the research team showed that the actual concrete strength at transfer was on

average 25% higher than the specified strength for transfer, while the concrete strength at 28 days was 45% higher than the specified 28-day strength. The cylinder tests also revealed that the elastic modulus for locally produced girders was on average 85% of the value predicted using the AASHTO equation. In addition, concrete properties can vary from girder to girder on the same casting bed since multiple batches of concrete are used for a single casting.

d) *Void deformation.* The deformation of the internal voids for box beams and cored slabs caused by hydrostatic pressure of the fresh concrete during casting can lead to overestimation of the camber by as much as 25% depending on the shape and size of the section. Camber predictions were improved when the section properties were modified to account for this factor.

e) *Temperature of the concrete.* Temporary thermal gradients through the depth of the girder caused by heat curing or solar effects can result in temporary changes in camber. This effect is most severe for box beams and cored slabs.

f) *Curing method.* The camber of girders at the time of prestress transfer can be significantly affected by the curing method used. Heat cured girders other than modified bulb-tees tend to have significantly less camber at transfer than moist cured girders, although there does not seem to be a significant difference in the camber at later stages, suggesting that the discrepancy could be due to temporary thermal gradients.

g) *Girder transport.* On occasion, camber was found to decrease slightly during transport from the storage yard to the jobsite, likely due to the dissipation of a thermal gradient within the girder.

h) *Project scheduling.* Girders that experience different amounts of time between casting and prestress transfer or between transfer and girder erection can have different cambers.

2) Due to the variations in production, some of which are unpredictable, the measured camber was observed to vary significantly among girders that were otherwise identical in design.

3) The measured camber at the time of transfer should not be used as a reliable indicator of the camber at later stages due to the variability caused by rapidly changing concrete properties and by temperature effects.

4) The current NCDOT method was shown to significantly overestimate the camber for most girder types. Camber was overestimated by an average of 52% among all of the girders studied.

5) The modified NCDOT method provided improved camber predictions compared to the current NCDOT method, but it still overestimated the camber by an average of 39% among all of the girders studied.

6) The proposed approximate method overestimated camber by an average of 16% among all of the girders studied, which was significantly better than the NCDOT methods.

7) The proposed refined method provided the best estimates of camber for most girder types. It underestimated camber by an average of only 6% among all of the girders studied, although it underestimated the camber by an average of approximately 25% for steam cured modified bulb-tee girders and moist cured Type IV girders.

8.2 Recommendations for Practice

Based on the findings of this research, the following design and production practices are recommended:

1) For deflection calculations, the specified concrete strength at transfer should be increased by 25%. The specified 28-day concrete strength should be increased by

45%. These changes account for the average relationship between specified and actual concrete strength.

2) The concrete unit weight should be assumed to be 150 lbs/ft^3.

3) To estimate elastic modulus, the equation provided in the 2010 AASHTO specifications should be multiplied by 0.85 and should be calculated using the adjusted concrete strength and the recommended unit weight of 150 lbs/ft^3.

4) The section properties of box beams and cored slabs should be adjusted to account for the void deformation caused by the hydrostatic pressure of the fresh concrete during casting. For girders made using typical void materials used at the time of this research, which includes paper tubes for cored slabs and EPS foam with 170 psi elastic modulus for box beams, the properties provided in Appendix A are recommended. The designer should also consider the effects of these modified properties in stress and strength assessments. As an alternative to adjusting the properties, the designer may specify void materials that are significantly stiffer than current materials.

5) If an internal hold-down system is used for box beams or cored slabs such that the internal voids are connected to the strands, it should be verified that the buoyancy force is not shifting the strands upward during casting.

6) The effect of debonding and transfer length should be accounted for in the camber predictions. The calculations for the proposed methods provided in Chapter 6 include this adjustment.

7) The proposed refined method provided in Section 6.5 should be used to predict camber. The proposed approximate method provided in Section 6.4 may be used to predict camber when a simple rough estimate is desired. The elastic shortening loss used in the approximate method may be calculated according to the AASHTO 2010 method instead of the PCI method, since this will not significantly affect the camber predictions and will provide consistency with the losses calculations that are performed for the proposed refined method.

8) Whenever practical, camber should be measured before dawn before the sun induces thermal gradients within the girders.

9) Girders should be stored with the supports as close as possible to their design bearing locations to minimize camber variability.

8.3 Recommendations for Future Research

The following topics for future research are recommended:

1) The effects of the strand temperature on the prestressing force should be analyzed in further detail. Field measurements as well as laboratory testing are required to determine how the prestressing force within the girder changes before and after the strands are released for both moist cured and heat cured girders.

2) Further research should be performed to ensure that the void deformation in box beams is not more severe than was estimated in this study. This could include cutting open a trial girder to view the deformed section directly. Analysis could also consist of detailed modeling of the effects of the hydrostatic pressure on the voids, including non-linear local effects at the hold-down supports.

3) The effect of void deformation should be analyzed further with respect to the flexural performance and limit-states of the girder.

9 IMPLEMENTATION AND TECHNOLOGY TRANSFER PLAN

The research team proposes the following for the implementation of the research findings and recommendations:

1) As proposed, the research team has prepared three spreadsheet files that can be used to predict prestress losses and camber for typical prestressed girders. The three files are:

   Camber and Losses (Proposed Approximate Method).xlsx

   This file predicts camber and prestress losses using only the proposed approximate method presented in Chapter 6.

   Camber and Losses (Proposed Refined Method).xlsx

   This file predicts camber and prestress losses using only the proposed refined method presented in Chapter 6.

   Camber and Losses (All Methods).xlsx

   This file predicts camber and prestress losses using each of the four methods considered in this report, including the current NCDOT method, the modified NCDOT method, the proposed approximate method, and the proposed refined method.

2) The research team has developed an additional spreadsheet file, **Modified Section Properties.xlsx**, that can be used to calculate the modified section properties of typical box beams and cored slabs by accounting for the effects of void deformation. This file was used to calculate the proposed section properties provided in Appendix A.

3) The final report includes a disc containing these files as well as camber data and cylinder test data. The research team is prepared to organize a workshop to demonstrate the use of the files for NCDOT engineers at their convenience.
4) An abstract of this research has been accepted for presentation and publication at the upcoming 2011 PCI Annual Convention and National Bridge Conference in Salt Lake City, Utah. The research team also plans to present the research findings in a comprehensive paper to be submitted to the PCI Journal for possible publication later this year.

10 REFERENCES

AASHTO. (2004). *AASHTO LRFD Bridge Design Specifications* (3rd ed.). Washington, DC: American Association of State Highway Transportation Officials.

AASHTO. (2006). *AASHTO LRFD Bridge Design Specifications: 2005-2006 Interim Revisions.* Washington, DC: American Association of State Highway and Transportation Officials.

ACI Committee 435. (1995). *Control of Deflection in Concrete Structures (ACI 435R-95).* Farmington Hills, MI: American Concrete Institute.

Ahlborn, T. M., French, C. E., & Leon, R. T. (1995). Applications of High-Strength Concrete to Long-Span Prestressed Bridge Girders. *Transportation Research Record*(1476), 22-30.

Bruce, R. N., Russell, H. G., Roller, J. J., & Hassett, B. M. (2001). *"Implementation of High Performance Concrete in Louisiana Bridges" (Report No. 310).* Baton Rouge, LA: Louisiana Transportation Research Center.

Byle, K. A., Burns, N. H., & Carrasquillo, R. L. (1997). *Time-Dependent Deformation Behavior of Prestressed High Performance Concrete Bridge Beams.* Austin, TX: Texas Department of Transportation.

Chen, Z., Liu, Z., & Sun, G. (2011). Thermal Behavior of Steel Cables in Prestressed Steel Structures. *Journal of Materials in Civil Engineering, 1*, 250.

Kelly, D., Bradbury, T., & Breen, J. (1987). *Time-Dependent Deflections of Pretensioned Beams.* Austin, TX: Center for Transportation Research.

Martin, L. D. (1977). A Rational Method for Estimating Camber and Deflection of Precast Prestressed Members. *PCI Journal*, 100-108.

PCI. (2004). *PCI Design Handbook* (6th ed.). Chicago, IL: Precast/Prestressed Concrete Institute.

Roller, J. J., & Russell, H. G. (2003, March-April). Effect of Curing Temperatures on High Strength Concrete Bridge Girders. *PCI Journal*, 72-79.

Stallings, J. M., & Eskildsen, S. (2001). *Camber and Prestress Losses in High Performance Concrete Bridge Girders (Research Report ALDOT 930-373).* Auburn, AL: Highway Research Center, Auburn University.

Tadros, M. K., Al-Omaishi, N., Seguirant, S., & Gallt, J. (2003). *Prestress Losses in Pretensioned High-Strength Concrete Bridge Girders (NCHRP report no. 496).* Washington, DC: National Cooperative Highway Research Program.

Tadros, M. K., Fawzy, F., & Hanna, K. (2011). Precast, Prestressed Girder Camber Variability. *PCI Journal*, 135-154.

Zia, P., Preston, H. K., Scott, N. L., & Workman, E. B. (1979). Estimating Prestress Losses. *Concrete International*, 32-38.

APPENDICES

Appendix A Proposed Modification of the Section Properties to Account for Void Deformation

This section presents the recommended section properties of the prestressed girder sections considered in this study to account for the deformation of the void forms that occurs during casting due to the local deformation, flexural deflection, and compressive deformation of the voids caused by the fresh concrete. The modified properties are calculated based on the use of typical void materials in use at the time of this study, which includes paper tubes for cored slabs and EPS foam blocks with an elastic modulus of 170 psi for box beams. Other assumptions used to calculate the modified section properties of the box beams and cored slabs are also presented in this section, along with examples of the evaluation of the effect of void deformation on the camber.

Since AASHTO girders and modified bulb-tee girders do not have internal voids, the section properties are not modified. However, for completeness, the original design section properties for these girder types are also presented.

The section properties presented in this section have the following notation:

A_g	area of the gross section
I_g	moment of inertia of the gross section
y_c	vertical distance from the centroid of the gross section to the bottom fibers
w_g	uniformly distributed dead load due to girder self-weight
V/S	volume-to-surface area ratio; for girders with internal voids, only half of the internal surface area is included.

A.1 AASHTO Girders

Since AASHTO girders do not have internal voids, the section properties are not modified to account for void deformation. The original section properties for these girders are given in Table A-1.

Table A-1 Original section properties of AASHTO girders.

	Girder Type	
	Type III	**Type IV**
A_g (in^2)	559.5	789
I_g (in^4)	125390	260741
y_c (in)	20.270	24.730
w_g (lb/ft)	583.0	822.0
V/S (in)	4.056	3.140

A.2 Modified Bulb-Tee Girders

Since modified bulb-tee girders do not have internal voids, the section properties are not modified to account for void deformation. The original section properties for these girders are given in Table A-2.

Table A-2 Original section properties of modified bulb-tee girders.

	Modified Bulb-Tee (Depth)	
	63"	**72"**
A_g (in^2)	770.1	833.1
I_g (in^4)	408315	570260
y_c (in)	32.290	36.790
w_g (lb/ft)	802.0	868.0
V/S (in)	3.246	3.264

A.3 Cored Slabs

Measurements taken during the site visits to the precasting plants were used to estimate the distance that the void tubes used for cored slabs shift upward during casting due to local deformation at the hold-down supports and flexural deflection between the supports caused by the buoyancy of the voids in the fresh concrete. Large diameter voids were found to shift upward more than smaller voids due to their greater buoyancy and reduced local stiffness. It was observed that 8-inch diameter voids were have an average upward shift of 1/2”; 10-inch diameter voids have an average upward shift of 5/8”; and 12-inch diameter voids have an average upward shift of 3/4” based on the measured local deformation and flexural deflection.

Six unique cored slab sections were considered. The original and modified section properties as well as the percent change in the properties due to the modifications are given in Table A-3.

Table A-3 Original and modified section properties of cored slabs.

	Cored Slab Depth/Void Diameter					
	18"/10"			**21"/8"**		
	Original	**Modified**	**% Change**	**Original**	**Modified**	**% Change**
A_g (in^2)	483.4	483.4	0.0%	647.9	647.9	0.0%
I_g (in^4)	16286	16189	-0.6%	27019	26982	-0.1%
y_c (in)	8.920	8.717	-2.3%	10.423	10.345	-0.7%
w_g (lb/ft)	503.5	503.5	0.0%	674.9	674.9	0.0%
V/S (in)	3.467	3.467	0.0%	4.657	4.657	0.0%

	Cored Slab Depth/Void Diameter					
	21"/10"			**21"/12"**		
	Original	**Modified**	**% Change**	**Original**	**Modified**	**% Change**
A_g (in^2)	591.4	591.4	0.0%	522.3	522.3	0.0%
I_g (in^4)	26439	26345	-0.4%	25384	25169	-0.8%
y_c (in)	10.415	10.249	-1.6%	10.404	10.079	-3.1%
w_g (lb/ft)	616.0	616.0	0.0%	544.0	544.0	0.0%
V/S (in)	4.067	4.067	0.0%	3.443	3.443	0.0%

	Cored Slab Depth/Void Diameter					
	24"/12"			**26"/12"**		
	Original	**Modified**	**% Change**	**Original**	**Modified**	**% Change**
A_g (in^2)	630.3	630.3	0.0%	702.3	702.3	0.0%
I_g (in^4)	38905	38699	-0.5%	49775	50022	0.5%
y_c (in)	11.902	11.633	-2.3%	13.224	12.982	-1.8%
w_g (lb/ft)	656.5	656.5	0.0%	731.5	731.5	0.0%
V/S (in)	3.997	3.997	0.0%	4.390	4.390	0.0%

Using the modified section properties in Table A-3 provided improved accuracy in the camber predictions when compared to field measurements. The following example provides a numerical illustration to highlight the effect of the deformation of the voids.

Example

This example determines the effect that the void deformation has on the camber of typical cored slabs due to the buoyancy of the voids in the fresh concrete during casting. For simplicity, the effects of debonding and transfer length are ignored.

The cored slab considered has the following properties:

depth	21 in	
void diameter	12 in	
P_i	700540 lbs	
y_c	original: 10.404 in	modified: 10.079 in
y_{ps}	4.412 in	
L	600 in (50 ft)	
w_g	45.33 lb/in (544 lb/ft)	
E_{ci}	3.99x10^6 psi	
I_g	original: 25384 in^4	modified: 25169 in^4

Initial net camber, calculated using the original properties:

$$\Delta_{ps,i} = \frac{P_i e L^2}{8 E_{ci} I_g} = \frac{(700540)(10.404 - 4.412)(600^2)}{(8)(3.99x10^6)(25384)} = 1.87\ in$$

$$\Delta_{sw,i} = \frac{5 w_g L^4}{384 E_{ci} I_g} = \frac{(5)(45.33)(600^4)}{(384)(3.99x10^6)(25384)} = 0.76\ in$$

$$\Delta_{net,i} = \Delta_{ps,i} - \Delta_{sw,i} = 1.87 - 0.76 = \mathbf{1.11\ in}$$

Initial net camber, calculated using the modified properties:

$$\Delta_{ps,i} = \frac{(700540)(10.079 - 4.412)(600^2)}{(8)(3.99x10^6)(25169)} = 1.78\ in$$

$$\Delta_{sw,i} = \frac{(5)(45.33)(600^4)}{(384)(3.99x10^6)(25169)} = 0.76\ in$$

$$\Delta_{net,i} = 1.78 - 0.76 = \mathbf{1.02\ in}$$

The percent change in net camber resulting from using the modified section properties to account for the effect of void deformation is as follows:

$$\frac{1.02}{1.11} - 1 = -0.08 = \mathbf{-8}\%$$

In this example, the initial net camber was reduced by 8% due to the deformation of the voids in this sample cored slab during casting. The typical reduction in camber among all of the cored slabs considered in the study ranged from 5% to 12%. In addition, since the creep is proportional to the initial stresses, the effect on the long-term camber is expected to be proportional to the initial effects.

A.4 Box Beams

Similar to the analysis used for cored slabs, the box beam analysis considers the local deformation of the voids at the hold-down supports and the flexural deflection between the hold-down supports. In this case, however, the compressive deformation of the void form used for the box beam due to the hydrostatic pressure of the fresh concrete must also be considered. The modified section properties of the three standard box beam sections considered in this study were calculated. Based on field measurements, the voids were found to shift upward by 1/4" due to local deformation. The flexural deflection of the void form was calculated using elastic beam theory. The net hydrostatic pressure pushing upward on the void was calculated by analyzing the voids as an inverted continuous span with hold-downs at 48 inches apart. The average elastic modulus of the expanded polystyrene (EPS) material used for the void forms was assumed to be 170 psi based on data from the manufacturers, which was verified by lab tests conducted at NCSU. Linear behavior of the material under the anticipated loads was also verified. (See Appendix F for details of the testing.) The average flexural deflection was assumed to be 50% of the maximum calculated deflection. The compressive deformation of the void in the horizontal direction was determined by applying the linearly varying hydrostatic pressure to the sides of the void. The vertical compressive deformation was calculated by assuming that the void is subject to uniform compression equal to the net hydrostatic pressure acting on the void. Figure A-1 illustrates the profile of the assumed hydrostatic loading and the deformed shape.

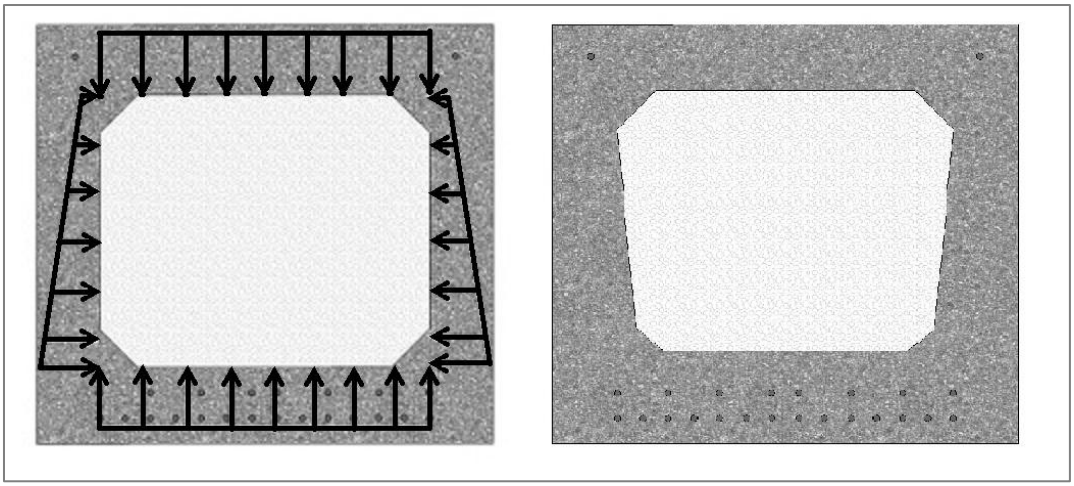

Figure A-1 Distribution of the hydrostatic pressure on the internal foam void of the box beam and the resulting deformed section.

The original and modified section properties for the box beams as well as the percent change in the properties resulting from the modifications are given in Table A-4.

Table A-4 Original and modified section properties of box beams.

Box Beam (Depth)	Property	Original	Modified	% Change
27 in	A_g (in^2)	574.3	581.3	1.2%
	I_g (in^4)	51007	50913	-0.2%
	y_c (in)	13.182	12.851	-2.5%
	w_g (lb/ft)	598.2	605.5	1.2%
	V/S (in)	3.502	3.502	0.0%
33 in	A_g (in^2)	634.3	646.5	1.9%
	I_g (in^4)	86465	86912	0.5%
	y_c (in)	16.090	15.686	-2.5%
	w_g (lb/ft)	660.7	673.5	1.9%
	V/S (in)	3.485	3.485	0.0%
39 in	A_g (in^2)	694.3	713.2	2.7%
	I_g (in^4)	133302	134993	1.3%
	y_c (in)	19.015	18.492	-2.7%
	w_g (lb/ft)	723.2	742.9	2.7%
	V/S (in)	3.471	3.471	0.0%

Using the modified section properties in Table A-4 provided improved accuracy in the camber predictions when compared to field measurements. The following example provides a numerical illustration to highlight the effect of the deformation of the voids on the camber of box beams.

Example

This example illustrates the effect that the void deformation during casting has on the camber of a given box beam. For simplicity, the effects of debonding and transfer length are ignored.

The box beam considered has the following properties:

depth	39 in	
P_i	1158208 lbs	
y_c	original: 19.015 in	modified: 18.492 in
y_{ps}	7.714 in	
L	1200 in (100 ft)	
w_g	original: 60.26 lb/in (723.2 lb/ft)	modified: 61.91 lb/in (742.9 lb/ft)
E_{ci}	4.29×10^6 psi	
I_g	original: 133302 in^4	modified: 134993 in^4

The initial net camber, calculated using the original section properties:

$$\Delta_{ps,i} = \frac{P_i e L^2}{8 E_{ci} I_g} = \frac{(1158208)(19.015 - 7.714)(1200^2)}{(8)(4.29x10^6)(133302)} = 4.12\ in$$

$$\Delta_{sw,i} = \frac{5 w_g L^4}{384 E_{ci} I_g} = \frac{(5)(60.26)(1200^4)}{(384)(4.29x10^6)(133302)} = 2.85\ in$$

$$\Delta_{net,i} = \Delta_{ps,i} - \Delta_{sw,i} = 4.12 - 2.85 = \mathbf{1.27\ in}$$

The initial net camber, calculated using the modified section properties:

$$\Delta_{ps,i} = \frac{P_i e L^2}{8 E_{ci} I_g} = \frac{(1158208)(18.492 - 7.714)(1200^2)}{(8)(4.29x10^6)(134993)} = 3.88\ in$$

$$\Delta_{sw,i} = \frac{5w_g L^4}{384E_{ci}I_g} = \frac{(5)(61.92)(1200^4)}{(384)(4.29x10^6)(134993)} = 2.89\ in$$

$$\Delta_{net,i} = \Delta_{ps,i} - \Delta_{sw,i} = 3.88 - 2.89 = \mathbf{0.99\ in}$$

The percent change in net camber resulting from the use of the modified section properties to account for the effect of void deformation:

$$\frac{0.99}{1.27} - 1 = -0.22 = -\mathbf{22}\%$$

This example illustrates that the local deformation, flexural deflection, and compressive deformation of the EPS foam void due to hydrostatic pressure caused by the fresh concrete during casting reduces the predicted initial net camber of the example box beam by 22%. The typical percent change in net camber among all of the box beams considered in the study ranged from 5% to 10% for 27-inch box beams, from 15% to 25% for 33-inch box beams, and from 20% to 25% for 39-inch box beams.

Appendix B Example: Prediction of Prestress Losses and Camber

The following example illustrates the calculation of the prestress losses and camber for a modified bulb-tee girder with harped strands using the four prediction models considered in this report, including the current NCDOT method (Chapter 3), the modified NCDOT method (Chapter 6), the proposed approximate method (Chapter 6), and the proposed refined method (Chapter 6). For each method, the camber is determined for transfer, 28 days, and 1 year assuming that the girder erection has not occurred.

The following information is needed:

Identification

Project #	R-2301A
County	Jones-Craven
Member Type	72in MBT (metric)
PC #	
Span	B
INT/EXT	

Environmental Factors

H (%)	70

Member Properties

L_m (member) (ft)	123.819
L_s (span) (ft)	122.375
A_g (in^2)	833.100
y_c (in)	36.790
I_g (in^4)	570260
d (in)	72.000
V/S	3.264

Concrete Properties

w_c (pcf)	150
f'_{ci} (psi)	7200
f'_c (psi)	9500

Debond Length

L_{db} (ft)	0

Prestressing Properties

f_{pu} (ksi)	270
E_p (psi)	2.850E+07
D_{ps} (strand Dia.) (in)	0.600
n_{str}	46
y_{psm} (in)	8.609
y_{pse} (in)	18.347
x_h (ft from CL)	5.000

Time Steps

t_i (days)	1
t_1 (days)	28
t_2 (days)	365

Diaphragm

# of Diaphragms	0
Length (each, inch, longitudinal direction of member)	0
D1 (ft)	0.000
D2 (ft)	0.000
D3 (ft)	0.000
D4 (ft)	0.000

Loads

w_g (self-wt) (lb/ft)	868
w_{sd} (SI Dead) (lb/ft)	0

B.1 Current NCDOT method

Using the current NCDOT method, the prestress losses and camber for the example girder given at the beginning of this appendix are predicted as follows:

1) Estimated elastic modulus of the concrete at prestress transfer (E_{ci}) and at 28 days (E_c):

$$E_{ci} = 33 w_c^{1.5} \sqrt{f'_{ci}}$$
$$= (33)(150\ pcf)^{1.5} \sqrt{7200\ psi}$$
$$= 5144190.9\ psi$$
$$E_c = 33 w_c^{1.5} \sqrt{f'_c}$$
$$= (33)(150\ pcf)^{1.5} \sqrt{9500\ psi}$$
$$= 5908981.5\ psi$$

2) Moment at midspan due to self-weight:

$$M_g = \frac{w_g L_m^2}{8} + M_{diaphragm}$$
$$= \frac{\left(868 \frac{\text{lb}}{\text{ft}}\right) (123.819\ \text{ft})^2}{8} + 0$$
$$= 1663429\ lb - ft$$
$$= 19961148\ lb - in$$

3) Eccentricity of the prestressing strands at midspan (e_m) and at the end of the girder (e_e):

$$e_m = y_c - y_{psm}$$
$$= 36.790\ in - 8.609\ in$$
$$= 28.181\ in$$
$$e_e = y_c - y_{pse}$$
$$= 36.790\ in - 18.347\ in$$

$$= 18.443\ in$$

4) The cross-sectional area for a 0.6-in prestressing strand is 0.217 in^2. Therefore, the total strand area is:

$$A_{ps} = A_{ps,str} n_{str}$$
$$= (0.217\ in^2)(46)$$
$$= 9.982\ in^2$$

5) Specified initial prestressing force before transfer:

$$P_j = 0.75 f_{pu} A_{ps}$$
$$= 0.75(270000\ psi)(9.982\ in^2)$$
$$= 2021355\ lbs$$

6) Prestress loss due to strand relaxation prior to prestress transfer:

$$\Delta f_{pR1} = \frac{log(24.0t)}{40}\left[\frac{f_{pj}}{f_{py}} - 0.55\right] f_{pj}$$
$$= \frac{log(24.0t)}{40}\left[\frac{0.75 * f_{pu}}{0.9 * f_{pu}} - 0.55\right](0.75 * f_{pu})$$
$$= \frac{log(24.0 * 2)}{40}\left[\frac{0.75 * 270000}{0.9 * 270000} - 0.55\right](0.75 * 270000)$$
$$= 2412\ psi$$

7) Prestress loss due to elastic shortening at transfer:

   a. Guess prestress force after transfer (1st iteration):

$$P_i(guess) = 0.7(f_{pu})A_{ps}$$
$$= 0.7(270000\ \text{psi})(9.982\ \text{in}^2)$$
$$= 1886598\ lbs$$

   b. Stress in the concrete at the level of the centroid of the strands (1st iteration):

$$f_{cgp} = \left[\frac{P_i}{A_g} + \frac{P_i e_m^2}{I_g}\right] - \frac{M_g e_m}{I_g}$$

$$= \left[\frac{1886598}{833.10} + \frac{(1886598)(28.181)^2}{570260}\right] - \frac{(19961148)(28.181)}{570260}$$

$$= 3905.5\ psi$$

c. Elastic shortening loss (1st iteration)

$$\Delta f_{pES} = \frac{E_p}{E_{ci}} f_{cgp}$$

$$= \frac{28500000\ psi}{5144190.9\ psi} 3905.5\ psi$$

$$= 21637\ psi$$

d. Prestress force after transfer (2nd iteration):

$$P_i = 2021355\ lbs - (2412\ psi + 21637\ psi)(9.982\ in^2)$$

$$= 1781298\ lbs$$

e. Stress in the concrete at the level of the centroid of the strands (2nd iteration):

$$f_{cgp} = \left[\frac{1781298}{833.10} + \frac{(1781298)(28.181)^2}{570260}\right] - \frac{(19961148)(28.181)}{570260}$$

$$= 3632.4\ psi$$

f. Elastic shortening loss (2nd iteration)

$$f_{pES} = \frac{28500000\ psi}{5144190.9\ psi} 3632.4\ psi$$

$$= 20124.3\ psi$$

g. Prestress force after transfer (3rd iteration):

$$P_i = 2021355\ lbs - (2412\ psi + 20124.3\ psi)(9.982\ in^2)$$

$$= 1796398\ lbs$$

h. Stress in the concrete at the level of the centroid of the strands (3rd iteration):

$$f_{cgp} = \left[\frac{1796398}{833.10} + \frac{(1796398)(28.181)^2}{570260}\right] - \frac{(19961148)(28.181)}{570260}$$

$$= 3671.6\ psi$$

i. Elastic shortening loss (final iteration):

$$f_{pES} = \frac{28500000\ psi}{5144190.9\ psi} 3671.6\ psi$$
$$= 20341.5\ psi$$

8) Prestress force after transfer:

$$P_i = 2021355\ lbs - (2412\ psi + 20341.5\ psi)(9.982\ in^2)$$
$$= 1794230\ lbs$$

9) Prestress loss due to concrete shrinkage:

$$\Delta f_{pSR} = 17.0 - 0.15H$$
$$= 17.0 - 0.15(70)$$
$$= 6.5\ ksi$$
$$= 6500\ psi$$

10) Stress in the concrete at the level of the centroid of the strands due to superimposed dead loads applied at girder erection:

$$f_{cds} = \frac{M_{sd} * e_m}{I_g}$$
$$= \frac{(0)(28.181)}{570260}$$
$$= 0\ psi$$

11) Prestress loss due to creep:

$$\Delta f_{pCR} = 12 f_{cgp} - 7 f_{cds}$$
$$= (12)(3671.6) - 7(0)$$
$$= 44059.2\ psi$$

12) Prestress loss due to strand relaxation that occurs after prestress transfer:

$$\Delta f_{pR2} = 0.3\left[20.0 - 0.4\Delta f_{pES} - 0.2\left(\Delta f_{pSR} + \Delta f_{pCR}\right)\right]$$

$$= 0.3\left[20.0 - 0.4\left(\frac{20341.5}{1000}\right) - 0.2\frac{6500 + 44059.2}{1000}\right]$$
$$= 0.525\ ksi$$
$$= 525\ psi$$

13) Final prestress force:

$$P_f = P_j - A_{ps} * \left(\Delta f_{pES} + \Delta f_{pSR} + \Delta f_{pCR} + \Delta f_{pR2}\right)$$
$$= 2021355 - 9.982 * (20341.5 + 6500 + 44059.2 + 525)$$
$$= 1308384\ lbs$$

14) Camber at prestress transfer:

a. Camber due to prestressing only:

$$\Delta_{ps,i} = \frac{P_i}{E_{ci}I_g}\left(\frac{e_m L_m^2}{8} - (e_m - e_e)\frac{(L_m/2 - x_h)^2}{6}\right)$$
$$= \frac{1794230}{(5144190.9)(570260)}\left(\frac{(28.181)(123.819 * 12)^2}{8} - (28.181 - 18.443)\frac{\left(\frac{123.819 * 12}{2} - (5 * 12)\right)^2}{6}\right)$$
$$= 4.294\ in$$

b. Deflection due to self-weight:

$$\Delta_{sw,i} = \frac{5w_g L_m^4}{384E_{ci}I_g} + \Delta_{diaphragm}$$
$$= \frac{5(868/12)(123.819 * 12)^4}{384(5144190.9)(570260)} + 0$$
$$= 1.565\ in$$

c. Net camber at prestress transfer:

$$\Delta_i = \Delta_{ps,i} - \Delta_{sw,i}$$
$$= 4.294 - 1.565$$

$$= 2.729\ in$$

15) Camber at girder erection (28 days):

$$\Delta_{28} = 2.26\Delta_{ps,i} - 2.31\Delta_{sw,i}$$
$$= 2.26(4.294) - 2.31(1.565)$$
$$= 6.089\ in$$

16) Camber at 1 year equals camber at 28 days for this study:

$$\Delta_{365} = 6.089\ in$$

17) Summary of prestress losses, prestress forces, and camber:

$$\Delta f_{pR1} = 2412\ psi$$
$$\Delta f_{pES} = 20341.5\ psi$$
$$\Delta f_{pSR} = 6500\ psi$$
$$\Delta f_{pCR} = 44059.2\ psi$$
$$\Delta f_{pR2} = 525\ psi$$

$$P_j = 2021355\ lbs$$
$$P_i = 1794230\ lbs$$
$$P_f = 1308384\ lbs$$

$$\Delta_i = 2.729\ in$$
$$\Delta_{28} = 6.089\ in$$
$$\Delta_{365} = 6.089\ in$$

B.2 Modified NCDOT Method

The modified NCDOT method for predicting the prestress losses and camber of prestressed, pretensioned concrete girders is similar to the current NCDOT method except that it uses the adjustments recommended in Section 5.10 to account for the production factors, material properties, and debonding and transfer length. For box beams or cored slabs, this method utilizes the modified section properties recommended in Appendix A. Using this method, the prestress losses and camber for the example girder given at the beginning of this appendix are determined as follows:

1) Estimated concrete compressive strength at transfer (f^*_{ci}) and at 28 days (f^*_c):

$$\begin{aligned} f_{ci}^* &= 1.25 f_{ci}' \\ &= (1.25)7200 \\ &= 9000\ psi \\ f_c^* &= 1.45 f_c' \\ &= (1.45)9500 \\ &= 13775\ psi \end{aligned}$$

2) Estimated elastic modulus of the concrete at prestress transfer (E_{ci}) and at 28 days (E_c):

$$\begin{aligned} E_{ci} &= (0.85)33 w_c^{1.5} \sqrt{f_{ci}^*} \\ &= (0.85)(33)(150\ pcf)^{1.5} \sqrt{9000\ psi} \\ &= 4888673.2\ psi \\ E_c &= (0.85)33 w_c^{1.5} \sqrt{f_c^*} \\ &= (0.85)(33)(150\ pcf)^{1.5} \sqrt{13775\ psi} \\ &= 6048052.6\ psi \end{aligned}$$

3) Moment at midspan due to self-weight:

$$M_g = \frac{w_g L_m^2}{8} + M_{diaphragm}$$

$$= \frac{\left(868 \frac{\text{lb}}{\text{ft}}\right)(123.819 \text{ ft})^2}{8} + 0$$
$$= 1663429\ lb - ft$$
$$= 19961148\ lb - in$$

4) Eccentricity of the prestressing strands at midspan (e_m) and at the end of the girder (e_e):

$$e_m = y_c - y_{psm}$$
$$= 36.790\ in - 8.609\ in$$
$$= 28.181\ in$$
$$e_e = y_c - y_{pse}$$
$$= 36.790\ in - 18.347\ in$$
$$= 18.443\ in$$

5) The cross-sectional area for a 0.6-in prestressing strand is 0.217 in^2. Therefore, the total strand area is:

$$A_{ps} = A_{ps,str} n_{str}$$
$$= (0.217\ in^2)(46)$$
$$= 9.982\ in^2$$

6) Specified initial prestressing force before transfer:

$$P_j = 0.75 f_{pu} A_{ps}$$
$$= 0.75(270000\ psi)(9.982\ in^2)$$
$$= 2021355\ lbs$$

7) Prestress loss due to strand relaxation prior to prestress transfer:

$$\Delta f_{pR1} = \frac{log(24.0t)}{40}\left[\frac{f_{pj}}{f_{py}} - 0.55\right] f_{pj}$$
$$= \frac{log(24.0t)}{40}\left[\frac{0.75 * f_{pu}}{0.9 * f_{pu}} - 0.55\right](0.75 * f_{pu})$$

$$= \frac{log(24.0 * 2)}{40}\left[\frac{0.75 * 270000}{0.9 * 270000} - 0.55\right](0.75 * 270000)$$
$$= 2412\ psi$$

8) Prestress loss due to elastic shortening at transfer:

a. Guess prestress force after transfer (1st iteration):

$$P_i(guess) = 0.7(f_{pu})A_{ps}$$
$$= 0.7(270000\text{ psi})(9.982\text{ in}^2)$$
$$= 1886598\ lbs$$

b. Stress in the concrete at the level of the centroid of the strands (1st iteration):

$$f_{cgp} = \left[\frac{P_i}{A_g} + \frac{P_i e_m^2}{I_g}\right] - \frac{M_g e_m}{I_g}$$
$$= \left[\frac{1886598}{833.10} + \frac{(1886598)(28.181)^2}{570260}\right] - \frac{(19961148)(28.181)}{570260}$$
$$= 3905.5\ psi$$

c. Elastic shortening loss:

$$\Delta f_{pES} = \frac{E_p}{E_{ci}} f_{cgp}$$
$$= \frac{28500000\ psi}{4888673.2\ psi} 3905.5\ psi$$
$$= 22768\ psi$$

d. Prestress force after transfer (2nd iteration):

$$P_i = 2021355\ lbs - (2412\ psi + 22768\ psi)(9.982\ in^2)$$
$$= 1794083\ lbs$$

e. Stress in the concrete at the level of the centroid of the strands (2nd iteration):

$$f_{cgp} = \left[\frac{1794083}{833.10} + \frac{(1794083)(28.181)^2}{570260}\right] - \frac{(19961148)(28.181)}{570260}$$

$$= 3665.6\ psi$$

f. Elastic shortening loss (2nd iteration)

$$f_{pES} = \frac{28500000\ psi}{4888673.2\ psi} 3665.6\ psi$$
$$= 21370\ psi$$

g. Prestress force after transfer (3rd iteration):

$$P_i = 2021355\ lbs - (2412\ psi + 21370\ psi)(9.982\ in^2)$$
$$= 1808043\ lbs$$

h. Stress in the concrete at the level of the centroid of the strands (3rd iteration):

$$f_{cgp} = \left[\frac{1808043}{833.10} + \frac{(1808043)(28.181)^2}{570260}\right] - \frac{(19961148)(28.181)}{570260}$$
$$= 3701.8\ psi$$

i. Elastic shortening loss (final iteration):

$$f_{pES} = \frac{28500000\ psi}{4888673.2\ psi} 3701.8\ psi$$
$$= 21581\ psi$$

9) Prestress force after transfer:

$$P_i = 2021355\ lbs - (2412\ psi + 21581\ psi)(9.982\ in^2)$$
$$= 1781857\ lbs$$

10) Prestress loss due to concrete shrinkage:

$$\Delta f_{pSR} = 17.0 - 0.15H$$
$$= 17.0 - 0.15(70)$$
$$= 6.5\ ksi$$
$$= 6500\ psi$$

11) Stress in the concrete at the level of the centroid of the strands due to superimposed dead loads applied at girder erection:

$$f_{cds} = \frac{M_{sd} * e_m}{I_g}$$
$$= \frac{(0)(28.181)}{570260}$$
$$= 0\ psi$$

12) Prestress loss due to creep:

$$\Delta f_{pCR} = 12 f_{cgp} - 7 f_{cds}$$
$$= (12)(3701.8) - 7(0)$$
$$= 44422\ psi$$

13) Prestress loss due to strand relaxation that occurs after prestress transfer:

$$\Delta f_{pR2} = 0.3\left[20.0 - 0.4\Delta f_{pES} - 0.2\left(\Delta f_{pSR} + \Delta f_{pCR}\right)\right]$$
$$= 0.3\left[20.0 - 0.4\left(\frac{21581}{1000}\right) - 0.2\frac{6500 + 44422}{1000}\right]$$
$$= 0.355\ ksi$$
$$= 355\ psi$$

14) Final prestress force:

$$P_f = P_j - A_{ps} * \left(\Delta f_{pES} + \Delta f_{pSR} + \Delta f_{pCR} + \Delta f_{pR2}\right)$$
$$= 2021355 - 9.982 * (21581 + 6500 + 44422 + 355)$$
$$= 1294086\ lbs$$

15) Camber at prestress transfer:

a. Camber due to prestressing only:

$$\Delta_{ps,i} = \frac{P_i}{E_{ci} I_g}\left(\frac{e_m L_m^2}{8} - (e_m - e_e)\frac{\left(\frac{L_m}{2} - x_h\right)^2}{6} - \frac{e_m (L_{db} + L_t)^2}{6}\right)$$

$$= \frac{1781857}{(4888673.2)(570260)}\left(\frac{(28.181)(123.819*12)^2}{8} - (28.181-18.443)\frac{\left(\frac{123.819*12}{2}-(5*12)\right)^2}{6} - \frac{28.181(0*12+36)^2}{6}\right)$$

$$= 4.483\ in$$

b. Deflection due to self-weight:

$$\Delta_{sw,i} = \frac{5w_g L_m^4}{384E_{ci}I_g} + \Delta_{diaphragm}$$

$$= \frac{5(868/12)(123.819*12)^4}{384(4888673.2)(570260)} + 0$$

$$= 1.647\ in$$

c. Net camber at prestress transfer:

$$\Delta_i = \Delta_{ps,i} - \Delta_{sw,i}$$

$$= 4.483 - 1.647$$

$$= 2.836\ in$$

16) Camber at girder erection (28 days):

$$\Delta_{28} = 2.26\Delta_{ps,i} - 2.31\Delta_{sw,i}$$

$$= 2.26(4.483) - 2.31(1.647)$$

$$= 6.327\ in$$

17) Camber at 1 year is assumed equal to camber at 28 days for this study:

$$\Delta_{365} = 6.327\ in$$

18) Summary of prestress losses, prestress forces, and camber:

$\Delta f_{pR1} = 2412\ psi$

$\Delta f_{pES} = 21581\ psi$

$\Delta f_{pSR} = 6500\ psi$

$\Delta f_{pCR} = 44422\ \ psi$

$\Delta f_{pR2} = 355\ psi$

$P_j = 2021355\ lbs$

$P_i = 1781857\ lbs$

$P_f = 1294086\ lbs$

$\Delta_i = 2.836\ in$

$\Delta_{28} = 6.327 in$

$\Delta_{365} = 6.327\ in$

B.3 Proposed Approximate Method

The proposed approximate method for prediction of prestress losses and camber for prestressed, pretensioned concrete girders uses the adjustments recommended in Section 5.10 to account for the production factors, material properties, and debonding and transfer length. For box beams or cored slabs, this method utilizes the modified section properties recommended in Appendix A. Using this method, the prestress losses and camber for the example girder given at the beginning of this appendix are determined as follows:

1) Estimated concrete compressive strength at transfer (f^*_{ci}) and at 28 days (f^*_c):

$$f^*_{ci} = 1.25 f'_{ci}$$
$$= (1.25)7200$$
$$= 9000\ psi$$
$$f^*_c = 1.45 f'_c$$
$$= (1.45)9500$$
$$= 13775\ psi$$

2) Estimated elastic modulus of the concrete at prestress transfer (E_{ci}) and at 28 days (E_c):

$$E_{ci} = (0.85)33 w_c^{1.5} \sqrt{f^*_{ci}}$$
$$= (0.85)(33)(150\ pcf)^{1.5} \sqrt{9000\ psi}$$
$$= 4888673.2\ psi$$
$$E_c = (0.85)33 w_c^{1.5} \sqrt{f^*_c}$$
$$= (0.85)(33)(150\ pcf)^{1.5} \sqrt{13775\ psi}$$
$$= 6048052.6\ psi$$

3) Moment at midspan due to self-weight:

$$M_g = \frac{w_g L_m^2}{8} + M_{diaphragm}$$

$$= \frac{\left(868 \frac{\text{lb}}{\text{ft}}\right)(123.819 \text{ ft})^2}{8} + 0$$
$$= 1663429\ lb - ft$$
$$= 19961148\ lb - in$$

4) Eccentricity of the prestressing strands at midspan (e_m) and at the end of the girder (e_e):

$$e_m = y_c - y_{psm}$$
$$= 36.790\ in - 8.609\ in$$
$$= 28.181\ in$$
$$e_e = y_c - y_{pse}$$
$$= 36.790\ in - 18.347\ in$$
$$= 18.443\ in$$

5) The cross-sectional area for a 0.6-in prestressing strand is 0.217 in^2. Therefore, the total strand area is:

$$A_{ps} = A_{ps,str} n_{str}$$
$$= (0.217\ in^2)(46)$$
$$= 9.982\ in^2$$

6) Specified initial prestressing force before transfer:

$$P_j = 0.75 f_{pu} A_{ps}$$
$$= 0.75(270000\ psi)(9.982\ in^2)$$
$$= 2021355\ lbs$$

7) Prestress loss due to elastic shortening at transfer:
   a. Stress in the concrete at the level of the centroid of the strands:

$$f_{cgp} = \left[\frac{0.9P_j}{A_g} + \frac{0.9P_j e_m^2}{I_g}\right] - \frac{M_g e_m}{I_g}$$

$$= \left[\frac{0.9(2021355)}{833.10} + \frac{0.9(2021355)(28.181)^2}{570260}\right] - \frac{(19961148)(28.181)}{570260}$$

$$= 3730.8\ psi$$

b. Elastic shortening loss:

$$\Delta f_{pES} = \frac{E_p}{E_{ci}} f_{cgp}$$

$$= \frac{28500000\ psi}{4888673.2\ psi} 3730.8 psi$$

$$= 21750\ psi$$

8) Prestress force after transfer:

$$P_i = P_j - \Delta f_{pES} A_{ps}$$

$$P_i = 2021355\ lbs - (21750\ psi)(9.982\ in^2)$$

$$= 1804247\ lbs$$

9) Prestress loss due to concrete shrinkage:

$$\Delta f_{pSR} = (8.2x10^{-6}) E_p \left(1 - 0.06\left(\frac{V}{S}\right)\right)(100 - H)$$

$$= (8.2x10^{-6})(28500000)\big(1 - 0.06(3.264)\big)(100 - 70)$$

$$= 5638\ psi$$

10) Stress in the concrete at the level of the centroid of the strands due to superimposed dead loads applied at girder erection:

$$f_{cds} = \frac{M_{sd} * e_m}{I_g}$$

$$= \frac{(0)(28.181)}{570260}$$

$$= 0\ psi$$

11) Prestress loss due to creep:

$$\Delta f_{pCR} = 2.0\frac{E_p}{E_c}\left(f_{cgp} - f_{cds}\right)$$
$$= 2.0\frac{28500000}{6048052.6}(3730.8 - 0)$$
$$= 35161\ psi$$

12) Prestress loss due to strand relaxation:

$$\Delta f_{pRE} = 5000 - 0.04\left(\Delta f_{pSR} + \Delta f_{pCR} + \Delta f_{pES}\right)$$
$$= 5000 - 0.04(5638 + 35161 + 21750)$$
$$= 2498\ psi$$

13) Final prestress force:

$$P_f = P_j - A_{ps} * \left(\Delta f_{pES} + \Delta f_{pSR} + \Delta f_{pCR} + \Delta f_{pRE}\right)$$
$$= 2021355 - 9.982 * (21750 + 5638 + 35161 + 2498)$$
$$= 1372056\ lbs$$

14) Camber at prestress transfer:

a. Camber due to prestressing only:

$$\Delta_{ps,i} = \frac{P_i}{E_{ci}I_g}\left(\frac{e_m L_m^2}{8} - (e_m - e_e)\frac{\left(\frac{L_m}{2} - x_h\right)^2}{6} - \frac{e_m(L_{db} + L_t)^2}{6}\right)$$

$$= \frac{1804247}{(4888673.2)(570260)}\left(\frac{(28.181)(123.819 * 12)^2}{8}\right.$$
$$\left. - (28.181 - 18.443)\frac{\left(\frac{123.819 * 12}{2} - (5 * 12)\right)^2}{6}\right.$$
$$\left. - \frac{28.181(0 * 12 + 36)^2}{6}\right)$$

$$= 4.539\ in$$

b. Deflection due to self-weight:

$$\Delta_{sw,i} = \frac{5w_g L_m^4}{384E_{ci}I_g} + \Delta_{diaphragm}$$
$$= \frac{5(868/12)(123.819 * 12)^4}{384(4888673.2)(570260)} + 0$$
$$= 1.647\ in$$

c. Net camber at prestress transfer:

$$\Delta_i = \Delta_{ps,i} - \Delta_{sw,i}$$
$$= 4.539 - 1.647$$
$$= 2.892\ in$$

15) Camber at 28 days:

$$\Delta_{28} = 1.80\Delta_{ps,i} - 1.85\Delta_{sw,i}$$
$$= 1.80(4.539) - 1.85(1.647)$$
$$= 5.123\ in$$

16) Camber at 1 year (365 days):

$$\Delta_{365} = 2.45\Delta_{ps,i} - 2.70\Delta_{sw,i}$$
$$= 2.45(4.539) - 2.70(1.647)$$
$$= 6.674\ in$$

17) Summary of prestress losses, prestress forces, and camber:

$$\Delta f_{pES} = 21750\ psi$$
$$\Delta f_{pSR} = 5638\ psi$$
$$\Delta f_{pCR} = 35161\ psi$$
$$\Delta f_{pRE} = 2498\ psi$$

$P_j = 2021355\ lbs$

$P_i = 1804247\ lbs$

$P_f = 1372056\ lbs$

$\Delta_i = 2.892\ in$

$\Delta_{28} = 5.123\ in$

$\Delta_{365} = 6.674\ in$

B.4 Proposed Refined Method

The proposed refined method for prediction of prestress losses and camber for prestressed, pretensioned concrete girders uses the adjustments recommended in Section 5.10 to account for the production factors, material properties, and debonding and transfer length. For box beams or cored slabs, this method utilizes the modified section properties recommended in Appendix A. Using this method, the prestress losses and camber for the example girder given at the beginning of this appendix are determined as follows:

1) Estimated concrete compressive strength at transfer (f^*_{ci}) and at 28 days (f^*_c):

$$f^*_{ci} = 1.25 f'_{ci}$$
$$= (1.25)7200$$
$$= 9000\ psi$$
$$f^*_c = 1.45 f'_c$$
$$= (1.45)9500$$
$$= 13775\ psi$$

2) Estimated elastic modulus of the concrete at prestress transfer (E_{ci}) and at 28 days (E_c):

$$E_{ci} = (0.85)33 w_c^{1.5} \sqrt{f^*_{ci}}$$
$$= (0.85)(33)(150\ pcf)^{1.5} \sqrt{9000\ psi}$$
$$= 4888673.2\ psi$$
$$E_c = (0.85)33 w_c^{1.5} \sqrt{f^*_c}$$
$$= (0.85)(33)(150\ pcf)^{1.5} \sqrt{13775\ psi}$$
$$= 6048052.6\ psi$$

3) Moment at midspan due to self-weight:

$$M_g = \frac{w_g L_m^2}{8} + M_{diaphragm}$$

$$= \frac{\left(868 \frac{\text{lb}}{\text{ft}}\right)(123.819 \text{ ft})^2}{8} + 0$$
$$= 1663429\ lb - ft$$
$$= 19961148\ lb - in$$

4) Eccentricity of the prestressing strands at midspan (e_m) and at the end of the girder (e_e):

$$e_m = y_c - y_{psm}$$
$$= 36.790\ in - 8.609\ in$$
$$= 28.181\ in$$
$$e_e = y_c - y_{pse}$$
$$= 36.790\ in - 18.347\ in$$
$$= 18.443\ in$$

5) The cross-sectional area for a 0.6-in prestressing strand is 0.217 in^2. Therefore, the total strand area is:

$$A_{ps} = A_{ps,str} n_{str}$$
$$= (0.217\ in^2)(46)$$
$$= 9.982\ in^2$$

6) Specified initial prestressing force before transfer:

$$P_j = 0.75 f_{pu} A_{ps}$$
$$= 0.75(270000\ psi)(9.982\ in^2)$$
$$= 2021355\ lbs$$

7) Prestress loss due to elastic shortening at transfer:
   a. Guess prestress force after transfer (1st iteration):

$$P_i(guess) = 0.9(P_j)$$
$$= 0.9(2021355)$$
$$= 1819220\ lbs$$

b. Stress in the concrete at the level of the centroid of the strands (1st iteration):

$$f_{cgp} = \left[\frac{P_i}{A_g} + \frac{P_i e_m^2}{I_g}\right] - \frac{M_g e_m}{I_g}$$

$$= \left[\frac{1819220}{833.10} + \frac{(1819220)(28.181)^2}{570260}\right] - \frac{(19961148)(28.181)}{570260}$$

$$= 3730.8\ psi$$

c. Elastic shortening loss (1st iteration):

$$\Delta f_{pES} = \frac{E_p}{E_{ci}} f_{cgp}$$

$$= \frac{28500000\ psi}{4888673.2\ psi} 3730.8\ psi$$

$$= 21750\ psi$$

d. Prestress force after transfer (2nd iteration):

$$P_i = P_j - \Delta f_{pES} A_{ps}$$

$$= 2021355\ lbs - (21750\ psi)(9.982\ in^2)$$

$$= 1804247\ lbs$$

e. Stress in the concrete at the level of the centroid of the strands (2nd iteration):

$$f_{cgp} = \left[\frac{1804247}{833.10} + \frac{(1804247)(28.181)^2}{570260}\right] - \frac{(19961148)(28.181)}{570260}$$

$$= 3692\ psi$$

f. Elastic shortening loss (2nd iteration)

$$f_{pES} = \frac{28500000\ psi}{4888673.2\ psi} 3692\ psi$$

$$= 21523\ psi$$

8) Prestress force after transfer:

$$P_i = 2021355\ lbs - (21523\ psi)(9.982\ in^2)$$

$$= 1806512\ lbs$$

9) Creep coefficients:

a. Factor to account for the effect of the volume-to-surface area ratio:

$$k_s = 1.45 - 0.13\frac{V}{S} \geq 0$$
$$= 1.45 - 0.13(3.264)$$
$$= 1.026$$

b. Humidity factor for creep:

$$k_{hc} = 1.56 - 0.008H$$
$$= 1.56 - 0.008(70)$$
$$= 1.000$$

c. Factor for the effect of concrete strength:

$$k_f = \frac{5}{1 + f_{ci}^*}$$
$$= \frac{5}{1 + (9\ kips)}$$
$$= 0.500$$

d. Time development factor for 28 days due to loading applied at transfer:

$$k_{td} = \frac{t_1 - t_i}{61 - 4f_{ci}^* + (t_1 - t_i)}$$
$$= \frac{28 - 1}{61 - 4(9\ kips) + (28 - 1)}$$
$$= 0.519$$

e. Creep coefficient at 28 days due to loading applied at transfer:

$$\Psi(28, t_i) = 1.9k_s k_{hc} k_f k_{td} t_i^{-0.118}$$
$$= 1.9(1.026)(1.000)(0.5)(0.519)(1)^{-0.118}$$
$$= 0.506$$

f. Time development factor for 1 year due to loading applied at transfer:

$$k_{td} = \frac{t_2 - t_i}{61 - 4f_{ci}^* + (t_2 - t_i)}$$
$$= \frac{365 - 1}{61 - 4(9\ kips) + (365 - 1)}$$
$$= 0.936$$

g. Creep coefficient at 1 year (365 days) due to loading applied at transfer:

$$\Psi(365, t_i) = 1.9 k_s k_{hc} k_f k_{td} t_i^{-0.118}$$
$$= 1.9(1.026)(1.000)(0.5)(0.936)(1)^{-0.118}$$
$$= 0.912$$

h. Time development factor for final time (5 years) due to loading applied at transfer:

$$k_{td} = \frac{t_f - t_i}{61 - 4f_{ci}^* + (t_f - t_i)}$$
$$= \frac{(5 * 365) - 1}{61 - 4(9\ kips) + (5 * 365 - 1)}$$
$$= 0.986$$

i. Creep coefficient at final time (5 years) due to loading applied at transfer:

$$\Psi(t_f, t_i) = 1.9 k_s k_{hc} k_f k_{td} t_i^{-0.118}$$
$$= 1.9(1.026)(1.000)(0.5)(0.986)(1)^{-0.118}$$
$$= 0.961$$

j. Creep coefficient for the period between 28 days and 1 year due to loading applied at transfer:

$$\Psi(365{,}28) = \Psi(365, t_i) - \Psi(28, t_i)$$
$$= 0.912 - 0.506$$
$$= 0.406$$

10) Shrinkage strains:

a. Humidity factor for shrinkage:

$$k_{hs} = 2.00 - 0.014H$$
$$= 2.00 - 0.014(70)$$
$$= 1.02$$

b. Shrinkage strain at 28 days:

$$\varepsilon_{bid} = k_s k_{hs} k_f k_{td} 0.48x10^{-3}$$
$$= (1.026)(1.02)(0.5)(0.519)(0.48x10^{-3})$$
$$= 0.0001304$$

c. Shrinkage strain at 1 year (365 days):

$$\varepsilon_{bid} = k_s k_{hs} k_f k_{td} 0.48x10^{-3}$$
$$= (1.026)(1.02)(0.5)(0.936)(0.48x10^{-3})$$
$$= 0.000235$$

11) Transformed section coefficient that accounts for time-dependent interaction between concrete and bonded steel in the section being considered for the time period between transfer and deck placement (This will be used for both 28 days and 1 year since the interest is in prestress losses and camber before deck placement):

$$K_{id} = \frac{1}{1 + \frac{E_p A_{ps}}{E_{ci} A_g}\left(1 + \frac{A_g e_m^2}{I_g}\right)\left(1 + 0.7\Psi(t_f, t_i)\right)}$$
$$= \frac{1}{1 + \frac{(28500000)(9.982)}{(4888673.2)(833.1)}\left(1 + \frac{(833.1)(28.181)^2}{570260}\right)\left(1 + 0.7(0.961)\right)}$$
$$= 0.798$$

12) Prestress loss at 28 days due to concrete shrinkage:

$$\Delta f_{pSR,28} = \varepsilon_{bid} E_p K_{id}$$
$$= (0.0001304)(28500000)(0.798)$$
$$= 2967\ psi$$

13) Prestress loss at 28 days due to creep:

$$\Delta f_{pCR,28} = \frac{E_p}{E_{ci}} f_{cgp} \Psi(28, t_i) K_{id}$$
$$= \frac{28500000}{4888673.2}(3692)(0.506)(0.798)$$
$$= 8691\ psi$$

14) Prestress loss at 28 days due to relaxation of prestressing strands:

$$\Delta f_{pRE,28} = \frac{f_{pi}}{30}\left(\frac{f_{pi}}{f_{py}} - 0.55\right)$$
$$= \frac{\frac{P_i}{A_{ps}}}{30}\left(\frac{\frac{P_i}{A_{ps}}}{0.9 f_{pu}} - 0.55\right)$$
$$= \frac{{}^{1806512}/_{9.982}}{30}\left(\frac{{}^{1806512}/_{9.982}}{0.9(270000)} - 0.55\right)$$
$$= 1175\ psi$$

15) Prestress loss at 1 year (365 days) due to concrete shrinkage:

$$\Delta f_{pSR,365} = \varepsilon_{bid} E_p K_{id}$$
$$= (0.000235)(28500000)(0.798)$$
$$= 5345\ psi$$

16) Prestress loss at 1 year (365 days) due to creep:

$$\Delta f_{pCR,365} = \frac{E_p}{E_{ci}} f_{cgp} \Psi(365, t_i) K_{id}$$
$$= \frac{28500000}{4888673.2}(3692)(0.912)(0.798)$$
$$= 15664\ psi$$

17) Prestress loss at 1 year (365 days) due to relaxation of prestressing strands:

$$\Delta f_{pRE,365} = \frac{f_{pi}}{30}\left(\frac{f_{pi}}{f_{py}} - 0.55\right)$$

$$= \frac{\frac{P_i}{A_{ps}}}{30}\left(\frac{\frac{P_i}{A_{ps}}}{0.9f_{pu}} - 0.55\right)$$

$$= \frac{{}^{1806512}/_{9.982}}{30}\left(\frac{{}^{1806512}/_{9.982}}{0.9(270000)} - 0.55\right)$$

$$= 1175\ psi$$

18) Prestress force at 28 days:

$$P_{28} = A_{ps}\left(f_{pj} - \left[\Delta f_{pES} + \Delta f_{pSR,28} + \Delta f_{pCR,28} + \Delta f_{pRE,28}\right]\right)$$
$$= 9.982(0.75(270000) - [21523 + 2967 + 8691 + 1175])$$

$$= 1678413\ lbs$$

19) Prestress force at 365 days:

$$P_{365} = A_{ps}\left(f_{pj} - \left[\Delta f_{pES} + \Delta f_{pSR,365} + \Delta f_{pCR,365} + \Delta f_{pRE,365}\right]\right)$$
$$= 9.982(0.75(270000) - [21523 + 5345 + 15664 + 1175])$$

$$= 1585072\ lbs$$

20) Camber at prestress transfer:

a. Camber due to prestressing only:

$$\Delta_{ps,i} = \frac{P_i}{E_{ci}I_g}\left(\frac{e_m L_m^2}{8} - (e_m - e_e)\frac{\left(\frac{L_m}{2} - x_h\right)^2}{6} - \frac{e_m(L_{db} + L_t)^2}{6}\right)$$

$$= \frac{1806512}{(4888673.2)(570260)}\left(\frac{(28.181)(123.819*12)^2}{8} - (28.181-18.443)\frac{\left(\frac{123.819*12}{2}-(5*12)\right)^2}{6} - \frac{28.181(0*12+36)^2}{6}\right)$$

$$= 4.545\ in$$

b. Deflection due to self-weight:

$$\Delta_{sw,i} = \frac{5w_g L_m^4}{384E_{ci}I_g} + \Delta_{diaphragm}$$

$$= \frac{5(868/12)(123.819*12)^4}{384(4888673.2)(570260)} + 0$$

$$= 1.647\ in$$

c. Net camber at prestress transfer:

$$\Delta_i = \Delta_{ps,i} - \Delta_{sw,i}$$

$$= 4.545 - 1.647$$

$$= 2.898\ in$$

21) Camber at 28 days:

a. Camber due to prestressing only:

$$\Delta_{ps,28} = \Delta_{ps,i} - \frac{P_i - P_{28}}{\left(\frac{E_{ci}+E_c}{2}\right)I_g}\left(\frac{e_m L_m^2}{8} - \frac{(e_m - e_e)\left(\frac{L_m}{2}-x_h\right)^2}{6} - \frac{e_m(L_{db}+L_t)^2}{6}\right)$$

$$= 4.545 - \frac{1806512 - 1678413}{\left(\frac{4888673.2 + 6048052.6}{2}\right)570260}\left(\frac{28.181(123.819 * 12)^2}{8} - \frac{(28.181 - 18.443)\left(\frac{123.819 * 12}{2} - 5 * 12\right)^2}{6} - \frac{28.181(0 + 36)^2}{6}\right)$$

$$= 4.257\ in$$

b. Deflection due to self-weight:

$$\Delta_{sw,28} = \Delta_{sw,i}$$

$$= 1.647\ in$$

c. Deflection due to creep:

$$\Delta_{cr,28} = \Psi(28, t_i)\left(\frac{\left(\frac{P_i + P_{28}}{2}\right)}{E_{ci} I_g}\left(\frac{e_m L_m^2}{8} - \frac{(e_m - e_e)\left(\frac{L_m}{2} - x_h\right)^2}{6} - \frac{e_m(L_{db} + L_t)^2}{6}\right) - \Delta_{sw,\mathrm{i}}\right)$$

$$= 0.506\left(\frac{\left(\frac{1806512 + 1678413}{2}\right)}{(4888673.2)(570260)}\left(\frac{(28.181)(123.819 * 12)^2}{8} - \frac{(28.181 - 18.443)\left(\frac{123.819 * 12}{2} - 5 * 12\right)^2}{6} - \frac{28.181(0 + 36)^2}{6}\right) - 1.647\right)$$

$$= 1.385\ in$$

d. Net camber at 28 days:

$$\Delta_{28} = \Delta_{ps,28} - \Delta_{sw,28} + \Delta_{cr,28}$$
$$= 4.257 - 1.647 + 1.385$$
$$= 3.995\ in$$

22) Camber at 1 year (365 days):

a. Camber due to prestressing only:

$$\Delta_{ps,365} = \Delta_{ps,28} - \frac{P_{28} - P_{365}}{E_c I_g}\left(\frac{e_m L_m^2}{8} - \frac{(e_m - e_e)\left(\frac{L_m}{2} - x_h\right)^2}{6} - \frac{e_m(L_{db} + L_t)^2}{6}\right)$$

$$= 4.257 - \frac{1678413 - 1585072}{(6048052.6)(570260)}\left(\frac{28.181(123.819 * 12)^2}{8}\right.$$
$$\left. - \frac{(28.181 - 18.443)\left(\frac{123.819 * 12}{2} - 5 * 12\right)^2}{6} - \frac{28.181(0 + 36)^2}{6}\right)$$

$$= 4.067\ in$$

b. Deflection due to self-weight:

$$\Delta_{sw,365} = \Delta_{sw,i}$$
$$= 1.647\ in$$

c. Deflection due to creep:

$$\Delta_{cr,365} = \Delta_{cr,28}$$
$$+ \Psi(365,28)\left(\frac{\left(\frac{P_{28} + P_{365}}{2}\right)}{E_{ci} I_g}\left(\frac{e_m L^2}{8} - \frac{(e_m - e_e)\left(\frac{L}{2} - x_h\right)^2}{6}\right.\right.$$
$$\left.\left. - \frac{e_m(L_{db} + L_t)^2}{6}\right) - \Delta_{sw,\mathrm{i}}\right)$$

$$= 1.385 + 0.406\left(\frac{\left(\frac{1678413 + 1585072}{2}\right)}{(4888673.2)(570260)}\left(\frac{(28.181)(123.819 * 12)^2}{8}\right.\right.$$

$$\left.\left. - \frac{(28.181 - 18.443)\left(\frac{123.819 * 12}{2} - 5 * 12\right)^2}{6} - \frac{28.181(0 + 36)^2}{6}\right)\right.$$

$$\left. - 1.647\right)$$

$$= 2.383\ in$$

d. Net camber at 365 days:

$$\Delta_{365} = \Delta_{ps,365} - \Delta_{sw,365} + \Delta_{cr,365}$$
$$= 4.067 - 1.647 + 2.383$$
$$= 4.803\ in$$

23) Summary of prestress losses, prestress forces, and camber:

$$\Delta f_{pES} = 21523\ psi$$
$$\Delta f_{pSR,28} = 2967\ psi$$
$$\Delta f_{pCR,28} = 8691\ psi$$
$$\Delta f_{pRE,28} = 1175\ psi$$
$$\Delta f_{pSR,365} = 5345\ psi$$
$$\Delta f_{pCR,365} = 15664\ psi$$
$$\Delta f_{pRE,365} = 1175\ psi$$

$$P_j = 2021355\ lbs$$
$$P_i = 1804247\ lbs$$
$$P_{28} = 1678413\ lbs$$
$$P_{365} = 1585072\ lbs$$

$\Delta_i = 2.898\ in$

$\Delta_{28} = 3.995\ in$

$\Delta_{365} = 4.803\ in$

B.5 Summary of the Predicted Camber

The predicted camber at transfer, at 28 days, and at one year for the example girder using each of the methods considered in this report as well as the measured values for two actual girders are presented in Figure B-1. The measured values shown suggest that the proposed approximate method provided a more accurate prediction of camber than the NCDOT methods for these two girders. However, due to the natural variability of camber, such a small number of girders should not be considered to provide a reliable comparison of the predictions. Based on the extensive database of field measurements of 382 girders developed for this research, the proposed approximate method and the proposed refined method provided significantly more accurate predictions of camber than the current NCDOT method and the modified NCDOT method.

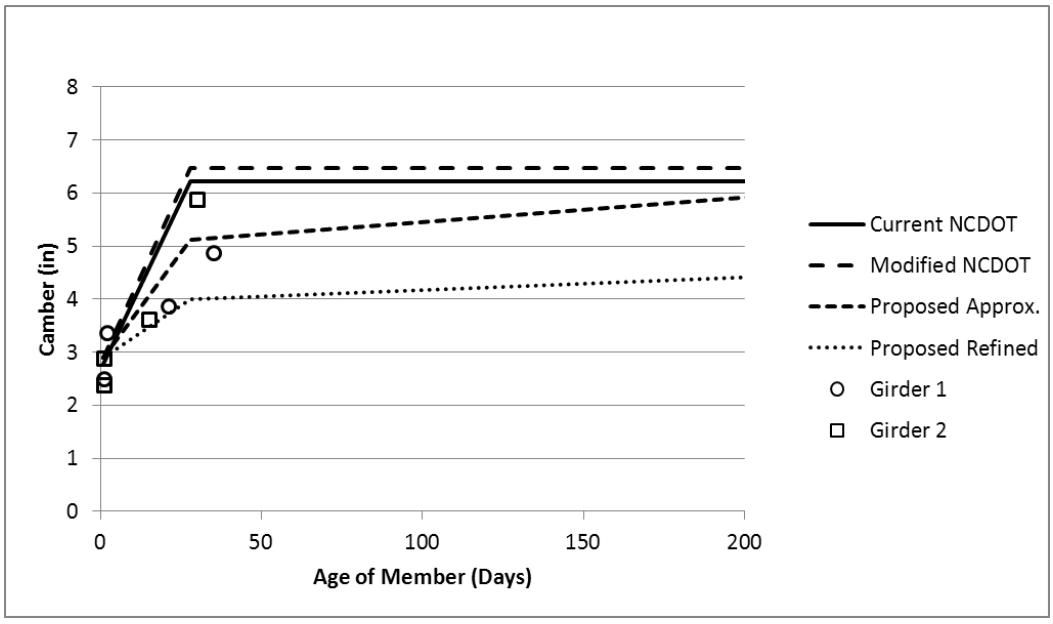

Figure B-1 Predicted and measured camber for two girders.

Appendix C Camber Experiences of Other States

A questionnaire regarding design practices and field experiences related to prestress losses and camber was answered by the Texas Department of Transportation, the Nebraska Division of Roads, and the Florida Department of Transportation. Their answers are provided below.

Texas Department of Transportation

1. Have you ever experienced any camber problems with prestressed concrete bridge beams that are often beyond normal construction tolerances? If so, please briefly describe them.

Yes. We have had instances where cambers greatly exceeded the normally expected values. In rare cases, these girders had to be re-cast because they could not be made to fit into the bridge elevation profiles using normal mitigation measures. Other more common cases involve girders fabricated at the same time but with large variations in storage duration due to project phasing. The second phase girders usually arrive with higher cambers than the 1st phase girders but no adjustment of the bridge grades can be made to accommodate the 2nd phase girders.

2. Do you use semi-lightweight concrete for your prestressed bridge beams? If so, do you experience more severe camber problems than using normal weight concrete?

No, all of our producers use normal weight concrete when fabricating prestressed beams. However, beams produced with limestone coarse aggregate typically have higher camber than those in which river rock is utilized.

3. What procedure or approach do you use to minimize the impact of the camber problem?

Smart contractors will lower the bearing seat elevations on their own if they suspect there could be a camber issue. Most contractors are aware that some fabricators have a history of producing beams with high cambers while others have a history of low cambers. The problem occurs mainly with widenings or phased construction where profile grade adjustments are not usually possible. For new construction, it is usually easy to adjust the profile grade to account for higher cambers.

4. What types and sizes of members (such as box beams, cored slabs, AASHTO girders, bulb tees, etc.) are more prone to cause the problem?

On the rare occasions that we see excess camber it usually occurs in the longer members with high strand patterns (bulb tees, U-beams, etc.). Differential camber in box beams is harder to overcome in the field since the members are typically placed immediately adjacent to one another but that is not an issue very often.

5. What is the maximum span that you normally use for each type of the members, and is the camber problem related more with the longer spans?

50' spans for slab beams, 110' spans for box beams, 120+' for U-beams, and 150+' for AASHTO beams and bulb tees.

6. What code(s) and design software(s) do you currently use to calculate prestress losses, camber, and deflection?

PSTRS14-TxDOT Prestressed Concrete Beam Design/Analysis Program (Version 5.0) - User may choose loss method of AASHTO 1994 Standard thru 2004 LRFD (old LRFD losses) or 2007 LRFD (new refined losses) Specifications. For LRFD the methods are uncoupled from the LRFD Specifications used for other aspects of design/analysis. For camber calculations note this excerpt from the PSTRS14 User Guide:

Camber

The maximum camber calculations are derived from the hyperbolic function method developed by Sinno [6]. Sinno formulated hyperbolic functions for unit shrinkage and unit creep from field data of full-sized, Texas Type B, prestressed concrete bridge beams.

The prestressing steel for the beams consisted of seven wire, 7/16-in. diameter, 250 ksi stress relieved strands. The beams were fabricated of both normal-weight and lightweight concrete and stored for a 300-day period. At the end of the storage period, the beams were installed in the 40 ft. and 56 ft. spans of a bridge on IH-610 over South Park Boulevard in Houston, Texas. The camber calculations are, therefore, strongly correlated with the particular structure they were calibrated to.

The calculation method developed by Sinno was fully implemented in the TxDOT "Camber Prediction Program" -- PSTRS11 (a.k.a. Prestressed Beam Stresses and Camber). PSTRS11 was written by Sinno and employs empirically based unit hyperbolic creep and shrinkage functions and a step-wise time-increment numerical procedure. This program was never used for predicting camber in bridge design production, so the source code was not incorporated into PSTRS10 or PSTRS14. Instead, a very simplified single step method of calculating the camber at mid-span, using a single set of assumed creep and shrinkage values, is included in PSTRS14. The justification for this simplification is the presumption that camber calculation is inherently inaccurate so there is no need to improve the prediction of what cannot be reliably predicted. The design engineer may not agree with this logic and may choose to employ other means to determine beam camber. But in practice, PSTRS14's calculated

camber is assumed to be good enough by most bridge design engineers in spite of some field data to the contrary.

PSTRS14's camber calculation method may not provide an adequately accurate prediction of beam camber for design purposes when applied to other beam types (i.e. volume/surface ratios) than I-beams, other material constituents, other storage periods, other final location and framing plan, as well as other factors not considered in Sinno's method. Some of these factors and other factors described by Kelly, Bradberry, and Breen [7] significantly influence camber at erection. Under no circumstances should the calculated camber be considered as having the same degree of certainty as, for example, the concrete strength required. The value printed for erection camber should be considered a rough estimate only and is not applicable to all possible design options, beam types, aggregate types, etc.

The user should verify that the calculated camber versus the dead load deflection due to placement of all superimposed dead load results in a beam with a positive net camber. If the camber needs to be increased, the user may do so by adding additional strands using the analysis option. This would not, however, guarantee that the profile of the beam will always have a net positive camber throughout the service life of the bridge.

Camber calculations performed by the program are thus insensitive to the beam type and many other factors that affect the actual camber of prestressed concrete beams. Furthermore, final concrete strength alone is used to determine beam stiffness so the method is not affected by the initial concrete stiffness associated with f'ci.
6. Sinno, Raouf. The Time-Dependent Deflections of Prestressed Concrete Bridge Beams, Ph.D. Dissertation, Texas A&M University, College Station, Texas, January 1968.
7. Kelly, D. J., Bradberry, T. E., and Breen, J. E. "Time-Dependant Deflections of Pretensioned Beams," Research Report 381-1, Research Project 3-5-84-381, Center for Transportation Research, Bureau of Engineering Research, The University of Texas at Austin, Austin, TX (August 1987) 211 pp.
URL: http://fsel.engr.utexas.edu/publications/docs/381-1.pdf

Deflections are simple span deflections and may be based on the moduli derived from final concrete strengths of beam and composite areas such as shear keys. However, TxDOT policy is to set all concrete moduli to 5000 ksi for both stress and deflection calculations and to indicate on the plans that the deflections shown are calculated assuming an E'c of 5000 ksi.

PGSuper, WSDOT/TxDOT Precast-Prestressed Girder design and analysis software Version 2.4 - AASHTO LRFD Bridge Design Specifications, 5th Edition, 2010. This software is capable of using the losses, creep, and shrinkage prediction based on AASHTO LRFD 1st Edition 1994 through AASHTO LRFD 5th Edition 2010. Losses are generally computed using the Refined Method.

By design policy TxDOT uses the loss method of the 2004 LRFD Specifications.

7. How do you determine the modulus of elasticity of concrete at different ages? If you calculate camber at prestress transfer, do you use the specified fci' for the calculation? How do you determine shrinkage and creep in your calculations?

In PSTRS14 - Regarding camber, see discussion above in response to question 6.

PSTRS14 does not calculate the camber at release nor does it perform a time step analysis. The losses calculations and camber calculations are not coupled in terms of using the same creep factors. The calculation of losses considers E'ci. The creep and shrinkage calculations follow the provisions of the various loss specifications (1994, 2004 or 2007) employed.

In PGSuper - Modulus of elasticity at transfer is computed using a modified form of AASHTO LRFD Equation 5.4.2.4-1 using f'ci. This equation is modified with the factors K1 and K2 as defined in NCHRP Report 496. Creep and shrinkage are computed with modified versions of AASHTO LRFD Equations 5.4.2.3.2-1 and 5.4.2.3.3-1. This equations are modified with K1 and K2 factors as defined in NCHRP Report 496. For girders having temporary top strand to control stability during transportation, the elastic shortening losses and Kid and Kdf transformed section coefficients are modified to compute the shortening, creep, and shrinkage losses in the permanent strands. Modifications account for the fact that the temporary strands raise the CG of the prestressing force while the majority of the creep and shrinkage losses are taking place.

8. Have you conducted or sponsored any research regarding prestress losses, camber, and deflection? If so, please send us your report or provide a reference to your report.

TxDOT - Research on prestress losses is ongoing through TxDOT Project 0-6374, "Effects of New Prestress Loss Predictions on TxDOT Bridges". Camber and deflection has been researched previously (see report link to reference 7 in answer to question 6, above). Results of this camber research have not been incorporated into PSTRS14.

WSDOT - Camber research was conducted at the University of Washington. Reference: Improving Predictions for Camber in Precast, Prestressed Concrete Bridge Girders, Rosa, Michael A; Stanton, John F; Eberhard, Marc O, Washington State Transportation Center; Washington State Department of Transportation; Federal Highway Administration, 2007. Results of this research have not been incorporated into PGSuper.

Nebraska Division of Roads

1. Have you ever experienced any camber problems with prestressed concrete bridge beams that are often beyond normal construction tolerances? If so, please briefly describe them.

Yes. Lately we have been getting some camber below the predicted values at 30 days which caused construction problems. We don't know if this due to design or fabrication or material use (we have been using SCC for the last few years).

So far we know we have potential problems (less camber than predicted at 30 days)when we ask for high strength concrete over 10 ksi for long spans (>160 ft

We also know sometimes the fabricator get concrete strength at release way more than the specified.

2. Do you use semi-lightweight concrete for your prestressed bridge beams? If so, do you experience more severe camber problems than using normal weight concrete?

No. Our fabricator use an approved SCC mix

3. What procedure or approach do you use to minimize the impact of the camber problem?

We have shown PCI tolerances (at release) on the plans so our inspectors can enforce it. We have required the fabricator to check the camber before shipping. We are in process of identifying the "K" factors due to our local ingredients so we can use it in our calculation for losses.

4. What types and sizes of members (such as box beams, cored slabs, AASHTO girders, bulb tees, etc.) are more prone to cause the problem?

We use NU section (I and IT section)

NU1600-2000

5. What is the maximum span that you normally use for each type of the members, and is the camber problem related more with the longer spans?

We have shipped 175 ft NU2000 section.

Camber problem on long spans

6. What code(s) and design software(s) do you currently use to calculate prestress losses, camber, and deflection?

We use CONSPAN software for design using LRFD .We use approximate losses method and sometimes refined losses. (Both give about the same camber prediction at 30 days)

7. How do you determine the modulus of elasticity of concrete at different ages? If you calculate camber at prestress transfer, do you use the specified f_{ci}' for the calculation? How do you determine shrinkage and creep in your calculations?

We provide two camber numbers on the plans: camber at release calculated based on the fci and camber at 30 days (assumed girder erection) based on the 28 days strength (design strength). In general we use AASHTO LRFD approximate method to determine creep and shrinkage.

8. Have you conducted or sponsored any research regarding prestress losses, camber, and deflection? If so, please send us your report or provide a reference to your report.

We haven't conducted any official research regarding these issues but we are fortunate to have Dr. Tadros around to guide us along.

Florida Department of Transportation

1. Have you ever experienced any camber problems with prestressed concrete bridge beams that are often beyond normal construction tolerances? If so, please briefly describe them.

On rare occasions, the camber is either underestimated or overestimated.

2. Do you use semi-lightweight concrete for your prestressed bridge beams? If so, do you experience more severe camber problems than using normal weight concrete?

No.

3. What procedure or approach do you use to minimize the impact of the camber problem?

The contractor is required to monitor the camber in storage. We are considering additional loads during design to allow for more tolerance when the camber is overestimated.

4. What types and sizes of members (such as box beams, cored slabs, AASHTO girders, bulb tees, etc.) are more prone to cause the problem?

The I-beam, possibly because we use them more frequently.

5. What is the maximum span that you normally use for each type of the members, and is the camber problem related more with the longer spans?

Florida uses Inverted Tees, adjacent slabs and I beams. The adjacent slabs have occasional camber issues and span up to 50'. The Inverted Tees are rarely used. The Florida I-beams are new and span up to 180'.

6. What code(s) and design software(s) do you currently use to calculate prestress losses, camber, and deflection?

We use the LRFD approximate method for calculating losses. We also use our in-house prestressed concrete design program. The camber calculation in our program is based on the UF research.

7. How do you determine the modulus of elasticity of concrete at different ages? If you calculate camber at prestress transfer, do you use the specified f_{ci}' for the calculation? How do you determine shrinkage and creep in your calculations?

See our Mathcad program.

8. Have you conducted or sponsored any research regarding prestress losses, camber, and deflection? If so, please send us your report or provide a reference to your report.

We are currently collecting data for the new Florida-I Beam to calibrate the camber calculation. This in-house research should be completed by June 2011.

Appendix D Camber Data Sheet Example

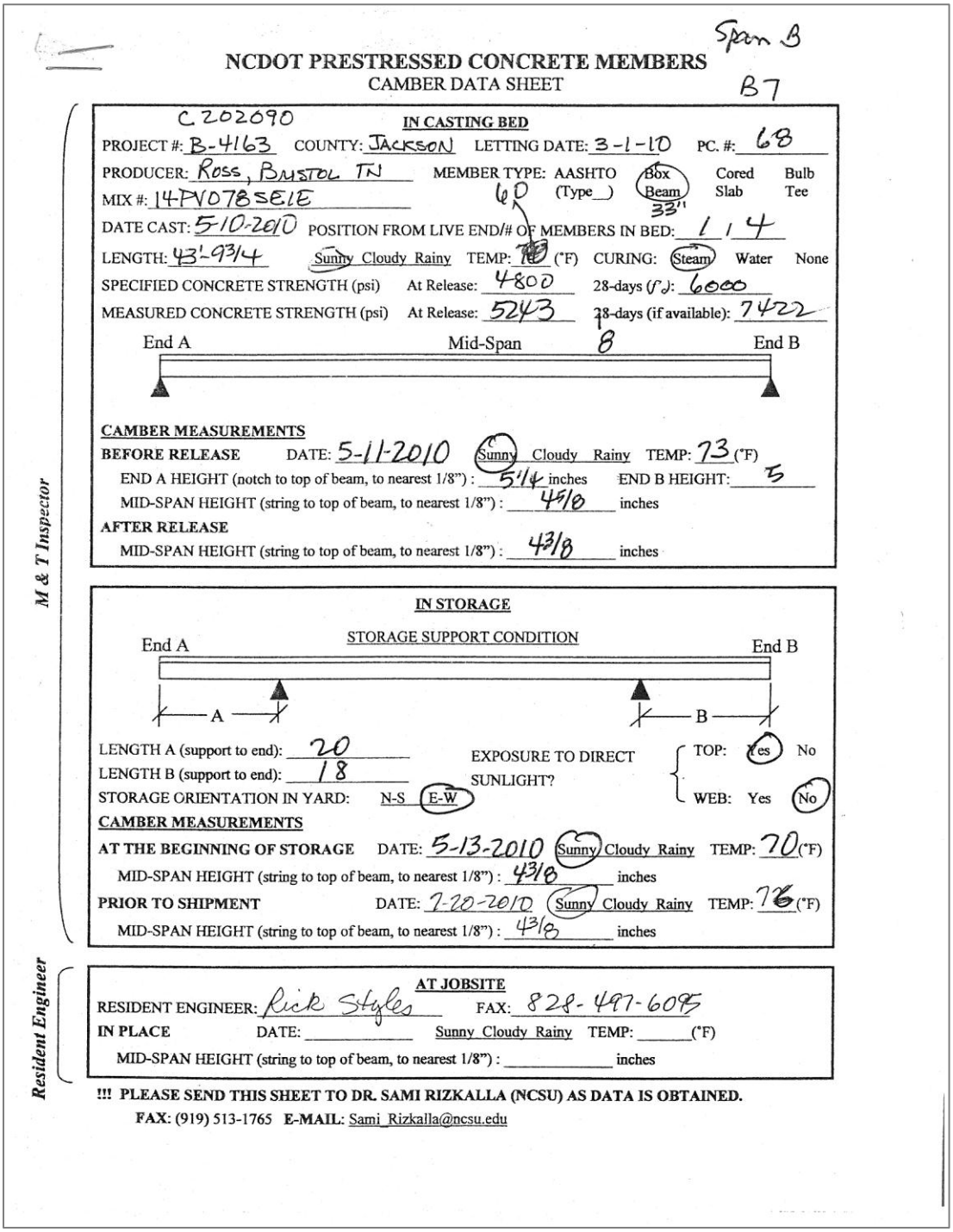

NCDOT PRESTRESSED CONCRETE MEMBERS
CAMBER DATA SHEET

Span B
B7

C202090 **IN CASTING BED**

PROJECT #: B-4163 COUNTY: JACKSON LETTING DATE: 3-1-10 PC. #: 68

PRODUCER: Ross, Bristol TN MEMBER TYPE: AASHTO (Type 60) Box Beam 33" Cored Slab Bulb Tee

MIX #: 14PV078SE1E

DATE CAST: 5-10-2010 POSITION FROM LIVE END/# OF MEMBERS IN BED: 1 / 4

LENGTH: 43'-9 3/4 Sunny Cloudy Rainy TEMP: 70 (°F) CURING: Steam Water None

SPECIFIED CONCRETE STRENGTH (psi) At Release: 4800 28-days (f'c): 6000

MEASURED CONCRETE STRENGTH (psi) At Release: 5243 28-days (if available): 7422

End A — Mid-Span 8 — End B

CAMBER MEASUREMENTS

BEFORE RELEASE DATE: 5-11-2010 Sunny Cloudy Rainy TEMP: 73 (°F)

END A HEIGHT (notch to top of beam, to nearest 1/8"): 5 1/4 inches END B HEIGHT: 5

MID-SPAN HEIGHT (string to top of beam, to nearest 1/8"): 4 5/8 inches

AFTER RELEASE

MID-SPAN HEIGHT (string to top of beam, to nearest 1/8"): 4 3/8 inches

M & T Inspector

IN STORAGE

STORAGE SUPPORT CONDITION

End A — A — B — End B

LENGTH A (support to end): 20

LENGTH B (support to end): 18

STORAGE ORIENTATION IN YARD: N-S E-W

EXPOSURE TO DIRECT SUNLIGHT? TOP: Yes No WEB: Yes No

CAMBER MEASUREMENTS

AT THE BEGINNING OF STORAGE DATE: 5-13-2010 Sunny Cloudy Rainy TEMP: 70 (°F)

MID-SPAN HEIGHT (string to top of beam, to nearest 1/8"): 4 3/8 inches

PRIOR TO SHIPMENT DATE: 7-20-2010 Sunny Cloudy Rainy TEMP: 76 (°F)

MID-SPAN HEIGHT (string to top of beam, to nearest 1/8"): 4 3/8 inches

Resident Engineer

AT JOBSITE

RESIDENT ENGINEER: Rick Styles FAX: 828-497-6095

IN PLACE DATE: _____ Sunny Cloudy Rainy TEMP: _____ (°F)

MID-SPAN HEIGHT (string to top of beam, to nearest 1/8"): _____ inches

!!! PLEASE SEND THIS SHEET TO DR. SAMI RIZKALLA (NCSU) AS DATA IS OBTAINED.

FAX: (919) 513-1765 **E-MAIL:** Sami_Rizkalla@ncsu.edu

Figure D-1 Sample camber data sheet used to collect field measurements and girder data.

Appendix E Material Properties of Concrete

A large number of concrete cylinders were tested by the research team to determine the unit weight, elastic modulus, and compressive strength for selected bridge projects. The use of the test results are discussed in Section 5.4.

The cylinders were produced at various precasting plants using a number of different concrete mix designs commonly used for prestressed concrete girders. Typically, twelve cylinders from each mix design were tested, although the number occasionally varied. The concrete cylinders were collected from a total of ten precasting plants that produce girders for NCDOT.

Cylinders were cured with the girder during the initial curing phase. In the case of girders that were moist cured, the cylinders were placed under the burlap that covered the casting bed, while a soaker hose was placed on top of the burlap. For girders that were steam cured, the cylinders were placed with the girders underneath the tarp that covered the bed. When the initial curing phase was complete, the cylinders were removed from the casting bed and delivered to NCSU, where they were stored and air-cured at room temperature until the time of testing. Some of the cylinders were left in the molds until testing, while others were removed from the molds when they were taken out of the casting bed. The cylinders were tested at various ages ranging from 1 day to 193 days.

Cylinders were tested in sets, as required by the testing standards. Early in the testing phase, cylinders were tested in sets of six cylinders from each batch of concrete. Three of the cylinders from each set were tested for strength, and three were tested for elastic modulus. Later in the testing phase, cylinders were tested in sets of three. The first cylinder was tested for strength, and the other two cylinders were tested initially to determine the elastic modulus and then were tested to failure to determine the compressive strength. The average of the two elastic modulus tests was taken as the elastic modulus for the set, and the average of the three strength tests was taken as the strength for the set. Approximately 30% of all of the cylinders tested were measured to determine the unit weight.

A total of 78 sets comprising 260 individual cylinders were tested, although not all of the cylinders were tested for each property. The details of the testing for each property are described below.

Unit Weight

The unit weight was determined by dividing the weight of the cylinder in pounds by the volume of the cylinder in cubic feet. The dimensions of the cylinder were measured using 18-inch digital calipers. The weight of the cylinders was measured using a digital scale calibrated to a precision of 0.005 lbs. A total of 29 sets of cylinders comprising 88 individual specimens were measured for unit weight.

Compressive Strength

Cylinders were tested for strength in accordance with ASTM C39 *Compressive Strength of Cylindrical Concrete Specimens* using a load-controlled, 500-kip capacity Forney compression-testing machine. Steel end-caps with high-strength neoprene inserts were used to distribute the load evenly to the end surfaces of the cylinders, in accordance with ASTM C1231 *Use of Unbonded Caps in Determination of Compressive Strength of Hardened Concrete Cylinders.*

In all, strength tests were conducted on 218 cylinders from 78 tested sets. As mentioned above, strength tests were conducted at various ages of the concrete.

Elastic Modulus

Cylinders were tested for elastic modulus using an electronic compressometer device. The device consisted of two rigid aluminum rings held 5 inches apart by braces. Four Duncan 9600 Series linear potentiometers with a 0.4-inch stroke were attached around the circumference of one of the rings, and the tip of the plunger on each potentiometer rested against plates attached to the other ring. The device was positioned over the cylinder so that the rings were concentrically aligned. The rings were then fastened to the cylinder by tightening six contact bolts, three on each ring, spaced circumferentially. After thus anchoring the rings, the braces were removed so that the rings were free to move with respect

to each other. As the cylinder was compressed, the rings moved closer together, and the plungers in the calibrated linear potentiometers were depressed. An electronic signal was sent from the potentiometers to an OPTIM data acquisition system to record the stroke of each potentiometer. The load reading was also sent from the Forney machine to the OPTIM. Load and stroke were recorded once every second.

Tests were performed by first applying a pre-load of 300 pounds to the cylinder, at which point the data recording was started. The test was stopped when the load reached 40% of the estimated ultimate strength.

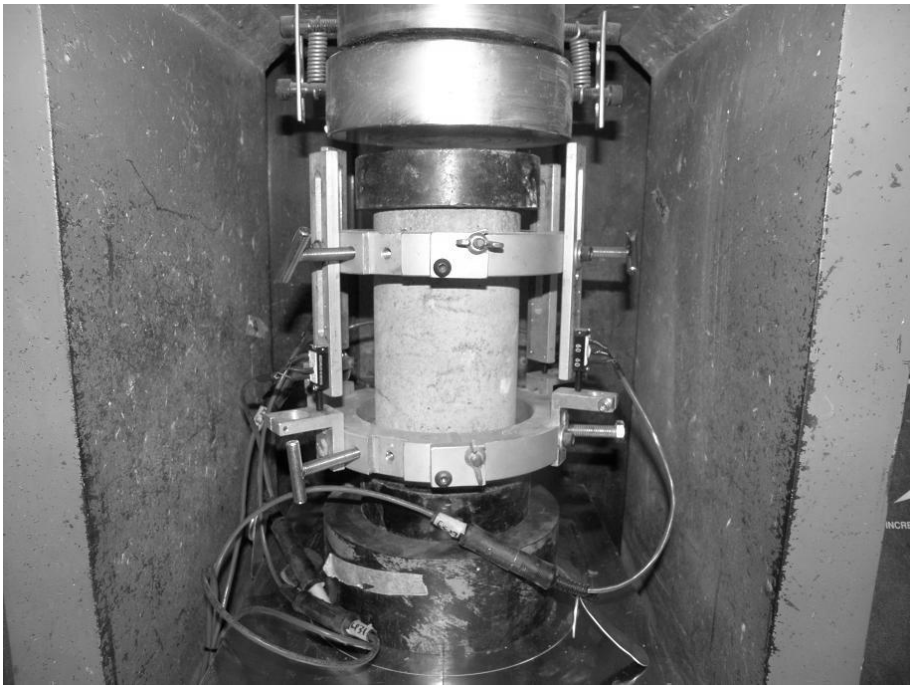

Figure E-1 Test setup for elastic modulus testing of concrete cylinders.

To determine the elastic modulus from the test data, the measured strokes from each of the four potentiometers at each time-step were averaged. The strain at each time-step was then calculated by dividing the average stroke by 5 inches, the distance between the rings. The stress at each time-step was calculated by dividing the recorded load by the cross-sectional area of the cylinder. The stresses and strains were then plotted. The slope of the

best-fit line through these points was considered the elastic modulus for the cylinder. The elastic modulus of all of the cylinders in a given set were then averaged. A plot of the stress-strain curves and average elastic modulus for one set of cylinders is shown in Figure E-2.

A total of 76 sets of cylinders comprising 153 individual specimens were tested for elastic modulus.

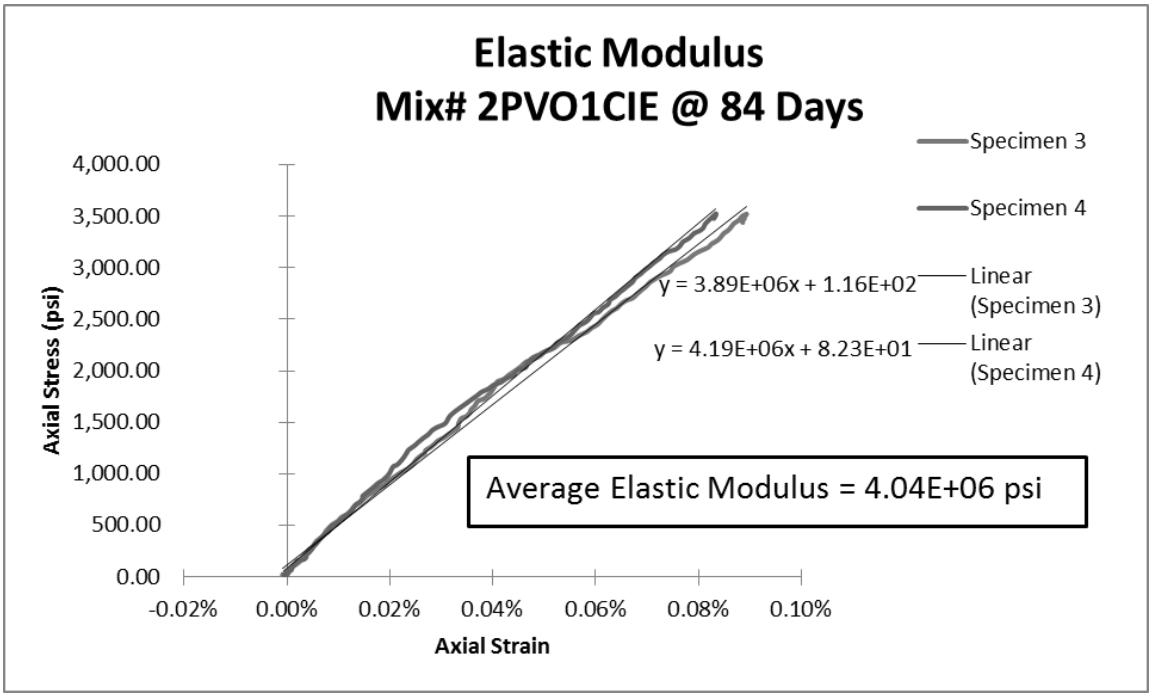

Figure E-2 Sample elastic modulus test results for a set of two concrete cylinders.

Appendix F Material Properties of the EPS Foam Void Used for Box Beams

To verify the average elastic modulus of the expanded polystyrene (EPS) material used to form the internal voids for box beams and to obtain the approximate yield stress of the material, a sample of the material was tested in the lab at NCSU. The following material properties were provided in the manufacturer's specifications for the material:

Minimum density: 0.90 lb/ft^3
Average elastic modulus: 180 psi

These material properties are typical of the material used by most of the precasting plants at the time of this study based on a review of the specifications from several plants.

Multiple test specimens were obtained from the sample. The specimens were divided into six groups of three specimens each, as shown in Table F-1.

Table F-1 Box beam void EPS specimens tested.

Group Name	# of specimens	Length (in)	Width (in)	Thickness (in)
2S	3	10	10	2
2L	3	16	10	2
2E	3	6	6	2
4S	3	10	10	4
4L	3	16	10	4
4E	3	6	6	4

All of the specimens were compressed through their thickness using a stroke-controlled compression testing machine as shown in Figure F-1. The test method for each group of specimens is described in Table F-2.

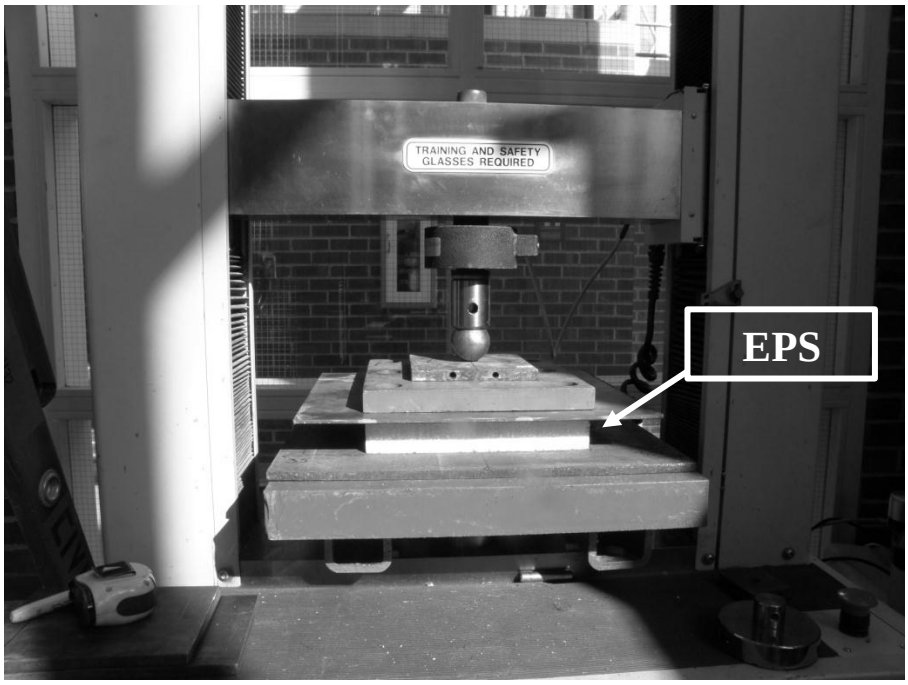

Figure F-1 Testing of EPS void material for elastic modulus and yield stress.

Table F-2 Compression test method for each group of EPS void specimens.

Group Name	Test Method
2S	Entire area in compression using a steel plate.
2L	Compression area consists of 10” x 6” steel plate laid transversely across the specimen so that 5” of the specimen on either side of the plate are not in compression.
2E	Entire area in compression using a steel plate.
4S	Same as 2S.
4L	Same as 2L.
4E	Same as 2E.

The average measured density of the specimens was 0.95 lb/ft^3, which is close to the manufacturer’s minimum density, suggesting that the sample is representative of the typical

characteristics of the material as given in the specifications. As shown in Figure F-2, the average measured elastic modulus of the sample was 170 psi, which is close to the manufacturer's specified value. In addition, the yield stress of the sample was found to be approximately 6 psi, which is well above the maximum hydrostatic pressure of 3 psi that is typically applied to the void for the box beams considered in this study. Therefore, it is concluded that the void material can be assumed to behave linearly under the hydrostatic pressure due to the fresh concrete during casting, and that the average elastic modulus is approximately 170 psi for the EPS material that is typically used for box beams at the time of this research. These characteristics were used in the analysis to determine the modified section properties for box beams.

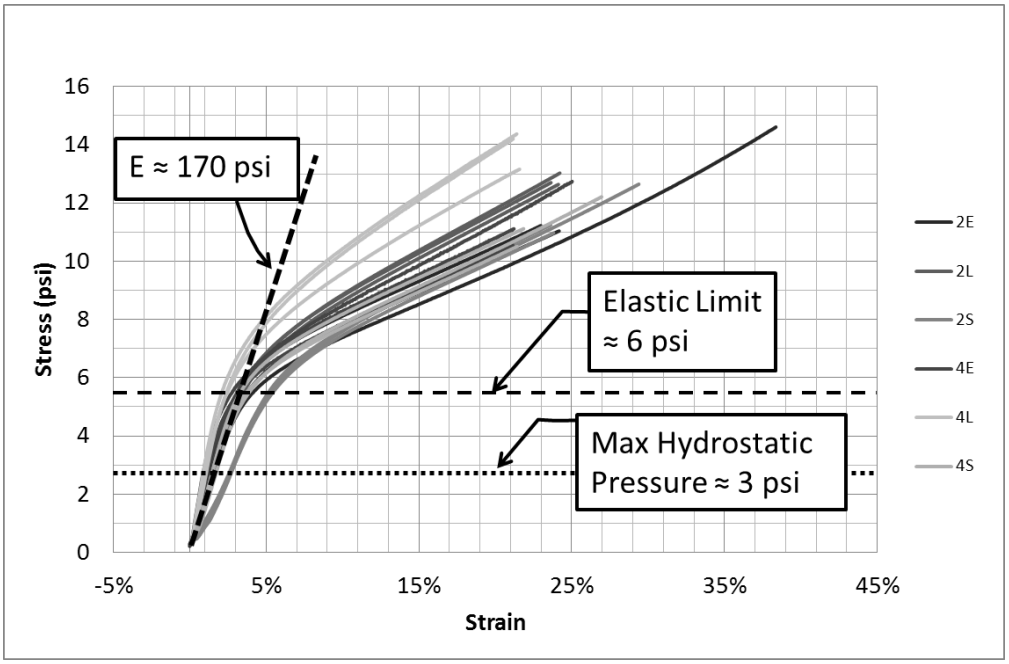

Figure F-2 Compression test results for EPS void material.